DISSERTATION | DOCTORAL THESIS

Titel | Title

Understanding the human health impacts of environmental micro- and nanoplastics: Test material development and environmental exposure studies

verfasst von | submitted by

Mag.pharm. Lukas Wimmer

angestrebter akademischer Grad | in partial fulfilment of the requirements for the degree of

Doktor der Naturwissenschaften (Dr.rer.nat.)

Wien | Vienna, 2025

Studienkennzahl lt. Studienblatt | Degree programme code as it appears on the student record sheet:	UA 796 610 449
Dissertationsgebiet lt. Studienblatt | Field of study as it appears on the student record sheet:	Pharmazie
Betreut von | Supervisor:	Univ.-Prof. Dr. Lea Ann Dailey

Acknowledgements

THE DECISION TO PURSUE A DOCTORATE MUST BE MADE ALONE, BUT SUCCESSFULLY COMPLETING IT IS UNIMAGINABLE WITHOUT THE STRONG SUPPORT OF MANY MORE PEOPLE.

First and foremost, I would like to thank my supervisor, Lea Ann Dailey, for my exceptionally great experience as a PhD student in her research group. You created a working environment based on immense mutual respect, deep trust, and scientific excellence, which has profoundly impressed me not only professionally but also personally. With your warm and motivating approach, you always managed to give me new drive, even when faced with setbacks, and you provided me with both the freedom I valued and the support I needed. I consider myself extremely fortunate and honored to have worked with you over the past few years and want to thank you from the bottom of my heart for making my time as a PhD student a truly wonderful experience.

Great thanks go to both my co-supervisor Gabriela Hädrich, as well as Gianluca Bello and Richard Harvey, for all the time invested and active support during countless experiments. I could always rely on your help, regardless of your own obligations, whether I needed additional brainpower in the lab or staying power during karaoke. Furthermore, I would like to thank my fellow PhD students Feng Li, Thuong Phan Xuan, Jacqueline Schwarzinger, and My Vanessa Nguyen Hoang, as well as my colleague Itziar Otazo Aseginolaza. You significantly contributed to making my time as a PhD student the great experience it was. The relaxed atmosphere, where there was always time for jokes and mutual support, is not to be taken for granted, but it is highly valued by me – a day in the office without you isn't the same. For countless smaller and larger problems, I could always count on Maria Anzengruber, Katharina Skoll, and Maria Lummerstorfer, for which I want to express my deep gratitude. Your advice and hands-on mentality are greatly appreciated. While I'm sad to have lost you all as colleagues, I'm incredibly happy to have gained you as friends.

I would also like to thank all my project partners, especially Tanja Ćirković Veličković, Korinna Altmann, Anya Sherman, Tassilo Waniek, Vesna Jovanovic, and Thomas C. Meisel, as well as the many others involved. Working with you allowed me to broaden my horizon across other scientific disciplines. It was an absolute pleasure to collaborate with you.

I am deeply grateful to my entire family, especially my parents Yvonne and Hermann, for enabling me to study through their hard work and for always supporting all my decisions without reservation. I would also like to thank my brother Tobias, who can cheer me up even on tougher days. I am incredibly happy to have you as my brother. My thanks also go to my grandparents, uncles, and aunts, who likewise never doubted my decisions.

Viktor, Maximilian, Alexander, Julia, Sabine, and Melanie, you have all endured difficult days and celebrated all successes with me. It is hard for me to describe how much I value all of you, and your friendship. A week without seeing you is a week too long.

The one and only Claudia: For almost 15 years, you have been continuously by my side, providing support, offering comfort, letting me dream, making me confident, making me happy. It is incredibly difficult to put into words how much you mean to me and how significant your contribution to my successes is. I hope these lines come close to doing it justice. Please bear with me, as so often.

List of paper contributions

First-authorships

1. Wimmer, L., Nguyen Hoang, M. V., Schwarzinger, J., Jovanović, V. B., Anđelković, B., Cirkovic Velickovic, T., Meisel, T., Waniek, T., Weimann, C., Altmann, K., & Dailey, L. A. A quality-by-design inspired approach to develop PET and PP nanoplastic test materials for use in in vitro and in vivo biological assays. *Environmental Science: Nano* **2025**, 12, 2667-2686. https://doi.org/10.1039/D4EN01186D
2. Altmann, K., Wimmer, L., Alcolea-Rodriguez, V., Waniek, T., Wachtendorf, V., Matzdorf, K., Ciornii, D., Fengler, P., Milczewski, F., Otazo-Aseguinolaza, I., Ferrer, M., Bañares, M. A., Portela, R., & Dailey, L. A. Quality-by-design and current good practices for the production of test and reference materials for micro- and nanoplastic research. *Journal of Hazardous Materials* **2025**, 139595. https://doi.org/10.1016/J.JHAZMAT.2025.139595

Co-authorships

3. Sherman, A., Masset, T., Wimmer, L., Maruschka, L. K., Dailey, L. A., Hüffer, T., Breider, F., & Hofmann, T. The Invisible Footprint of Climbing Shoes: High Exposure to Rubber Additives in Indoor Facilities. *ACS ES&T Air* **2025**, 2(5), 930–942. https://doi.org/10.1021/acsestair.5c00017
4. Kaseke, T., Jovanovic, V., Wimmer, L., Vasovic, T., Mutic, T., Acimovic, J., Dailey, L. A., & Cirkovic Velickovic, T. Polypropylene micro- and nanoplastics affect the digestion of cow's milk proteins in infant model of gastric digestion. *Environmental Pollution* **2025**, 383, 126803. https://doi.org/10.1016/J.ENVPOL.2025.126803
5. Lessiak, U., Brandstoetter, T., Nell, B., Klein, K., Mlynek, G., Wimmer, L., Scheiblecker, L., Tichy, A., & Hoelbl-Kovacic, A. Preserved bevacizumab (Avastin®) eye drops for application in multidose containers – an in-vitro characterisation. *BMC Veterinary Research* **2025**, 21(1), 129. https://doi.org/10.1186/s12917-025-04592-4
6. Lujic, T., Gligorijevic, N., Stanic-Vucinic, D., Krstic Ristivojevic, M., Mutic, T., Wimmer, L., Dailey, L. A., & Cirkovic Velickovic, T. Effects of Polypropylene and Polyethylene Terephthalate Microplastics on Trypsin Structure and Function. *International Journal of Molecular Sciences* **2025**, 26(13). https://doi.org/10.3390/ijms26135974
7. Krishna de Guzman, M., Stanic-Vucinic, D., Gligorijevic, N., Wimmer, L., Gasparyan, M., Lujic, T., Vasovic, T., Dailey, L. A., van Haute, S., & Cirkovic Velickovic, T. Small polystyrene microplastics interfere with the breakdown of milk proteins during static in vitro simulated human gastric digestion. *Environmental Pollution* **2023**, *335*, 122282. https://doi.org/10.1016/j.envpol.2023.122282

Declarations

ChatGPT-4 and Google Gemini 2.5 Flash were occasionally used to check grammar and spelling. Parts of Chapter 1 and 2 were first published on the 18st of August 2025 in the Journal of Hazardous Materials (https://doi.org/10.1016/j.jhazmat.2025.139595) and reproduced with permission from Elsevier[1]. Parts of Chapters 1, 3, and 5 were first published on the 1st of April 2025 in Environmental Science: Nano (https://doi.org/10.1039/D4EN01186D) and reproduced with permission from the Royal Society of Chemistry[2]. I have made every effort to identify all copyright holders and have obtained their consent to use the images in this work. Should any copyright infringement nevertheless become known, I ask that you notify me.

Abstract

Plastics enabled significant technological advancements but the ever-increasing production volume and insufficient waste management lead to accumulation of those materials in nature. Consequently, plastics have become major environmental pollutants. While plastics are durable, they continuously fragment under environmental influences forming micro- and nanoplastics (MNPs). This size reduction enhances their spread *via* wind or water bodies, leading to almost unavoidable exposure to MNPs through food or air. Despite the increasing number of reports detecting MNPs in various regions of the human body, knowledge gaps exist regarding possible health implications. Particularly particles < 10 µm are of concern as they can be inhaled and are associated with both acute and long-term negative health effects. While this is especially true for traffic related aerosols, the impact of inhaled MNPs remains understudied. One reason for the existing knowledge gaps is the lack of suitable test materials. Commercially available MNPs are often not designed for use in biological assays and can contain undisclosed or even potentially interfering substances. Published methods to produce materials in-house on the other hand often neglect characterization of biologically relevant properties. Another reason for uncertainties regarding health implications is limited data on environmental concentrations of inhalable MNPs, particularly in aerosols. While initial research detected MPs in seaside aerosols, the inhalable fraction < 10 µm remained unstudied.

This thesis aims to address these gaps, firstly by developing microplastic (MP) and nanoplastic (NP) test materials specifically for use in biological assays, and secondly through implementation and validation of a novel sampling technique for the quantification of MNPs in aerosols. Test materials are developed following a systematic approach known as quality-by-design, where critical material attributes are pre-defined to ensure product quality already from the conceptual phase onwards. Polypropylene (PP) MPs for use in inhalation toxicology studies with a size range from 1-10 µm was the first material developed. PP was subjected to milling to mimic the environmental fragmentation process, followed by a multi-step procedure for size fractionation. The obtained material was then suspended in glycerol as biocompatible storage medium and dispersion aid. Thorough material characterization showed that irregularly shaped fragments with a highly

reproducible median particle size were obtained. In none of the MP suspensions in glycerol were viable microorganisms detected, including particles stored for 2.5 years. Furthermore, the material was fully redispersible in biorelevant medium (Dulbecco's Modified Eagle's Medium, DMEM) after production but showed signs of agglomeration after 2.5 years of storage. The practical utility, however, was severely constrained by the low particle yield per batch.

NPs comprised of polyethylene terephthalate (PET) and PP for use in *in vitro* and *in vivo* assays were the second material type developed with a targeted size fraction < 1 µm of > 85%. High yields per batch were achieved through polymer dissolution and subsequent reprecipitation (nanoprecipitation), which enabled the creation of highly concentrated stock suspensions for dose escalation studies. In-depth investigation of the glycerol vehicle revealed that cytotoxicity was caused by hyperosmolarity but was not problematic for usually tested NP concentrations. The produced NPs were free of contaminants and their bulk chemistry was not altered through production. Batch-to-batch variability of the final glycerol product was low and the size fraction < 1 µm exceeded the target for both polymers. Endotoxin levels were below the limit of detection and physical and microbial stability was demonstrated over 12 months. Full dispersibility in biorelevant medium was achieved for PET NPs, whereas the more hydrophobic PP NPs agglomerated.

In the last part of this thesis, a glass liquid impinger (GLI) was explored as a novel sampling device for MNPs in aerosols. Due to the low expected concentrations, thermal extraction-desorption gas chromatography mass spectrometry (TED-GC-MS) was chosen for sample analysis. Since the GLI is not a standard device in air pollution science, extensive method validation was conducted to assess its performance. The robustness of the washing and sample collection was demonstrated through high recovery rates of spiked NPs. However, nebulization of PET and PP NPs to establish their deposition patterns was challenging. The more hydrophobic PP could not be nebulized, which correlated with their agglomeration status after nebulization. While small amounts of PET were detected inside the GLI, the majority stayed in the nebulizer reservoir although the particles remained well dispersed throughout the experiment. Finally, two field sampling campaigns were conducted comparing MNP concentrations in lakeside versus seaside aerosols, utilizing

the developed GLI and TED-GC-MS method. Preliminary data from the lakeside campaign did not detect MNPs above procedural blank levels. The limit of detection and, thus, the methods suitability need to be determined in future work, as data analysis is ongoing.

Zusammenfassung

Kunststoffe ermöglichten beachtliche technologische Fortschritte, doch das stetig steigende Produktionsvolumen bei gleichzeitig inadäquater Entsorgung resultierten in der Akkumulation dieser Materialien in der Natur. Kunststoffe stellen mittlerweile eines der größten Umweltprobleme der Moderne dar, denn sie sind einerseits sehr langlebig, aber fragmentieren andererseits unter Umwelteinflüssen in immer kleinere Mikro- und Nanoplastikpartikel (MNP). Diese Größenreduktion begünstigt ihre Verbreitung durch Wind oder Wasser, was zu einer nahezu unvermeidbaren Exposition über die Nahrung oder Luft führt. Trotz der zunehmenden Anzahl von Studien, in denen MNP in verschiedenen Bereichen des menschlichen Körpers nachwiesen wurden, bestehen Unsicherheiten bezüglich möglicher gesundheitlicher Auswirkungen. Von besonderer Relevanz sind Partikel < 10 µm, da sie leicht inhaliert werden können und mit akuten sowie langfristigen negativen gesundheitlichen Folgen verbunden sind. Während dies besonders auf verkehrsbedingte Aerosole zutrifft, sind die Auswirkungen von inhalierten MNP nach wie vor unzureichend erforscht. Ein Grund für die bestehenden Wissenslücken ist der Mangel an geeigneten Testmaterialien. Kommerziell erhältliche MNP sind oft nicht für den Einsatz in biologischen Assays konzipiert und können nicht deklarierte oder sogar potenziell interferierende Substanzen enthalten. Wissenschaftliche Publikationen von Methoden zur Eigenproduktion von Testmaterialien vernachlässigen hingegen oft die Charakterisierung biologisch relevanter Eigenschaften. Ein weiterer Grund für Unsicherheiten bezüglich der gesundheitlichen Auswirkungen sind die sehr limitierte Verfügbarkeit von Daten zu Umweltkonzentrationen inhalierbarer MNP, insbesondere in Aerosolen. Während erste Studien größere Mikroplastikpartikel (MP) in Meeres-Aerosolen nachweisen konnten, wurden jedoch die inhalierbaren Partikel < 10 µm nicht untersucht.

Diese Arbeit zielt darauf ab die beschriebenen Wissenslücken zu schließen, erstens durch die Entwicklung von MP und Nanoplastikpartikel (NP) als Testmaterialien, speziell für die Anwendung in biologischen Assays und zweitens durch die Implementierung und Validierung einer neuartigen Methode zur Probenahme und Quantifizierung von MNP in Aerosolen. Die Testmaterialien wurden mithilfe eines systematischen Ansatzes, bekannt als "Quality-by-Design", entwickelt. Dabei wurden entscheidende Materialeigenschaften vorab definiert, um die Produktqualität bereits von der Konzeptphase an zu gewährleisten. Das erste entwickelte

Material waren Polypropylen (PP) MP (1-10 µm) für inhalationstoxikologische Studien. PP wurde einem Mahlprozess unterzogen, um den Fragmentierungsprozess in der Umwelt zu imitieren, gefolgt von einem mehrstufigen Verfahren zur Größenklassierung. Die erhaltenen Partikel wurden anschließend in Glycerol suspendiert, als biokompatibles Lagermedium und Dispergierhilfe. Eine umfassende Materialcharakterisierung zeigte, dass unregelmäßig geformte Fragmente mit einer hoch reproduzierbaren medianen Partikelgröße erhalten wurden. In keinem der in Glycerol gelagerten MP-Suspensionen wurden lebensfähige Mikroorganismen nachgewiesen, selbst bei Partikeln die 2.5 Jahre gelagert wurden. Darüber hinaus war das Material nach der Produktion in biorelevantem Medium (Dulbecco's Modified Eagle's Medium, DMEM) vollständig redispergierbar, zeigte jedoch nach 2.5 Jahren Anzeichen von Agglomeration. Der praktische Nutzen wurde jedoch durch die geringe Partikelausbeute pro Charge stark eingeschränkt.

Als zweiter Materialtyp wurden Polyethylenterephthalat (PET) und PP NP für den Einsatz in *In-vitro*- und *In-vivo*-Assays entwickelt, mit einem angestrebten Größenanteil unter 1 µm von > 85 %. Hohe Ausbeuten pro Charge wurden durch Lösen und anschließende Repräzipitation (Nanopräzipitation) der Polymere erzielt, was die Herstellung hochkonzentrierter Stammsuspensionen in Glycerol für Dosis-Eskalations-Studien ermöglichte. Eine detaillierte Untersuchung des Glycerol-Vehikels zeigte, dass die Zytotoxizität durch Hyperosmolarität verursacht wurde, was jedoch für die üblicherweise getesteten NP-Konzentrationen unproblematisch war. Die produzierten NP waren frei von Verunreinigungen und ihre chemische Zusammensetzung wurde durch die Produktion nicht verändert. Die Batch-zu-Batch-Variabilität des fertigen Glycerolprodukts war gering und der angestrebte Größenanteil < 1 µm wurde für beide Polymere übertroffen. Die Endotoxinkonzentrationen lagen unterhalb der Nachweisgrenze und die physikalische sowie mikrobielle Stabilität war über 12 Monate hinweg gegeben. PET NP konnten in biorelevantem Medium vollständig redispergiert werden, während die hydrophoberen PP NP agglomerierten.

Im letzten Teil dieser Arbeit wurde ein Glas-Flüssigkeits-Impinger (GLI) als neuartiges Probenahmegerät für MNP in Aerosolen untersucht. Aufgrund der erwarteten geringen Konzentrationen wurde die thermische Extraktions-Desorptions-Gaschromatographie-Massenspektrometrie (TED-GC-MS) für die Probenanalyse gewählt. Da der GLI kein

Standardgerät in der Umweltwissenschaft ist, wurde eine umfassende Methodenvalidierung zur Bewertung der Leistungsfähigkeit durchgeführt. Die Robustheit des Wasch- und Probenahmeverfahrens wurde durch hohe Wiederfindungsraten von dotierten NP demonstriert. Die Vernebelung von PET und PP NP zur Bestimmung ihrer Abscheidungsmuster im Gerät erwies sich jedoch als herausfordernd. Die hydrophoberen PP NP konnten nicht vernebelt werden, was mit ihrem Agglomerationszustand nach der Vernebelung korrelierte. Während geringe Mengen an PET innerhalb des GLI nachgewiesen wurden, verblieb der Großteil im Verneblerreservoir, obwohl die Partikel während des gesamten Experiments gut dispergiert blieben. Abschließend wurden zwei Feldstudien durchgeführt, um die MNP-Konzentrationen in Aerosolen an See- und Meeresstandorten zu vergleichen, wobei das entwickelte GLI und TED-GC-MS-Verfahren angewendet wurde. Vorläufige Daten aus der See-Studie zeigten keine MNP-Konzentrationen über den prozeduralen Blindwerten. Die Nachweisgrenzen und somit letztendlich die Eignung der Methode müssen in zukünftigen Arbeiten bestimmt werden, da die Datenanalyse noch läuft.

List of figures

List of tables

List of equations

List of acronyms

Acronym	Full form
ATR-FTIR	Attenuated total reflectance – Fourier transform infrared spectroscopy
BRM	Biorelevant media
BSA	Bovine serum albumin
CFU	Colony forming units
CI	Carbonyl index
CMA	Critical material attribute
CMC	Critical micelle concentration
CPP	Critical process parameter
CQA	Critical quality attribute
CRM	Certified reference material
D_{10}	10^{th} percentile
D_{50}	50^{th} percentile = median
D_{90}	90^{th} percentile
DCM	Dichloromethane
DLS	Dynamic light scattering
DMEM	Dulbecco's Modified Eagle's Medium
DQA	Desired quality attribute
F8BT	Poly-[(9,9-di-n-octylfluorenyl-2,7-diyl)-alt-(benzo[2,1,3]thiadiazol-4,8-diyl)]
FBS	Fetal bovine serum
FTIR	Fourier transform infrared spectroscopy
GLI	Glass liquid impinger
HD-PE	High-density polyethylene
HPW	High purity water
ISO	International Organization for Standardization
LC	Lower compartment
LD	Laser diffraction
LD-PE	Low-density polyethylene
LOD	Limit of detection
LOQ	Limit of quantification
LRT	Lower respiratory tract
MNPs	Micro- and nanoplastics
MPs	Microplastics
MTP	Mouth and throat piece
NIST	National Institute of Standards and Technology

Acronym	Full form
NPs	Nanoplastics
PAH	Polycyclic aromatic hydrocarbon
PE	Polyethylene
PET	Polyethylene terephthalate
PM_{10}	Particulate matter < 10 µm
$PM_{2.5}$	Particulate matter < 2.5 µm
PMMA	Poly(methyl methacrylate)
PP	Polypropylene
PS	Polystyrene
PSD	Particle size distribution
PUR	Polyurethane
PVC	Polyvinyl chloride
Py-GC-MS	Pyrolysis gas chromatography mass spectrometry
QbD	Quality by design
QC	Quality control
RGTM	Research grade test materials
RI	Refrective index
RM	Reference material
SEM	Scanning electron microscopy
SOP	Standard operating procedure
SRM	Standard reference material
SSA	Sea spray aerosols
TED-GC-MS	Thermal extraction-desorption gas chromatography mass spectrometry
Tg	Glass transition temperature
TPP	Target product profile
TPU	Thermoplastic polyurethane
UC	Upper compartment
URT	Upper respiratory tract
WHO	World Health Organization

Table of contents

Chapter 1

Introduction to the knowns and unknowns of plastic pollution

1 Introduction

Parts of this chapter were first published on the 18st of August 2025 in the Journal of Hazardous Materials (https://doi.org/10.1016/j.jhazmat.2025.139595) and the 1st of April 2025 in Environmental Science: Nano (https://doi.org/10.1039/D4EN01186D). Reproduced with permission from Elsevier[1] and the Royal Society of Chemistry[2].

1.1 Part I – The plastic life cycle

Since the 1970s[3], plastic pollution has been recognized as an environmental issue and has reached a concerning extent. Thus, this problem has gained significant attention from policymakers[4–6] and the general public[7] in recent years. In 2022, the worldwide production volume of plastics exceeded 400 Mt[8]. The high share of single-use plastic items and insufficiently high recycling rates[9] resulted in a likewise steady increase of plastic waste[10]. The majority of this waste is transferred to landfills[11], where even well-managed sites fail to avoid the release of this waste into the environment[12]. Synthetic polymers are exceptionally durable by design. However, they fragment under environmental influences like UV-irradiation, chemical processes, and mechanical stress[13,14], even down to the nanoscale[15]. This fragmentation process favors their spread *via* aquatic[16–18] or atmospheric[19,20] transport mechanisms. An increasing number of studies detect these particles in many different environments (urban, remote, indoor, outdoor, land, or sea)[21–24], which suggests that exposure to micro- and nanoplastics (MNPs) through food or air is almost unavoidable[25]. Despite increasing research efforts, many questions about possible impacts of MNPs on the environment and human health remain due to lacking standardization, insufficient controls, or a lack of test materials or suitable analytical methods[26]. This chapter will explore what plastics are, what their fate is when they enter the environment, and what the challenges are when trying to assess the risk of these materials.

Plastic – A generic term

In the early 20th century, Leo Hendrik Baekeland developed a process to synthesize the first fully synthetic plastic, later marketed under the name Bakelite[27]. This invention marked the starting point of a rapid development in polymer science, especially since the

1950s, which increasingly impacted society. Initially developed as an insulator for the emerging electrical industry, Bakelite and other polymers soon enabled countless other applications across all industries[28,29].

Today, plastic polymers are divided into four major groups (thermoplastics, thermoplastic elastomers, elastomers, and thermosets) of which thermoplastics dominate the global production. They have a linear structure, consist of one (homopolymer) or different (copolymer) repeating building blocks (monomers) and can be branched. The individual chains are not cross-linked and chain lengths can vary. The aforementioned characteristics and the macromolecular state – either amorph or semi-crystalline – define the final material properties of native polymers[30]. However, the performance of certain plastics can be altered by adding additives like flame retardants to enhance fire resistance, antioxidants to prevent material degradation through oxidative stressors, or plasticizers to increase flexibility and softness[31]. There are thousands of different additives available, further diversifying the options within the same polymer group.

In 2022, global annual plastic production exceeded 400 million tons (Mt), whereby the packaging industry accounts for 39% of the total demand. Thermoplastics like polypropylene (PP), polyethylene (PE; high-density and low-density PE), polyvinyl chloride (PVC), polyethylene terephthalate (PET) and polystyrene (PS) are the dominating polymer types, accounting for over 75% of total plastic production. They are extensively used in packaging due to their heat resistance, durability, hygienic properties, lightweight nature, and cost-effective mass-production. However, packaging is mainly designed to be single-use and disposed of immediately, generating a significant amount of plastic waste. Often, different polymers are combined in one item to achieve a desired performance, which makes recycling challenging or even impossible and economically unappealing[32,33]. Geyer, Jambeck and Lavender estimated that by 2015, only 9% of all plastic waste was recycled and 12% was incinerated[34]. The vast majority ends up in landfills where even well-managed sites fail to prevent the release of plastic waste into the environment[35].

Degradation mechanisms

Conventional plastics are durable by design. While this is beneficial during their life span, it becomes a problematic feature after plastic waste enters the environment. Although research on biodegradable plastics is increasing, the total production share remains negligible[8]. Therefore, it can take thousands of years until a plastic item is mineralized (degraded into CO_2 and H_2O under aerobic or also CH_4 under anaerobic conditions) depending on polymer type, size, shape, surface area, and environmental conditions among others[36]. The relevant degradation pathways in nature can be summarized under biotic or abiotic mechanisms, where usually the latter initiates the deterioration process. Through mechanical stress like wave action, UV irradiation, or hydrolyzation, larger objects break down into smaller pieces to a point where the surface is altered enough for microorganisms to attach and eventually mineralize those particles[37]. However, mineralization takes longer under environmental conditions than mechanical breakdown processes, which is the reason for the large number of microscopic plastic particles generated per single item[38].

Classification of plastic debris

Even before their end of life and throughout their intended use, plastic items can produce smaller pieces through wear[39]. Examples are polymeric fibers or fiber fragments released through washing textiles[40], peel-offs of paints that utilize polymers as binders[41], or abrasion of rubber tires[42]. Those unintentionally generated particles are defined as “secondary” microplastics. Conversely, if they are produced on purpose they are referred to as “primary” microplastics[43], which are commonly used as exfoliants in cosmetics[44] or fertilizers with coatings for controlled release[45]. This distinction is often irrelevant or impossible to determine in environmental samples but is used by policymakers in the US[46] and the EU[47], where bans on certain primary microplastics have already been implemented and may be expanded. However, Mitrano & Wohlleben (2020) argue that solely banning all primary microplastics might not be effective in reducing the microplastic burden in the environment since the vast majority are secondary MPs originating from improperly

disposed of items. Hence, they suggest focusing on efficient waste collection to mitigate the initial release of plastics into the environment[48].

Degradation with respect to conventional (non-biodegradable) plastics means a breakdown into ever smaller pieces. Depending on their size, the terms microplastics (MPs) and nanoplastics (NPs) were introduced – among others – to summarize the highly diverse composition of plastic debris. Although there is still no generally accepted size definition of micro- and nanoplastics (MNPs), Hartmann *et al.* (2019) provided definitions based on the largest dimension **(Table 1.1)**[43]. While the NP definition has been widely adopted by the scientific community, regulators[49], and organizations like the International Organization for Standardization (ISO)[50] or the World Health Organization (WHO)[25], the upper size limit of MPs is still contentious. MPs are often defined as < 5 mm as this is a threshold where ingestion is increasingly likely to happen[43]. Despite the ongoing discussion about the exact size definition, it has been shown that smaller particles are increasingly relevant for risk assessment because they spread more easily[51] and are possibly able to cross biological barriers[52].

Table 1.1: Proposed size classes of plastic items by Hartmann et al. where the size is defined by the largest dimension of the investigated object. This definition excludes fibers, which should be classified by their diameter [43].

Term	Size class (largest dimension)	Rationale
Macroplastics	> 1 cm	"[...] the largest dimension of an item will mainly determine the ingestion by biota."[43]
Mesoplastics	< 1 cm – 1 mm	
Microplastics (MPs)	< 1 mm – 1 µm	
Nanoplastics (NPs)	< 1 µm – 1 nm	

Transportation mechanisms and sources

MPs have been detected in diverse and remote environments, including glaciers in the Alps[53] and the Tibetan Plateau[54], the depths of the Mariana Trench[55], and other isolated regions such as the Arctic[56], Antarctic[57], and Iranian deserts[58]. These findings highlight that plastic debris can travel vast distances through aquatic and atmospheric transport, which are considered the two major transport mechanisms. Potential sources are manifold, but it

is estimated that around 80% of plastics in the ocean originate from land and only 20% are originally directly released into the oceans. Land-based sources that contribute significantly are littering, waste mismanagement, agriculture, and traffic. The released fragments are then transported *via* wind and rain into rivers, ultimately ending up in the ocean[59,60]. There they accumulate together with ocean-based sources from industrial fishing and shipping **(Figure 1.1)**[38]. Today, six major garbage patches formed by ocean gyres are known and they are projected to grow[61]. Surprisingly, it has been shown that the ocean does not only act as a sink for plastic waste but is also a source. MNPs can be released through bubble burst ejection and transported in the atmosphere for long distances until they deposit through atmospheric fallout **(see Chapter 1.3)**[62].

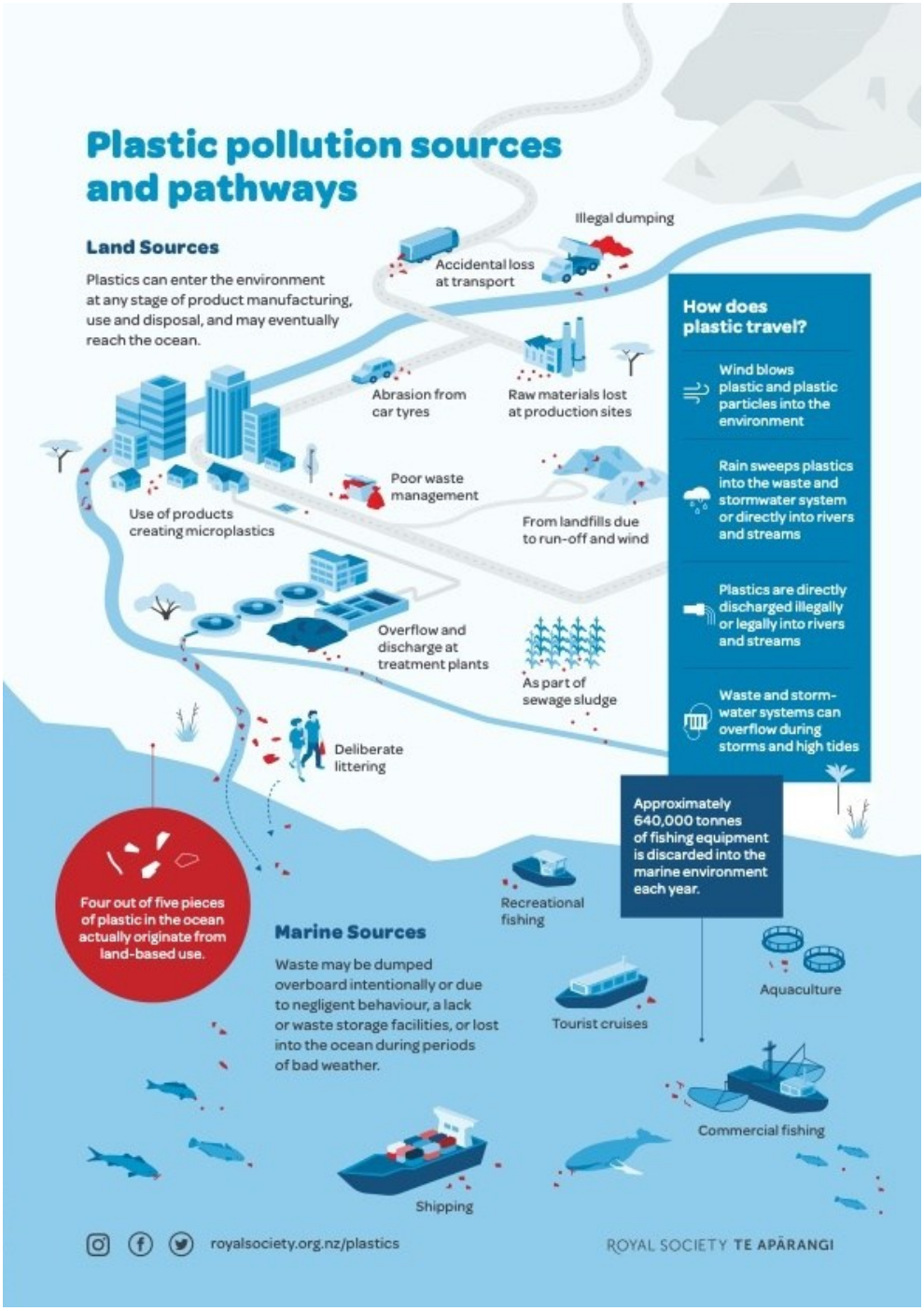

Figure 1.1: Sources of plastic pollution are land and marine based. In the environment, plastic items degrade into small pieces which facilitates their distribution across the planet. Main distribution pathways include transport *via* atmospheric deposition (wind and precipitation), discharges into rivers and streams, and wastewater overflows during storm events. Reprinted from "Plastics In The Environment - Te Ao Hurihuri - The Changing World" by the Royal Society of New Zealand Te Apārangi, 2019, p.6, https://www.royalsociety.org.nz/major-issues-and-projects/plastics, CC BY 3.0 NZ, with permission from the Royal Society of New Zealand Te Apārangi.

Possible health implications and current knowledge gaps

Despite intensive effort and resources invested in MNP research, the implications for human health are still unknown. The hydrophobic nature and large surface area of MNPs facilitate the adsorption of hydrophobic contaminants like polycyclic aromatic hydrocarbons (PAHs), biomolecules like toxins or allergens[63], or heavy metals, which are known for their potential adverse health effects[64]. Emecheta *et al*. (2024) studied the desorption behavior of benzo[*a*]pyrene as representative PAH from eleven different MPs in simulated digestion fluids. They showed that the estimated relative intake of PAHs *via* MPs was ≤ 0.1% compared to the total daily intake of PAHs under realistic scenarios. However, uncertainties remained due to the high variability of MNP and PAH concentrations at different locations[65]. It is also known that the previously described additives can leach into the surrounding medium and may further contribute to the toxicity profile of MNPs and their cargo[31,66]. A recent review by Li *et al*. (2024) highlighted that *in vitro* and *in vivo* studies in human derived cells, and mammals respectively, showed adverse effects through physical damage, inflammation, oxidative stress, apoptosis, or other unknown mechanisms. However, the following shortcomings remain: i) in most studies to date mainly pristine PS beads were tested, ii) effects were mainly observed at environmentally unrealistic concentrations, iii) effects from other organisms or cells cannot be directly extrapolated to or linked with human diseases, and iv) epidemiological studies only investigated occupational settings, thus data regarding exposure levels for the general public is not available[67]. Many of the current knowledge gaps are a direct result of the limited availability and sensitivity of suitable analytical methods to identify and quantify MNPs, a lack of standardization, and the complexity when the wide variety of relevant polymer types, environmental cargo, or plastic additives are considered. Thus, well-characterized test and reference materials for calibration, validation, and comparison studies are urgently needed[68–74].

IMPTOX – An EU funded research project investigating possible links between micro- and nanoplastics exposure and the development of allergic diseases

To address some of the mentioned knowledge gaps, five research projects – specifically investigating potential effects of MNPs on human health – got funded by the EU's Horizon2020 framework program: Aurora (focus on early life)[75], IMPTOX (focus on the development of allergic diseases)[76], PlasticsFatE (focus on additives, contaminants, and exposure levels)[77], plasticheal (focus on risk assessment and modeling)[78], and POLYRISK (focus on occupational and consumer exposure assessment)[79]. Together they form the European Cluster on Health Impacts of Micro- and NanoPlastic (CUSP)[80], where collaboration between the projects was expected. This thesis was conducted within the IMPTOX project, which covers three main areas: i) the development of suitable analytical techniques for the detection and characterization of MNPs in food, water, and air, ii) the investigation of MNPs in combination with potentially harmful cargo like toxins, or heavy metals, and iii) the role of MNPs in food allergy and allergic asthma. Two main objectives from these areas were assigned to our group and are described in detail in the following chapters. Briefly, the first objective was the development of suitable test materials. For study within IMPTOX, PET and PP were chosen because they are extensively used for packaging and are among the most abundant polymers in environmental and human samples[81–84]. The reasons for this abundance are outlined in **Chapter 1.1** and include a large production volume[8], a short service life, and low recycling rates of packaging materials or other single-use products[9]. Despite their relevance, suitable test materials are currently unavailable, especially in sizes < 50 µm **(see Chapter 0)**. The aim was therefore to develop well-characterized PET and PP test materials in sizes from the nano to the micron range. The second objective was to investigate the abundance of MNPs in air and compare fresh water (lakeside) with marine (seaside) locations. Studies showed that the ocean is a source of MNPs which can be part of sea spray aerosols[62]. Similarly, lakes are contaminated with plastics[85] and eject particles into the air[86], which could include plastic particles. Evidence, however, is lacking and technical or methodological limitations excluded NPs from those studies. **Chapter 1.3** describes the rationale in detail and provides the current state and gaps of knowledge regarding MNPs in sea spray and freshwater aerosols.

1.2 Part II – Current state and unmet needs of available micro- and nanoplastic test materials

Researchers have begun to develop methods for the in-house production of MNPs to overcome the shortage of test materials **(see Chapter 0)**. Due to the urgent need of materials for *in vitro* and *in vivo* toxicity assays, many materials are being used prior to thorough characterization and standardization, which limits comparability across different studies. There also appears to be a general confusion of terminology regarding the grades of test materials. Often, materials are referred to as "reference materials", even though they do not meet the specifications required for that designation. This chapter will introduce test material terminology, give an overview of available methods and materials, and outline concepts derived from the product design space which may help guide the development of MNP test materials.

Definitions of different test material grades

The National Institute of Standards and Technology (NIST) and the International Organization for Standardization (ISO) categorize materials into four major groups dependent on the specified intended use and level of characterization provided in the form of a suitable data and information sheet: i) research grade test materials, ii) reference materials, iii) certified reference materials, and iv) standard reference materials **(Table 1.2)**[2]. Research grade test materials (RGTM) represent the bottom of the hierarchy[87]. Their benefit of a fast batch release is offset by the lower degree of characterization compared to higher-grade materials. A reference material (RM) must show sufficient homogeneity and stability with respect to chosen key parameters but provides only a report of investigation rather than a certificate. A certified reference material (CRM) is of the highest grade and comes with a certificate stating the specified values and providing information on uncertainty and traceability[88]. Additionally, there are special CRMs issued by national authorities like NIST's standard reference material (SRM), which meets additional specific criteria[89].

Table 1.2: Test material categories and their definitions according to NIST and ISO.

Category	Definition
Research grade test material (RGTM)	Exploratory materials developed for current research needs, which are subject to continuous stability measurements. The benefit of a fast batch release opposes the lower degree of characterization compared to higher-grade materials[87].
Reference material (RM)	A "material, homogeneous and stable with respect to one or more specified property values, which has been established to be for its intended use in a measurement process"[88].
Certified reference material (CRM)	A "material characterized by a metrologically valid procedure for one or more specified properties, accompanied by a reference material certificate that provides the value of the specified property, its associated uncertainty, and a statement of metrological traceability"[88].
NIST standard reference material® (SRM)	"A CRM issued by NIST that also meets additional NIST-specific certification criteria and is issued with a certificate or certificate of analysis that reports the results of its characterizations and provides information regarding the appropriate use(s) of the material"[89].

An extensive list of commercially available MNP test materials was published by Crosset-Perrotin *et al.* (2025)[90]. The list includes information on the size, shape, label, manufacturing method, and composition or additives used, and reveals four key observations: i) PS (57%) and PE (16%) are overrepresented, ii) only 25% of non-PS materials include sizes < 50 µm, which is reduced to only 13% when PE is also excluded , iii) the production methods are disclosed for only 16% of the non-PS materials (PS is usually produced *via* emulsion-polymerization), and iv) the composition (e.g. used additives or stabilizers) is often not disclosed. Furthermore, the material grade is only known for NIST materials, which are certified or traceable size standards with an intended use for instrument calibration. While there are reference and certified reference materials available for different polymer types in the micron size range, there are only certified reference materials in the submicron size range comprised of PS **(Table 1.3)**. A selection of commercially available research grade test materials ≤ 1 µm is included in **Table 1.3** to highlight ranges of polymer compositions and particle sizes currently available for research purposes.

Table 1.3: Currently available materials for MNP research. This table is not comprehensive but should provide an overview. RGTM = research grade test material; RM = reference material; CRM = certified reference material; SRM = standard reference material. Abbreviations of the listed polymer types: PE = polyethylene; PET = polyethylene terephthalate; PMMA = poly(methyl methacrylate); PP = polypropylene; PS = polystyrene; PUR = polyurethane; PVC = polyvinyl chloride; TPU = thermoplastic polyurethane.

Polymer type	Certified/Property value (sizes = D_{50})	Grade	Supplier	Form	Intended use
PE (milled, aged)	61.2 µm	RM	BAM[91]	Dry powder, fragments	Instrument calibration
PET (milled)	62.6 µm	RM			
PS (milled)	206 µm	RM			
PS	Molecular weight, intrinsic viscosity, polydispersity	CRM		Pellet	
PS spheres	0.1 µm to 30 µm	SRM	NIST[92]	Suspension No additives stated	Instrument calibration
PP	1 µm	RGTM	CD Biopar-ticles[93]	Suspension Containing 0.1% Tween®20 + 2mM NaN3 as biocide	Not specified / multi purpose
PE	50 nm to 1 µm (and larger)	RGTM			
PVC	250 nm and 400 nm	RGTM			
PMMA	25 nm to 1 µm	RGTM			
PE, PET, PP, PS, PUR, PVC, TPU	10-1000 µm	Material status unclear; Certificate of analysis available but stability not demonstrated	Micro-plastic-solution[94,95]	Suspension in EtOH or dry powders Fragments, beads or fibers RSD < 20%	Method validation

Table 1.3 also illustrates that there is scope for broadening the spectrum of test and reference materials. The overrepresentation of PS is also evident in most of the studies to date on the health impacts of plastics because of their wide commercial availability, ease of handling, and monodisperse size distribution[96]. However, none of the materials cited above have been specifically validated for an intended use as comparator materials in *in vitro* and *in vivo* biological assays. The specified intended use for most certified reference materials is as a standard for instrument calibration. Off-label usage as comparator materials in biological assays, such as toxicity tests, is widespread but not without limitations[97–100]. For example, when reference materials are used as instrument calibration standards, the addition of disclosed or undisclosed additives, such as surfactants for colloidal stability and preservatives to prevent microbial growth in aqueous preparations is common and unproblematic, since these additives are important for the intended use. In contrast, such additives can be problematic for biological assays, as they may interfere with the assay or complicate the interpretation of results[101–104]. Furthermore, it is widely accepted that PS beads are not representative of environmental plastics and the general lack of suitable PP and PET reference materials is a major reason for the current knowledge gaps[70,105]. As a response, many groups have recently reported methodologies to prepare nanoplastic test materials in-house for use in biological assays[68,71,73,106]. However, many studies focus primarily on particle size and surface charge as the defining material attributes of these systems[107–110], which are important but not the only criteria necessary for use in many types of biological assays. To overcome these shortcomings a systematic approach that considers all relevant aspects and guides researchers throughout the development phase is needed. Such a concept exists and is extensively used in the pharmaceutical industry.

Material development through a quality-by-design inspired approach

The development of new drugs is time consuming and requires enormous resources because they must meet highest quality standards to satisfy regulatory needs and ensure safe products on the market. In many industries, but particularly in the pharmaceutical industry, the concept of quality-by-design (QbD) was introduced to ensure quality of a

product already from its conceptual phase onwards[111]. The discussed shortcomings of available MNP test materials highlighted the need for a systematic strategy for the development of high-quality test materials. Therefore, a QbD inspired approach was utilized in this work program to develop MNP test materials specifically for an intended use in *in vitro* and *in vivo* biological assays **(Figure 1.2)**. The QbD strategy consists of three main pillars: i) define, ii) develop, and iii) control. In the first phase (define), a target product profile (TPP) is defined, which includes the intended use und critical quality attributes (CQAs). By pre-defining CQAs, quality is already designed into the product and the development is directed towards desired criteria. In the second phase (develop) all critical process parameters (CPPs) are identified and knowledge of their influence on product quality is acquired. This knowledge is then used in the third phase (control), in which these parameters are controlled to ensure consistent quality and low (batch-to-batch) variability[112,113]. This concept provides a useful framework that considers all relevant aspects for the development of a (certified) reference material candidate.

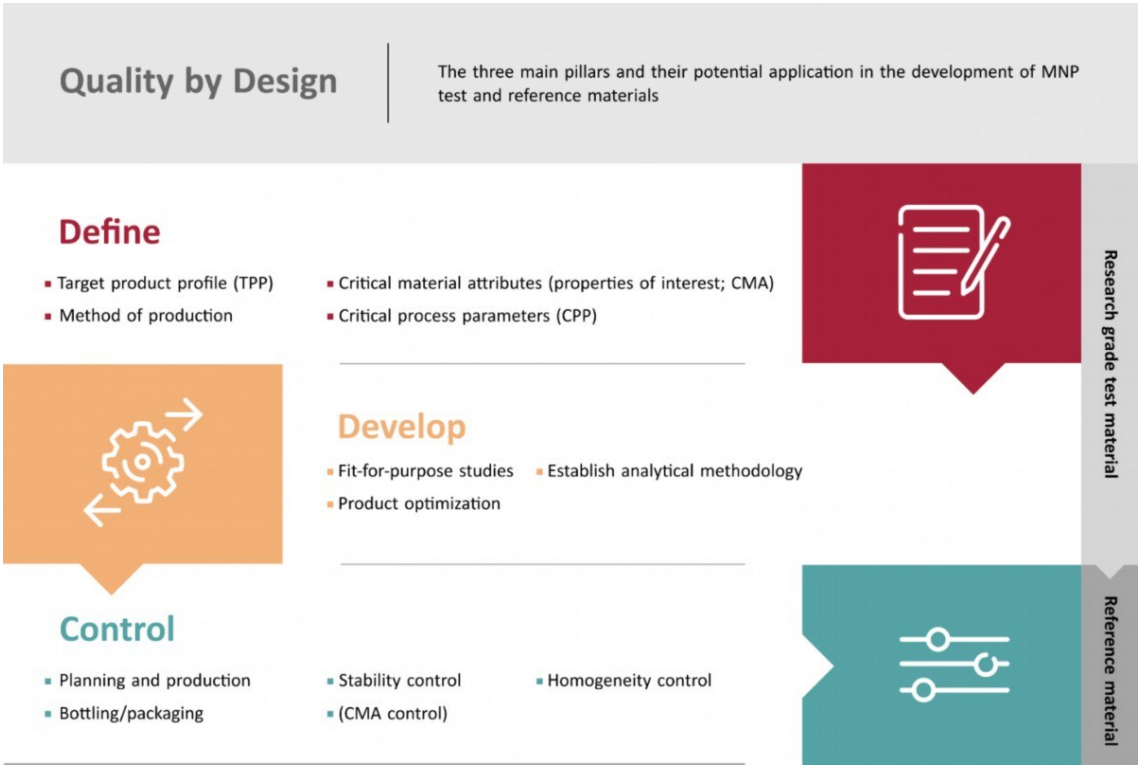

Figure 1.2: The three main pillars i) define, ii) develop, and iii) control of a QbD inspired approach for the development of MNP test and (certified) reference materials. Bullet points of each phase highlight key activities. Key activities of the certification process are defined in ISO 33401[114] and ISO 33405[115].

Available production methods for PET and PP test materials

With respect to the scope of the IMPTOX project, the literature was reviewed to identify production methods for PET and PP test materials in the micro and nano size range **(Table 1.4)**. The published methods could be categorized into four main groups: i) laser ablation, ii) ultrasonic treatment, iii) milling, and iv) dissolution with subsequent drying or nanoprecipitation. Milling and dissolution/precipitation methods were described for both materials, whereas laser ablation and ultrasonic treatment were only studied with PET. For PET, different size ranges could be produced. Methods such as ultrasonic treatment formed materials with a mixture of sizes, while milling tended to produce mainly MPs. In contrast, nanosized PET materials could be fabricated using either laser ablation, milling, or nanoprecipitation. The two primary methods to fabricate PP test materials (milling, nanoprecipitation) have been used to produce both MPs and NPs.

Table 1.4: Published production methods for PET and PP test materials. The obtained sizes are described as microplastics (MPs), nanoplastics (NPs) or a mixture of micro- and nanoplastics (MNPs), as defined in Chapter 1.1.3.

Method	Polymer	Size (MPs/NPs/MPNs)	Reference
Laser ablation	PET	NPs	Magri (2018)[116]
Ultrasonic treatment	PET	MNPs	Von der Esch (2020)[117]
		NPs	Peller (2022)[74]
Milling	PET	MPs	Seghers (2021)[70]
		NPs	Gerdes (2019)[118]
	PP	MPs	Hwang (2019)[119]
		NPs	Hildebrandt (2023)*[72]
	PET and PP	NPs	Caldwell (2020)[120]
Dissolution and drying / nanoprecipitation	PET	NPs	Rodriguez-Hernandez (2019)[121]
			Johnson (2021)[122]
			Santizo (2025)*[123]
	PP	MPs	Jeyavani (2022)[124]
			Fang (2019)[125]
		NPs	Tanaka (2021)[68]
			Lee(2022)[69]
	PET and PP	Not characterized	Achilias (2009)[126]

**Published after method development within this thesis but are included for comprehensiveness*

When analyzed in more detail, the following shortcomings were noted for many of the published production methods: i) many materials required the use of exogenous dispersion aids, which can affect toxicological assays (Seghers, Caldwell, Rodriguez-Hernandez), ii) many studies report low yields or omit to report the yields, which may limit the practicality of certain production methods for certain applications (Magri, Peller, Gerdes, Hwang, Hildebrandt, Johnson), and iii) many materials have not been sufficiently characterized (Jeyavani, Fang, Achilias).

Dispersion and dispersion aids

Johnson *et al.* (2021) utilized bovine serum albumin (BSA) as biocompatible dispersing aid[122], which is certainly an interesting approach but may not be suitable for all use cases, as will be seen in later chapters of this thesis. In contrast, the methods from

Tanaka *et al.* (2021)[68] and Lee *et al.* (2022)[69] avoided the use of surfactants and specified an intended use for toxicological testing, which made them a valuable starting point for further investigations. Dry powders are often used and provide advantages regarding microbial stability but they come with two major drawbacks. Electrostatic charging makes handling difficult and negatively influences dosing accuracy. The second reason is that drying hydrophobic polymers can lead to irreversible particle agglomerates. This becomes particularly relevant for particles < 40 µm[127], where those agglomerates can often not be redispersed into aqueous media, even when applying harsh conditions. Hence, a biocompatible liquid matrix would be preferred for MNP test and reference materials developed for biological assays.

Stability and homogeneity controls

Seghers *et al.* (2022)[70] provided a good overview of the challenges associated with dry powder handling and is one of the few studies to address dispersion issues. Furthermore, they highlighted the importance of the material's glass transition temperature (Tg) for efficient milling and defined a specific use case (measurement of irregular PET particles in water). What made this study particularly interesting was the number of samples produced (> 500 sample kits) which allowed them to investigate homogeneity and conduct an inter-laboratory comparison.

The recently described approaches from Hildebrandt *et al.* (2023)[72] and Santizo *et al.* (2025)[123] were also among the most promising for the development of reference material candidates. Hildebrandt *et al.* investigated homogeneity and stability, both crucial for gaining reference material status[72]. Santizo *et al.* pre-defined inhalation studies as the intended use case, did not use stabilizers and included also biological testing of their materials[123]. However, both papers were published after the completion of all studies of this thesis and could therefore not be considered at the beginning of this project but are listed for comprehensiveness. Although there were examples of well characterized MNPs, none of the listed (and at the time available) publications investigated batch variability, had pre-defined quality criteria, or discussed long-term stability (≥ 12 months).

Chapters scope: material production and characterization

Chapters 2 and 3 of this thesis describe the development and characterization of well-defined and characterized test materials developed specifically for use in biological assays, and more specifically *in vitro* and *in vivo* toxicology studies. **Chapter 2** describes in detail the production and isolation of micron-sized PP test materials within a narrow size range of 1-10 µm. This size range is of high interest for inhalation toxicology assessment, because particulate matter in this size range can deposit in deeper regions of the respiratory tract and are part of the already monitored particulate matter < 10 µm (PM_{10})[25], which will be discussed in the next chapter. PP test materials were produced *via* a top-down procedure and different types of comminution approaches were compared. It was interesting to note that efforts to isolate PET test materials in this size range were not successful, despite extensive investigation. This is likely due to technical limitations of the ultra-centrifugal mill used. It utilizes centrifugal forces to push the input material through a ring sieve with holes of a defined size. The ring sieve with the smallest available hole size is 80 µm, which roughly marks the lowest achievable particle size. Therefore, **Chapter 2** will focus only on a single polymer type, PP.

In **Chapter 3**, methods to produce NPs from both PET and PP using a bottom-up, i.e. nanoprecipitation, approach are described. Although milling methods could produce test materials in the submicron size range, the overall product yields were too low (unmeasurable gravimetrically) to satisfy the demand for materials by project partners. In contrast, nanoprecipitation into an anti-solvent was able to generate submicron-sized materials at a high yield, thus making this approach feasible for further studies. The characteristics of optimized nanoplastic test materials are described in **Chapter 3** [128]. Parts of this chapter have been published in Environmental Science: Nano (Royal Society of Chemistry) under "A quality-by-design inspired approach to develop PET and PP nanoplastic test materials for use in *in vitro* and *in vivo* biological assays" (DOI: 10.1039/D4EN01186D)[2].

Research questions and hypotheses: material production and characterization

Within IMPTOX, it was proposed that the two polymers, PET and PP, will be investigated. They have distinct physicochemical properties and are commonly found in environmental samples. Despite the narrow selection of only two polymer types, the requirement for different size ranges needed in different biological assays or applications broadened the spectrum of test material categories required to meet project goals. The required sizes varied from 500 µm to 0.1 µm with different particle size distribution ranges. Ultimately, two target size ranges were investigated in depth in this thesis: i) 1-10 µm, and ii) 0.1-1 µm. Among the many and diverse applications, project partners used the test materials for example to: i) investigate microbial attachment behavior (biofilm formation) with possible antibiotic resistance gene transfer; ii) evaluate adsorption of cargo, such as heavy metals, organic toxins and pollutants, allergens (single proteins and protein mixtures e.g. from ragweed pollen), or enzymes (e.g. facilitating digestion) to the MNP surface; iii) assess *in vitro* and *in vivo* toxicity; iv) track particle migration after administration in mice or after uptake by plants (an application requiring labelling of the test materials); v) validate new analytical methods; and vi) to train machine learning algorithms for particle identification and counting. These experiments were almost exclusively conducted in aqueous media and required well-dispersed samples. Pristine plastics, however, are prone to agglomeration in polar or high ionic strength environments due to their hydrophobic surface[128–130], thus the investigation of a range of suitable dispersion conditions also became nearly as important as test material production and characterization. A list of critical material and production process attributes was created to account for the diverse research applications and is presented in **Table 1.5**.

Table 1.5: Critical attributes of the production method and the produced material at different production steps.

Stage of manufacturing	Critical attributes
Production method	Standardized manufacturing procedure
	Pre-defined quality criteria
	Low inter-batch variability
Characterization of the test material	Chemical composition and integrity
	Sterility and endotoxin content
	Conforms to specified size distribution
	Shape reflects environmental samples
Handling and storage	Supplied in a non-toxic matrix
	Shows excellent chemical, physical (particularly colloidal) and microbial storage stability at high concentrations
	No use of specific surfactant additives to achieve high compatibility
	Stable as a dispersion when proteins of interest are mixed with the test materials
	Easy to handle by a variety of users with different study designs

Very early on, the use of glycerol as storage medium for MNPs was explored because of several potentially valuable properties. Glycerol is polar and miscible with water in all ratios, but is highly viscous in its pure form, which was expected to prevent irreversible agglomeration of the hydrophobic MNPs during long storage periods, even at high particle concentrations. Additionally, the absence of water and the high osmotic pressure have a preservative effect and should guarantee long shelf lives at room temperature. Furthermore, glycerol is well tolerated in biological systems due to its low toxicity profile. On the other hand, glycerol does exhibit a high hygroscopicity, which could reduce shelf-life, and at the start of the project, it was unknown which particle concentrations could be stabilized effectively. Considering the knowledge gaps and research needs, the following research questions for **Chapters 2 and 3** were identified:

- Is the chemical or physical integrity of the test materials influenced during manufacturing?
- Are the test materials free of contaminants (endotoxins, viable microorganisms, fungal spores)?
- What is the shelf life of the test materials?
- Which are critical quality parameters to ensure low variability and high inter-batch comparability?
- Are the test materials dispersible into different biologically relevant media and do they retain their original size distribution characteristics after dispersion?
- Can the materials be fluorescently labeled without leaching of the label?

These questions provided the framework for the scientific investigation and optimization of test materials conducted within this project. The overarching hypothesis investigated in the two chapters was that the use of glycerol as a liquid storage medium would enable the production of PET and PP test materials which could be packaged in multiple-dose units at high particle mass concentrations. The product would be stable in terms of size following dispersion and microbial quality for at least one year.

1.3 Part III – Background to sea spray aerosol as a source of enhanced exposure

Within IMPTOX, our group was also responsible for a second task, which was to collect environmentally relevant air samples and quantify the amount of respirable MNPs within these samples, using innovative aerosol sampling methods and state-of-the-art analytical techniques for plastic quantification in air matrices. The primary study question described in **Chapter 4** investigated whether sea spray aerosols (SSA) could represent a source of enhanced exposure to inhaled MNPs.

It is known that living near the ocean positively influences human health as it encourages physical activity and can reduce stress[131]. Green or blue environments, like the ocean, can improve the conditions of patients suffering from pulmonary diseases[132]. This

knowledge is utilized in the so-called climatotherapy, where patients are advised to spend extended periods at high altitude[133] or near the marine environment[134]. It is likely that cleaner air in these areas is one of the main drivers for the observed health improvements, although other factors are also discussed[135]. Especially in coastal regions, aerosols ejected from the sea (sea spray aerosols, SSA) contribute significantly to the total aerosol mass and their number based size distribution shows that the majority is <1 µm, thus, in the inhalable and respirable size range[136]. This classification is based on the aerodynamic equivalent Harrison diameter of a particulate, which considers its shape and density besides its size and therefore describes the possible total and regional deposition pattern of airborne particles into different regions of the lung[137]. In a report on dietary and inhalation exposure to MNPs, the WHO defines the inhalable fraction as particles with an aerodynamic diameter of > 2.5-10 µm but can include particles up to 100 µm (coarse fraction). The respirable fraction is referred to as particles with and aerodynamic diameter < 2.5 µm (fine fraction)[25].

The composition of SSA is complex and can include various organic compounds. The organic composition of SSA is greatly influenced by the composition of the sea surface micro layer, a thin layer on the sea surface. Hydrophobic compounds (e.g. anthropogenic pollutants), heavy metals, surfactants, and other organic compounds are known to enrich on the sea surface, forming the sea surface micro layer[138]. The total organic mass fraction can make up to 23% of submicron aerosols[139]. A study from Asselman *et al.* (2019) argues that biologically active compounds produced by various microorganisms can be part of SSA. When inhaled in environmentally relevant concentrations, some of these compounds are known for their interaction with different cell signaling pathways such as mTOR[140]. The inhibition of this pathway promotes anti-inflammatory effects and could contribute to the overall positive health effect[141]. Despite such health promoting effects, generally efforts are made to reduce the particulate burden in air[142]. Airborne particulate matter < 10 µm (PM_{10}) and < 2.5 µm ($PM_{2.5}$) are complex mixtures of various sources and used as a measure for air quality as they are associated with both acute and long-term negative health effects. Especially traffic related aerosols are of concern but there are other understudied pollutants emerging[143].

Current knowledge gaps - Aerosol exposure assessment

In the past decade, several reports about MNPs as air contaminants have been published, affecting both urban and remote rural areas[144,145]. After Wright and Kelly postulated that MNPs could be a component of SSA, Allen *et al*. (2020) showed that this was indeed true for MPs >10 µm, and that the sea is a source of MNPs in the air[62,64]. Using µ-FTIR, they provided a quantitative demonstration of the presence of MNPs in SSA sampled from the French Atlantic coast. Extrapolations based on their study results suggest that potentially 136,000 tons of MNPs annually could be released from the marine environment into the online air by sea spray. In their study, 18 m^3 air per sample were actively pumped through a solid filter system and an average of 3 MPs (>10 µm diameter)/m^3 air with an estimated mass range of 0.024-0.159 µg/m^3 air was found, depending on weather conditions[62].

Interestingly, a more recent study focusing on the presence of MNPs in SSA contradicted the claims put forward by Allen et al (2020). Lambert *et al*. (2024) further studied the aerosolization process of MNPs dispersed in sea water and estimated the human exposure to MPs *via* inhalation. The number of captured MPs after aerosolization was extrapolated to the number of particles inhaled per day spent on the coast based on reports on environmental MP and SSA concentrations and intake. Their calculations showed that 6.67×10^{-6} to 1.05×10^{-4}particles with a size between 1-5 µm will be inhaled per day *via* SSA and that even in the year 2100 – following the business-as-usual scenario on plastic production – the number of inhaled MPs is far below 1 particle per day. Thus, they concluded that human exposure to MPs through SSA is negligible compared to other sources like urban areas (1.5 particles per m^3) or indoor air (60 particles per m^3). However, those calculations were based on experiments in a controlled environment and do not consider NPs due to the existing knowledge gaps on their behavior and environmental concentration[146]. Thus, there is a strong need to validate these findings through field sampling campaigns.

Another multi-national study from Nava *et al*. (2023) found that lakes, too, are a reservoir for plastic debris and need to be considered in future studies[85]. Indeed, May *et al*. (2023) showed that freshwater lakes contribute to the total inland PM through generation of

lake spray aerosols[86]. However, the methodological limitation of the above-mentioned studies was that μ-FTIR was the primary method used to detect MPs. FTIR spectroscopy is known to resolution issues with particles smaller than 10 μm in size, and while a spatial resolution down to 3 μm can be achieved with μ-FTIR depending on the wavelength used, the effective special resolution for routine measurements is somewhat larger[147]. Therefore, in most cases, sizes > 5 μm were reported (average 20 μm ± 13 μm).

In terms of the potential for adverse respiratory health impacts, particle size matters. Particles with an aerodynamic diameter of 5-10 μm will primarily deposit in the extrathoracic airways, while particles with aerodynamic diameters < 5 μm can enter the deeper lung and are therefore very relevant for assessing the impact on human respiratory health[148]. Once in the atmosphere, MNPs can travel long distances in a short time, compared to aquatic transport mechanisms. Low densities and small sizes of plastic debris influence their mobility[20]. Despite the knowledge about these mechanisms, the health implications are unclear[149]. One study reported finding MPs in the lung but again used μ-FTIR as the measurement technique, which has technical and methodological limitations, thus, the results of this study must be interpreted with care[83].

Raman spectroscopy is another commonly used technique for detecting MNPs. Caldwell *et al.* (2024) achieved comparably low limits of detection (LOD) with Raman for PS and PET NPs (5 and 0.625 μg/mL, respectively) that were spiked into environmental water samples. However, the LOD strongly depended on the polymer type among other factors like particle size or the environmental matrix. While this was a promising approach for PS and PET, aliphatic polymers like PE and PP provided a challenge. PE NPs could only be detected in one out of four different environmental water samples, whereas PP NPs could not be detected in any of the samples spiked[150]. In an earlier study, Caldwell *et al.* (2023) used surface-enhanced Raman scattering (SERS) spectroscopy for detecting NPs in a simple Milli-Q water matrix. With this approach they reached a LOD in the ng region (625 ng/mL) for PS NPs. However, highlighting again differences between polymer types and particle sizes[151]. It shows that analytical tools suitable for the detection and identification of respirable sized MNPs comprised of different polymers in both environmental and

biological samples are still lacking,[149,152–154] leaving significant knowledge gaps vital for exposure assessment.

One way to overcome methodological size limitations of the described studies is to use a combination of an aerosol sampling device which first separates aerosols according to their aerodynamic diameter (e.g. an impactor or impinger) with a mass-based analytical method to measure the mass of the size fractions, such as thermal extraction-desorption gas chromatography mass spectrometry (TED-GC-MS). Mass-based methodologies are often more sensitive and robust compared to number-based detection methods, provided that the amount of collected mass is above the detection limit[155]. This approach was recently demonstrated elegantly by Rindelaub and Miskelly (2025), who used a standard impactor to collect $PM_{2.5}$ and PM_{10} from 100 m^3 air in different indoor laboratory environments. Pyrolysis GC-MS was then used to quantify the plastic and additive content in these samples. They reported mean total plastic concentrations of 0.51 µg/m^3 ($PM_{2.5}$ samples) and 1.14 µg/m^3 (PM_{10} samples) from n = 10 samples. Polycarbonate, polyvinylchloride, and polyethylene had the highest airborne concentrations in the inhalable fraction of air[156]. Importantly, this study convincingly demonstrated that the amounts of plastics detected in the active sampling campaign were significantly increased compared to amounts found in procedural controls, marking this study as a positive example in the literature, since several studies in the field omit the appropriate controls and may be prone to reporting artifacts arising through sample contamination.

Chapter scope: sea spray aerosols as a source of enhanced exposure

In a similar strategy to Rindelaub and Miskelly (2025), **Chapter 4** describes a methodological approach whereby a glass liquid impinger (GLI) was used as sampling device for capturing MNPs from air and separating the aerosols according to aerodynamic diameter into two size fractions representing aerosols that deposit in the upper respiratory tract (> 6.4 µm) and aerosols that deposit in the lower respiratory tract (<6.4 µm; **Figure 1.3**). Aerosol samples collected in the device were then analyzed by collaborators using TED-GC-MS as a mass-based analytical technique.

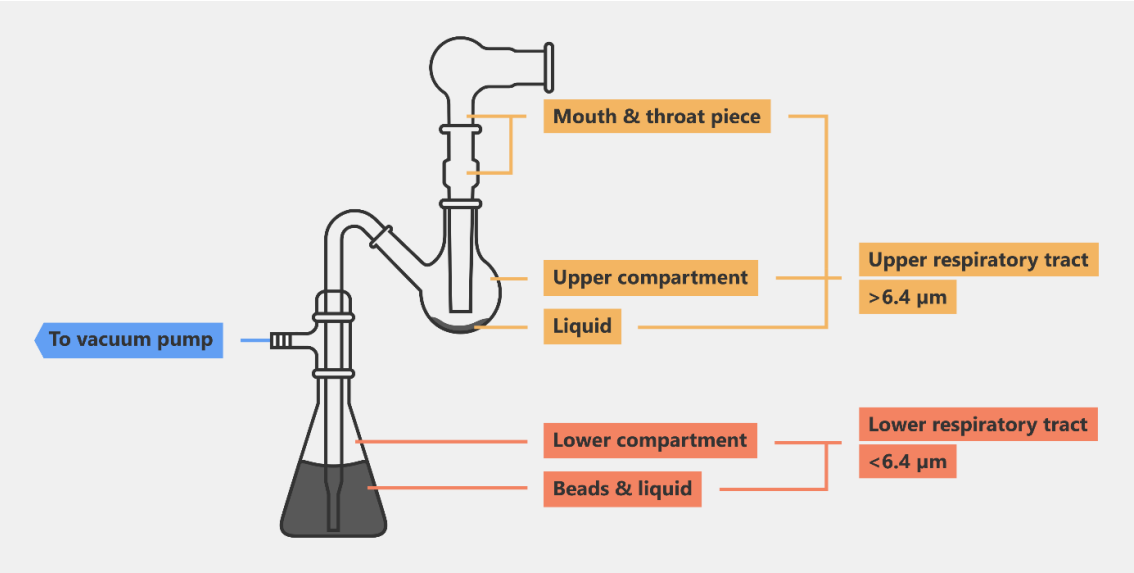

Figure 1.3: Scheme of the glass liquid impinger (GLI). Samples from the mouth and throat piece (MTP) and upper compartment (UC) are combined and separated from samples from the lower compartment (LC).

Since the GLI was developed for characterization of pharmaceutical aerosols and has not been used to analyze environmental aerosols, validation studies were performed prior to use of the instrument in two field studies. Fluorescent labeling of the NP test materials described in **Chapter 3** was explored for this purpose, as this is a commonly used strategy to simplify their detection and quantification and validate experimental and analytical approaches. A method for the incorporation of a large molecular weight polymeric dye with favorable optical properties like a large Stokes' shift (low background) and commonly used excitation and emission wavelengths was therefore investigated.

For validation, first the collection efficiency of the GLI and the recovery rate of washing process were evaluated. In a second step, the deposition pattern and recovery of nebulized fluorescently labeled NPs was investigated. Finally, a mixture of unlabeled NPs was nebulized into the GLI and the recovered mass was determined by TED-GC-MS to assess the limit of detection of the entire process under controlled conditions. The validated method was then used to sample air at two different rural locations. One field study was carried out in Austria at the Neusiedler Lake (lakeside) and served as baseline due to expected low MNPs concentrations. The second sampling site was on Brač island,

Croatia (seaside), where higher concentrations were expected. A manuscript with parts of this chapter is currently under preparation.

Research questions and hypotheses: SSAs as a source of enhanced exposure

The knowledge gaps on environmentally relevant concentrations of MNPs in air, more specifically in seaside and lakeside aerosols, provided the starting point for the second objective of this thesis. The foundation of **Chapter 4** are three main research questions:

- Is the glass liquid impinger a suitable sampling device to capture MNPs from air?
- Are the concentrations of inhalable MNPs at rural lakeside and seaside locations above the methods limit of detection?
- Is the concentration of MNPs at the seaside location higher than at the lakeside location?

It was hypothesized that there would not be detectable quantities of MNPs in air samples collected near the Neusiedler Lake because it is located in a rural and partly protected area. A Greenpeace report from 2023 on plastic contamination of Austrian lakes showed a low plastic abundance in the Neusiedler Lake samples[157]. In contrast, it has been shown that the Adriatic Sea is highly affected by plastic pollution. Sea currents drag plastic litter from the Mediterranean Sea into the Adriatic region, where it accumulates. Intake through rivers, heavy marine traffic, agriculture, fishing and high touristic activity in this area are further potential sources. Thus, it is no surprise that plastic debris was already detected on beaches, surface waters, sediments, and various organisms like fish or mussels[158]. However, studies that investigate a possible connection between plastic pollution in seawater and MNP content in seaside aerosols are still lacking. This was the rationale for the second hypothesis, that the aerosol samples from the Adriatic coastline show a higher abundance of MNPs than the lakeside aerosols.

Chapter 2

Small polypropylene microplastics: Method development to produce 1-10 μM test materials for study in biological assays

2 Test material development – Polypropylene microplastics

Parts of this chapter were first published on the 18th of August 2025 in the Journal of Hazardous Materials (https://doi.org/10.1016/j.jhazmat.2025.139595) and reproduced with permission from Elsevier[1].

2.1 Introduction and background

The goal was to produce PP MPs that reflect environmental samples with a size relevant for the ingestion and inhalation route. A very promising example for the development of a MP reference material was described by Seghers *et al*. (2022)[70], who described a standard for instrument calibration/validation in routine analysis of large volume aqueous samples, such as drinking water. This particular material contains a low, environmentally relevant concentration of PET MPs, which were embedded in a solid sodium chloride matrix *via* lyophilization. For this application, a sample kit was designed which included the lyophilizate plus a rinsing solution containing a Triton X-100 surfactant and a glass bottle filled with 950 mL pure water. To use the standard, the lyophilizate should be first dispersed in the surfactant fluid before transferring it into the final large-volume container. The production process could be scaled up to a batch size of 500 samples per batch with a three-day processing time. The batch-to-batch variability was fit-for-purpose when using the PET MPs as a reference material for instrument calibration when detecting plastics in water samples. This approach was reported to be user-friendly and reproducible in an interlaboratory comparison[70].

Employing a similar philosophy, we were interested in developing benchmark materials for use across a wide range of *in vitro* and *in vivo* toxicity assays. However, instead of choosing a solid storage matrix as described above, we explored the use of glycerol as a liquid storage medium and dispersant aid, which has several advantages for both *in vitro* and *in vivo* toxicology study designs. These include: i) colloidal stability in the storage medium at high plastics concentrations (up to 40 mg MPs per gram glycerol) without the need for exogenous surfactants in the storage vials, ii) microbial stability at ambient room temperature due to the non-aqueous matrix and preservative effects of glycerol, iii) biocompatibility with cells, tissues and organisms, and iv) reproducible dilution into a wide

variety of other dispersants. For the definition of all relevant parameters, a target product profile (TPP) was defined at the beginning of the development process **(see Chapter 0)**. Subsequently, critical quality attributes (CQAs) and desired quality attributes (DQAs) were identified, along with target values and acceptable ranges to ensure that the final product is fit for the intended purpose.

Definition of the target product profile and the critical and desired quality attributes

The development of the TPP was based on the following proposed applications for this test material: i) administration to animals in *in vivo* experiments, i) investigation of protein binding affinity and protein corona formation, and iii) *in vitro* particle-cell interaction studies. To reduce complexity, the decision was taken to use (additive free) food grade PP granules and produce test materials with characteristics similar to the pristine plastic (without ageing, surface functionalization, fluorescent labels). Since irregular shaped fragments were reported as one of the dominating MP types in human lung tissue samples[83,159,160], air[145,161], or water samples[162], this was defined as the favored particle shape. The target particle size range was defined as 1-10 µm, to include particles in the inhalable (< 10 µm) and respirable (< 4 µm) size range and comply with established air quality guidelines **(see Chapter 1.3)**. Furthermore, a review by Mortensen *et al*. (2021) on unintentionally ingested MNPs demonstrated that MPs from 1-5 µm represented the highest abundance in drinking water and other beverages[163], highlighting the relevancy for this exposure route. Particles < 1 µm were excluded since NP test materials were developed separately **(see Chapter 3)**. Final considerations of the TPP concerned the purity, final form, packaging, dispersibility, and stability of the material. No exogenous dispersing aids, proteins, or stabilizers should be added, so that users can choose from a wider range of bespoke dispersing aids that do not interfere with their assay of choice. Sterility and an acceptably low endotoxin content must be demonstrated, especially for use in *in vitro* and *in vivo* assays. Literature in this regard exists for nanomaterials but is equally relevant for MNPs[164–166]. A biocompatible storage matrix should be used to ensure dosing accuracy and easy handling. Thus, the matrix must be miscible with aqueous media and able to promote full redispersion of the MPs in aqueous test liquids. Furthermore, the final product should

contain a high MP concentration to enable flexible dosing, preferably in a multi-dose container. Finally, the chosen matrix and packaging must ensure the physical and microbial stability of the MPs over the shelf-life and in-use life span of at least one year. From this TPP, critical and desired quality attributes were extracted **(Table 2.1)** and include the specifications for the desired size range, limits for viable microorganisms, endotoxin content, batch-to-batch reproducibility, shelf-life stability, quality control (QC) vs. biorelevant media (BRM) dispersibility, and yield.

Table 2.1: Critical quality attributes (CQAs) and desired quality attributes (DQAs) of a PP test material 1-10 µm in size for use in in vitro and in vivo studies as well as protein corona investigations.

CQAs	Specification	Recommended methods/comments
Must not contain viable microorganisms and show a sufficiently low endotoxin content	Viable microorganisms: 0 colony forming units (CFU/mL) Endotoxins: < 0.1 EU/mL	No microbial growth on LB and Sabouraud agar; Endotoxin level according to LAL-assay; Required for parenteral administration in animal studies, desired for *in vitro* studies
Must be sufficiently concentrated to enable dilution to relevant test concentrations with a biocompatible osmolarity	*In vivo:* 300–312 mOsmol *In vitro:* < 400 mOsmol	Measured *via* freezing point depression; Required for animal and cell studies
Must not contain exogenous dispersing agents, such as Tween® surfactants or serum albumin	No addition of interfering dispersing aids	Required for protein corona studies
Must show sufficiently high batch-to-batch reproducibility within the 1-10 µm size range	RSD of all three percentiles (D_{10}, D_{50}, D_{90}) < 25%	PSD measured *via* laser diffraction; Required to assure comparability
Must be fully dispersible in various biorelevant media (QC vs. BRM dispersion)	≥ 90% of the test material is < 10 µm in size	PSD measured *via* laser diffraction; Reduction of the fraction < 10 µm compared to the QC dispersion would indicate agglomeration
DQAs	**Specification**	**Recommended methods/comments**
Shape should resemble real world samples	Irregularly shaped fragments	Top-down procedures mimic environmental comminution processes best
Should have a high particle concentration per unit product	Dispersions: 40 mg plastics per g glycerol matrix are desired	This allows flexible planning of dose escalation studies
Should be packaged in a "multi-dose" container	Resealable glass container	To avoid contamination with other polymer types; Reduces the need for multiple single-unit containers
Should maintain chemical, physical and microbial stability over shelf-life	Over at least one year shelf life and in-use life span	Chemical stability: FTIR Physical stability: PSD Microbial stability: sterility test
Should have an acceptable product yield and manufacturing time per batch	Yield per batch: > 10% Manufacturing time: < 2 days	Lower yields and longer manufacturing times could be acceptable depending on the concentration needed for specific assays

Study design and hypotheses

Three different mills (ball mill, ultra-centrifugal mill, and knife mill) were tested, and the resulting particle shape, size distribution, and yield were assessed. It was hypothesized, that top-down procedures would generate irregular shaped particles in the desired size range of 1-10 µm. In preliminary experiments, the ultra-centrifugal mill and the ball mill showed major flaws that excluded them from further investigations. The comparably low glass transition temperature (Tg) of PP (-20 to 0°C)[167] caused melting of the PP granules when introduced into the ultra-centrifugal mill, even when pre-treated with dry ice or liquid nitrogen. When using the ball mill with stainless steel accessories, the generated powder was visually contaminated with metal components from the milling balls, which has also been described in the literature[106]. Efforts to avoid this contamination were not successful because shorter grinding cycles or a reduced total milling time did not yield particles in the desired size range. This left the knife mill as the method of choice for in-depth investigation. Preliminary experiments showed no visual signs of metal contamination, the particles were irregularly shaped fragments, and a sieve cut with a 38 µm stainless steel sieve showed promising yields for the fraction < 38 µm. Thus, a wet milling procedure in ethanol was developed that consisted of the following main steps: Pre-treatment of the starting material, milling, size fractionation, and medium exchange to glycerol.

Pre-treatment

PP was provided as oval pellets (~4x3x3 mm) but milling them directly did not result in sufficiently high yields of the fraction < 38 µm. It was hypothesized that the yield could be increased through pre-treatment of the pellets by i) increasing their initial size *via* molding, and ii) freezing the starting material to increase its brittleness. The influence of the pre-treatment on the chemical integrity was evaluated *via* ATR-FTIR after applying different melting times.

Milling

It was hypothesized that the milling efficiency could be increased by keeping the temperature below the Tg of PP. To avoid overheating, grinding was conducted in cycles and their duration, intermediate pauses, grinding speeds, and grinding accessories to reduce the volume of the grinding container were explored.

Size fractionation

To obtain the desired size fraction, multiple fractionation methods were combined. Sieving was the first step for separating particles with high throughput that were too large to pass a 38 µm stainless steel sieve. Particles below that threshold were then subjected to filtration for removing plastics above 10 µm and below 1 µm. In a final step, the obtained MPs were centrifuged to fine-tune the particle size distribution (PSD). It was hypothesized that more sieving cycles would increase the overall yield, and a multistep centrifugation procedure would reduce the spread of the desired MP fraction. Thus, sieving cycles, and centrifugation parameters such as speed, time, and cycles were investigated.

Medium exchange to glycerol

Re-dispersibility of small MPs into aqueous media is a challenge, especially for highly hydrophobic materials like PP. Without dispersion aids, those particles tend to agglomerate irreversibly in dry powder form and aqueous suspension. Thus, glycerol as liquid and biocompatible matrix for the produced MPs was assessed. Five batches of PP MPs were produced employing the optimized production procedure to test the hypothesis that the obtained glycerol stocks fulfill the quality attributes described in the TPP. The conducted study characterized relevant parameters including the PSD profile at various production steps and after dispersion in aqueous media, sterility, and stability after long-time storage.

2.2 Materials and methods

Materials

Food grade PP (CAS: 9003-07-0) pellets were kindly provided by PlasticsEurope. Ethanol (96%, v/v) was sourced from Brenntag (Brenntag Austria GmbH, Vienna, Austria), and glycerol (≥ 99%, anhydrous for synthesis, 8.18709) and Tween®80 (polysorbate 80, P1754) from Sigma-Aldrich (Merck KGaA, Darmstadt, Germany). Filters were purchased from Whatman (0.8 µm, membrane filters, WHA7408004, Whatman plc, Maidstone, UK) and Merck Millipore (10 µm, nylon mesh, NY1004700, Merck Millipore KGaA, Billerica, USA). BSA (Bovine serum albumin, Fraction V, 1ET6.3) was provided by Carl Roth (Carl Roth GmbH + Co. KG, Karlsruhe, Germany) and DMEM/F-12 (Dulbecco's Modified Eagle Medium/Nutrient Mixture F-12, [+] L-Glutamine, no phenol red, 21041-025) from Fisher Scientific (Fisher Scientific GmbH, Schwerte, Germany)

Production method

Pre-treatment

Eight pellets (~200 mg) were transferred into each chamber of a silicone mold (10x10x10 mm) and melted into cuboids (10x10x3 mm) at 180°C for 1 hour. The resulting 0.3 cm thin cuboids were frozen (-70°C, minimum of 12 h) to increase brittleness.

Milling

Frozen PP cuboids (20 ± 2 g) were subsequently milled in ethanol (96%, v/v, 40 mL) with a knife mill (GM200, Retsch GmbH, Haan, Germany) using the cryogenic stainless-steel accessories (Cat. No.: 22.354.0005). The material was cooled with dry ice, which was occasionally replenished. The optimized milling procedure is shown in **Table 2.2**. To avoid rapid heating, the protocol consisted of multiple 30 sec milling cycles followed by a 3-5 min pause. The first cycle was carried out with the "hit-mode", where the knives rotate backwards and bluntly comminute the pre-treated PP. All further cycles were carried out with the "cut-mode" while increasing the rotation speed (revolutions per minute; rpm). After the third cycle, a volume reduction lid was introduced which increased the contact time of the material with the knives and led to a higher grinding efficiency. The last cycle consisted

of six runs at high speed to further increase the yield of the fine fraction and the obtained PP suspension was then size fractionated.

Table 2.2: Steps of the optimized milling protocol.

Mode	RPM	Duration	Pause	Repetitions
Hit	4,000	30 sec	3-5 min	1
Cut	5,000	30 sec	3-5 min	1
- - Introducing the volume reduction lid - -				
Cut	5,000	30 sec	3-5 min	1
Cut	6,500	30 sec	3-5 min	1
Cut	7,500	30 sec	3-5 min	1
Cut	8,500	30 sec	3-5 min	1
Cut	10,000	30 sec	3-5 min	5

Optimized size fractionation method

A stack of stainless-steel mesh sieves (woven wire mesh, Ø 200 mm, 50 mm height, Retsch GmbH, Haan, Germany) with the following mesh sizes: 800 µm, 500 µm, 180 µm, 63 µm and 38 µm were used for wet sieving the ethanolic PP suspension. The sieve stack was agitated with a vibratory sieve shaker (Rhewum GmbH, Remscheid, Germany) for 5 min with intensity and interval set to 7. All fractions > 38 µm were collected separately, dried and stored in glass beakers for later use. The smallest fraction passing the 38 µm sieve was used for further processing. For the isolation of PP particles 1-10 µm from the fraction < 38 µm, a two-step vacuum filtration followed by centrifugal fractionation was employed. Filters were placed on a glass filter holder system from VWR (511-0666, VWR International LLC., Radnor, USA) and the first filtration step required passing the < 38 µm suspension through a 10 µm nylon mesh filter. The filtrate (< 10 µm) was then filtered through a 0.8 µm nylon membrane filter and the residues from the 0.8 µm filter were resuspended in ethanol (20 mL). The obtained suspension was then split into two equal volumes and transferred into two clean glass centrifugation tubes (Pyrex, 11.5 mL). The suspensions were homogenized using vortex and sonication (1 min each) and immediately centrifuged, employing a benchtop centrifuge (Rotanta 460 R, Hettich Instruments, Beverly, USA) equipped with a swinging

bucket rotor (5699-R, r = 196 mm). Suspensions were centrifuged twice at 232 × g (1030 rpm, 24°C, 1 min) to sediment particles/agglomerates > 10 µm. After each centrifugation run, the supernatant was transferred into two clean tubes and ethanol was added to balance the weight. Subsequently particles < 1 µm were removed by two further centrifugation cycles using 1459 × g (2580 rpm, 24°C, 10 min). After each centrifugation, the supernatant was removed (and used to characterize the submicron fraction) and the tubes were refilled with ethanol. Following the second run, the sedimented particle pellets were collected, redispersed in ethanol to a defined volume and stored in a glass vial for later characterization and use.

Transfer to glycerol

Glycerol was pre-heated to 60°C in a water bath. Separately, the PP suspension in ethanol (1 mL) was fully dispersed by alternate cycles of vortexing and sonication (1 min each). The mass of heated glycerol required for the desired final concentration (typically 1 mg PP / g glycerol) was added to a round bottom flask followed by addition of the PP suspension in ethanol. The mixture was immediately mixed *via* alternate cycles of vortexing and sonication (1 min each). A rotary evaporator (water bath at 60°C) was then used to gradually remove the ethanol *via* incremental decreases in pressure (increments of approx. 50 mbar over 1 h until 40 mbar was reached). The flask was weighed in regular intervals and the process was considered complete when the weight of the flask reached the theoretical weight of the empty flask, PP, and glycerol combined.

Carbonyl index value

Spectra were recorded with the Nicolet iN10 MX Microscope (Thermo Fisher Scientific Inc., Waltham, USA) using the ATR module and DTGS detector with 64 scans and a resolution of 8 cm^{-1} in the range from 4000 to 650 cm^{-1}. The Omnic Picta and Omnic 7 software were used for recording and processing (baseline correction and peak normalization), respectively. The carbonyl index (CI) value was determined through dividing the area of the peak of interest ($A_{C=O}$) from 1820-1650 cm^{-1} by the area of the reference peak ($A_{ref.}$) from 1500-1420 cm^{-1} **(Equation 2.1)** according to Almond *et al.* (2020)[168].

Equation 2.1: Determination of the carbonyl index (CI) value.

$$CI = \frac{A_{C=O}}{A_{ref.}} \quad \textbf{(2.1)}$$

Product yield

The weight of the ethanolic PP MP suspension was first determined gravimetrically ($m_{susp.}$). After homogenization of the suspension *via* bath sonication, an aliquot (1 g) was transferred into an Eppendorf tube (2 mL) and the ethanol was removed under reduced pressure with a rotary evaporator. The weight of the PP microplastics (m_{MP}) was determined and the absolute yield (mg) was calculated according to **Equation 2.2**.

Equation 2.2: Determination of the absolute yield (mg) of PP MPs.

$$Yield\ (mg) = m_{susp.} \times m_{MP} \quad \textbf{(2.2)}$$

The yield (%) of the desired fraction was calculated **(Equation 2.3)** relative to the used mass of PP pellets (m_{PP}).

Equation 2.3: Determination of the relative yield (%) of PP MPs.

$$Yield\ (\%) = \frac{m_{susp.} \times m_{MP} \times 100}{m_{PP}} \quad \textbf{(2.3)}$$

Dispersion and analysis of particle size distribution: Quality control (QC)

PSDs were measured *via* laser diffraction employing a Mastersizer 3000 (Malvern Panalytical, Malvern, United Kingdom). To achieve full dispersion, glycerol suspensions were first heated to 60°C and subjected to three alternating cycles of vortexing and sonication (1 min each). Ethanolic suspensions were not heated but also underwent three vortex/sonication cycles as described above. Subsequently, 0.2 mL dispersion containing ~200 µg PP were dispersed in 0.2 mL Tween®80 (5%, w/w) solution (1:1) to promote full surface coverage of the PP by the surfactant during the process transfer to water. The mixture was sonicated for 5 min followed by dilution of 50-400 µL suspension into 6 mL water containing 0.33% Tween®80, which typically achieved the recommended obscuration

level (optical concentration) of 5-10% in the Mastersizer. Instrument settings included: Particle shape: “non-spherical”, Mie-Theory was applied (refractive index of PP: 1.49[169], absorption of PP: 0.01, refractive index of water: 1.33), and stirring speed: 1000 rpm. The background was measured with 6 mL of distilled water containing 0.33% Tween®80.

Dispersion and analysis of particle size distribution: Biorelevant media (BRM)

Similarly to the QC dispersion protocol, the glycerol stock was first homogenized by heating it to 60°C and alternately vortex/sonicate for 1 min each in three cycles. In contrast to the QC protocol, 0.2 mL of a filtered BSA solution (10%, w/w) was used to disperse 0.2 mL of the PP microplastic glycerol stock (1:1). The mixture was gently shaken to avoid foaming and subsequently sonicated for 30 s. This ensured that the glycerol was fully mixed with the BSA solution. Finally, the obtained suspension was sonicated for 5 min directly before the final dilution and size distribution measurement in DMEM/F-12 without FBS (to avoid air bubble formation) by laser diffraction. Instrument settings: Particle shape: “non-spherical”, Mie-Theory was applied (refractive index of PP: 1.49[169], absorption of PP: 0.01, refractive index of DMEM: 1.34[170]), and stirring speed: 1000 rpm. The background was measured with 6 mL DMEM/F-12.

Determination of viable microorganisms

Test material production was conducted under non-aseptic conditions, thus, 14 batches of 1-10 µm PP (eleven dry powders obtained after filtration and three dispersed in glycerol) were assessed for viable microorganisms according to the pour plate method described by the FDA[171] and the Ph.Eur.[172]. Briefly, the samples (1 mg) were dispersed *via* bath sonication (1 min) in complete cell culture medium (1 mL, cDMEM, DMEM+10% FBS + penicillin/streptomycin) to obtain 1 mg/mL sample stocks. Subsequently, the stocks were further diluted with cDMEM to the final test concentrations of 10, 50 and 200 µg/mL. MP samples were tested in Lysogeny broth (LB) agar for evaluation of aerobic bacteria and Sabouraud 4% glucose agar for fungi detection. Dispersions (1 mL) were added to the agar plates and incubated for 3 days at 30°C (LB plates) or 7 days at 20°C (Sabouraud plates).

The number of colony forming units (CFU) were counted and reported as CFU/mL. *Escherichia coli* and *Saccaromyces cerevisiae* were used as positive controls employing 10^{-9} and 10^{-5} serial dilutions, respectively.

Storage stability

The MPs were stored in a glycerol matrix at ambient room temperature in sealed HPLC glass vials (1.5 mL). The vials were kept in a cardboard box to avoid light exposure. Determination of the PSD and viable microorganisms were assessed directly after production (0 months) and after 2.5 years (32 months) of storage according to **Chapters 0and 0**, respectively. Sample vials remained sealed until the day of measurement.

Osmolarity

The freezing point depression of glycerol serial dilutions in cDMEM and saline solution (0.9% NaCl) ranging from 6.2 to 0.05% (w/v) glycerol was measured using a K-7400S Semi-Micro Osmometer (Knauer Wissenschaftliche Geräte GmbH, Berlin, Germany) and the average osmolarity values (mOsmol) were calculated from n = 3 replicates.

Data visualization and statistics

Raw data from LD measurements, was exported with Malvern's Mastersizer software and plotted with Python (3.11.0) using the Matplotlib library (3.9.2). Statistical tests were performed with a CI of 95% using the SciPy (1.14.1), NumPy (2.1.1), and Pandas (2.2.3) libraries for Python (3.11.0).

2.3 Results and discussion

Statement of transparency

FTIR spectra of heat-treated PP (0 h, 1 h, 1.5 h, 3h and 5 h) were provided by our collaborator Boban Anđelković from the University of Belgrade. Data on milling efficiency was obtained with help from Selena Margherita Prantner for her Bachelor's thesis

performed under my supervision, and Dr. Itziar Otazo Aseguinolaza. Data regarding the sieving and centrifugation process was generated with help from Markus Falkenstätter during his Master's project and Lauren Saveyn during her Bachelor's project, both performed under my supervision. SEM images were kindly provided by Dipl.-Ing. (FH) Christiane Weimann from the Federal Institute for Materials Research and Testing in Berlin (BAM). Microbial contamination was tested by my colleague, My Vanessa Ngyuen Hoang.

Optimization efforts for the production of pristine PP microplastics 1-10 µm

Pre-treatment

Through pre-treatment of PP granules (i.e. melting into larger cuboids), it was expected to improve the milling efficiency as a result of the geometry of both the material and the knife mill, i.e. less material accumulates underneath the rotating knives which are set about 5 mm above the bottom of the milling container. However, PP can degrade (e.g. through oxidation) also during comparably short heating times. Thus, the effect of the pre-treatment (molding process) on the material chemistry and mass yield of the desired fraction < 38 µm were assessed. Polyolefins like PP show no features in the carbonyl region (~1700 cm^{-1}) of an FTIR spectrum in their native state. However, heating (e.g. during the molding process) can introduce a carbonyl peak that can be used to calculate the CI value, which is indicative of degradation. Thus, FTIR spectra of heat-treated PP (0 h, 1 h, 1.5 h, 3h and 5 h) were recorded, and CI values were calculated. **Figure 2.1** shows the relationship between molding time and the CI value. Even 1 h at 180°C increased the CI value slightly from 0.02 (0 h) to 0.06 (1 h). However, this was considered acceptable compared to the increase seen in the other samples (0.29, 2.21, 3.86 for 1.5 h, 3 h, and 5 h, respectively). Lower temperatures or shorter heating times were not assessed as they did not liquify the material enough to be molded.

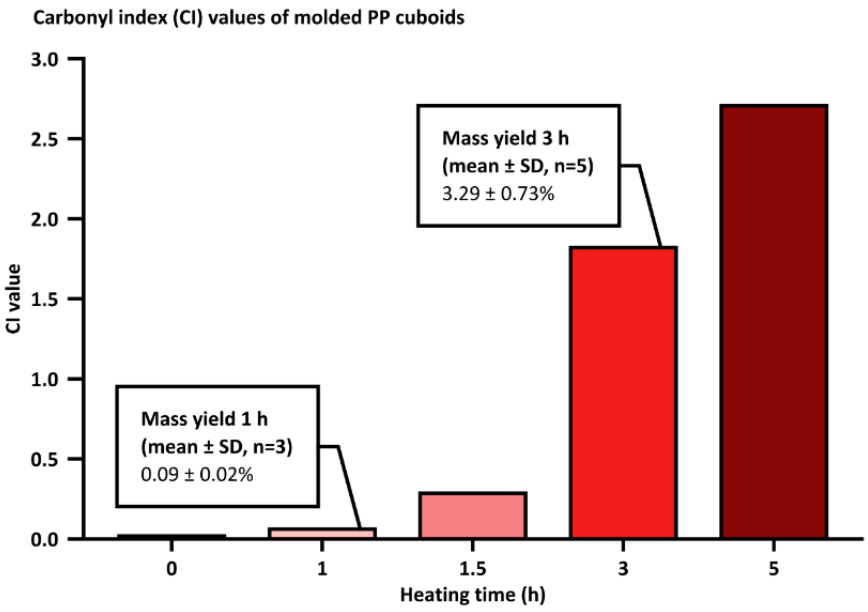

Figure 2.1: Impact of heating time (1, 1.5, 3, 5 h at 180°C) on the carbonyl index (CI) values of molded PP cuboids compared to the native PP pellets (0 h). n = 1 sample. Insets show the mass yield relative to the starting material mass of the fraction < 38 µm when using cuboids after 1 h (n = 3) and 3 h (n = 5) of heating at 180°C.

The mass yield of the fraction < 38 µm was considerably higher when the 3 h pre-treated cuboids were used (see insets in **Figure 2.1**), as expected. However, this increase in milling efficiency (brittleness) was achieved through surface oxidation, which can potentially affect the surface chemistry of produced MPs and subsequently their interaction with cells in various assays[173]. This shows the importance of thorough material characterization with respect to the intended use. To minimize pre-treatment effects on the material integrity, it was decided to use the 1 h pre-treated cuboids for milling.

Milling

The optimized milling procedure presented in **Table 2.2** successfully prevented excessive heating during milling. With the introduction of dry ice, pauses of 3-5 min were only necessary when dry ice was replenished to avoid material spilling through rapid dry ice sublimation when directly milled. Through minimizing pauses, the overall processing time

could be reduced by 30 min per batch. The surface temperature of dry ice (-78.5°C[174]) does not freeze ethanol (melting point -114°C[175]) and thus, can be used to keep the temperature of PP below its Tg (-20 to 0°C) during milling. This was ensured by stopping the milling process and replenishing dry ice when the dew on the outside of the milling container started to melt.

Sieving

Smaller MP size fractions require a wet sieving process to overcome agglomeration caused by electrostatic charge interactions[127,176]. However, water would also facilitate agglomeration due to its polarity, thus ethanol utilized for milling was also used for sieving. To test the hypothesis that prolonged sieving would increase the yield of the fraction < 38 µm, three conditions were tested: sieving the PP suspension once (n = 3), twice (n = 2), and five (n = 1) times for 5 min. Subsequently, the mass yield of the dried fraction < 38 µm relative to the sieved mass was calculated. The limited number of repeats for the two- and five-times sieving experiments does not allow a definitive conclusion but the current dataset shows that the highest obtained relative mass yields were similar for all three sieving procedures (once: 0.70%, twice: 0.72%, five times: 0.72%). Additionally, multiple sieving steps negatively influenced the PSD by increasing the 50th and 90th percentile from 11.6 and 33.5 µm (sieved once) to 24.0 and 64.4 µm (sieved five times). Since sieve meshes only provide a two-dimensional barrier, they can allow irregularly shaped particles to pass through in a time-dependent manner, even if one dimension is larger than the mesh size[177]. Therefore, a sieving time of 5 min and a single pass was found to be optimal to maintain the desired size cutoff where 22.3 ± 1.2% (n = 5) of the volume-based size distribution was within the desired 1-10 µm fraction. However, additional size separation steps were necessary to further narrow the PSD.

Filtration

Similar to sieving, vacuum filtration did not provide a clear cutoff at the given mesh size (10 µm) but reduced all three percentiles (D_{10}: p=0.0003, D_{50}: p=0.0006, D_{90}: p=0.01) statistically significant **(Figure 2.2A)**. A pilot study – performed by our collaborator Dr.

Tassilo Waniek from the Federal Institute for Materials Research and Testing in Berlin (BAM) – with milled PET MPs showed that specialized 10 µm silicon filter membranes (SmartMembranes) outperformed the 10 µm nylon filters due to their increased thickness and pore structure[178]. It ensures that particles can only pass if they are smaller than the pore diameter in all three dimensions, thus, providing a clear cutoff and interesting approach for milled PP particles **(Figure 2.2B)**. It hast to be noted that this approach requires much longer filtration times (hours) compared to the nylon filters (minutes) and therefore further investigations are needed.

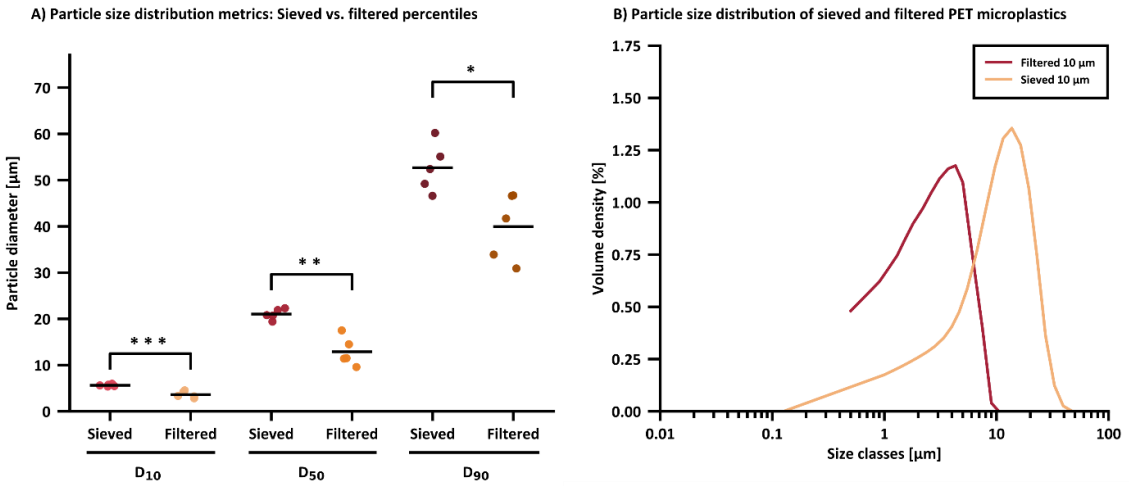

Figure 2.2: Comparison of the 10th, 50th, and 90th percentile of sieved (red) and additionally filtered (orange) PP microplastic suspensions (A). Comparison of the volume-based particles size distribution after sieving (orange) or filtering (red) a PET microplastic suspension through a 10 µm stainless steel mesh or 10 µm silicon membrane, respectively (B). Figure B was replotted with kind permission from Tassilo Waniek from BAM Berlin. Statistical significance was tested using a paired t-test (CI: 95%) where n.s. = $p > 0.05$, * = $p < 0.05$, ** = $p < 0.01$, and *** = $p < 0.001$.

After the first filtration step, submicron-sized material was detected in four out of five batches. A second filtration step was employed for removing this fraction using a 0.8 µm nylon membrane. Unfortunately, this second filtration was not effective in removing the submicron fraction but nonetheless helpful to quickly remove excess ethanol before further processing.

Centrifugation

Centrifugation was explored to fine-tune the PSD obtained after filtration. A pilot study revealed that repeated centrifugation using the same parameters continuously decreased the fraction < 1 µm. Thus, the final protocol was developed as a two-step procedure where each step was carried out twice. The first step was designed to remove particles > 10 µm followed by the second step for removing particles < 1 µm. In contrast to sieving and filtration, centrifugation did remove submicron particles in 3 out of 3 experiments but was less effective in separating particles > 10 µm from the product. Rapid agglomeration led to the removal of not only particles outside the desired range but also agglomerates that contain particles within the 1-10 µm size range. Thus, multiple centrifugation cycles can narrow the PSD but simultaneously reduce the yield. Furthermore, centrifugation increases the workload because it requires manual handling (pipetting). This also makes the result highly dependent on the skill and experience of the operator. **Figure 2.3A** shows the impact of combining filtration and centrifugation on the PSD of PP MPs. After producing five batches using the optimized procedure, a paired t-test was used to compare the 10^{th}, 50^{th}, and 90^{th} percentile of filtered and subsequently centrifuged PP MPs of the same batches **(Figure 2.3B)**. Only the D_{50} was statistically significantly smaller ($p = 0.03$) after centrifugation, whereas the differences of the D_{10} ($p = 0.3$) and D_{90} ($p = 0.2$) were not significant. However, the SD was reduced for both the 10^{th} and 50^{th} percentile from 0.63 and 2.79 µm to 0.31 and 1.09 µm respectively which is nonetheless useful for minimizing batch-to-batch variability.

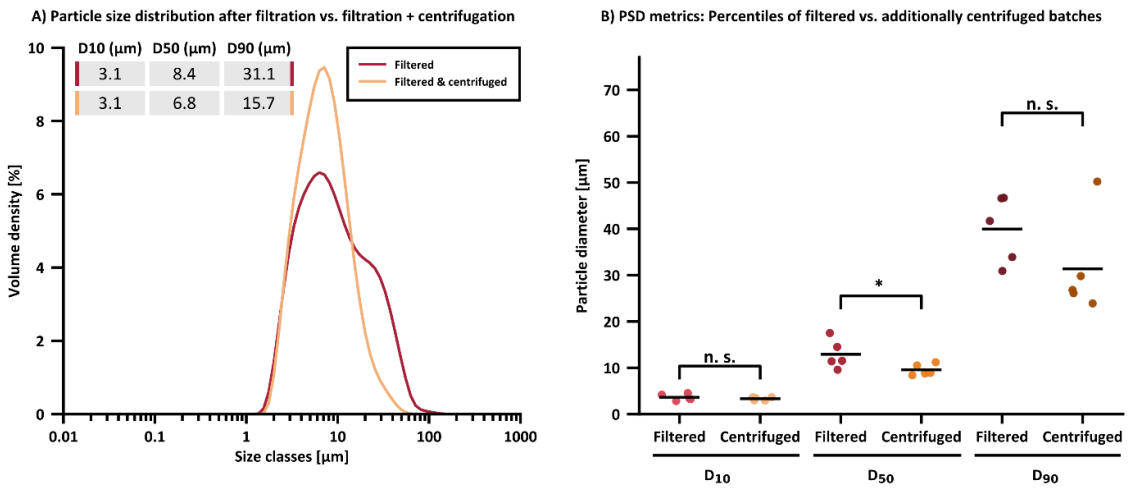

Figure 2.3: Fine-tuning the particle size distribution (PSD). The red trace shows the PSD of an ethanolic PP microplastic suspension (batch 029) following filtration. The orange trace shows the PSD of the same material following subsequent centrifugation fractionation (A). Comparison of the 10th, 50th, and 90th percentile of filtered and subsequently centrifuged PP MPs (B). Statistical significance was tested using a paired t-test (CI: 95%) where n.s. = $p > 0.05$, * = $p < 0.05$, ** = $p < 0.01$, and *** = $p < 0.001$.

Particle shape, product yield, and production time

The optimized production procedure was ultimately used to assess the material characteristics. SEM images **(Figure 2.4A-B)** of the produced PP MPs show a range of particle sizes and irregularly shaped fragments. This variety of shapes (excluding fibers) is expected for milled materials and in line with the TPP. Different agglomeration states can also be observed likely due to glycerol removal by washing with ethanol and subsequent drying prior to SEM imaging.

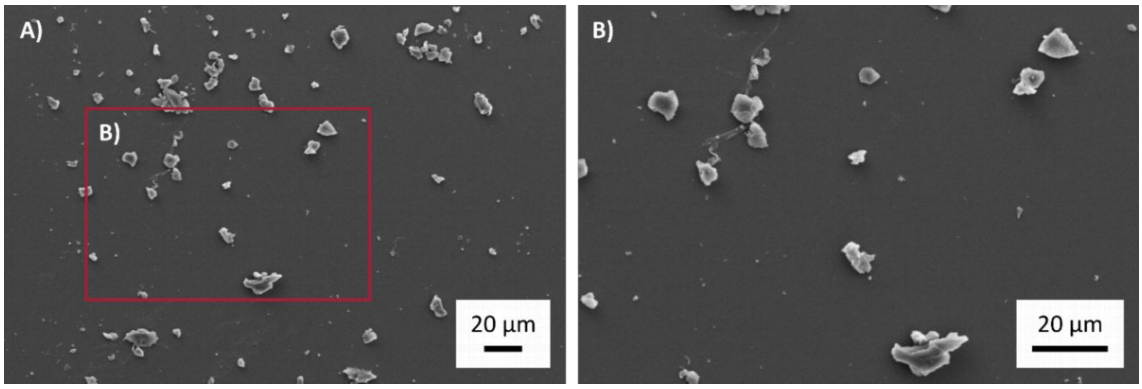

Figure 2.4: Representative SEM images of milled PP particles 1-10 µm after filtration and centrifugation. Overview with 1000x magnification (A). Detailed image with 2000x magnification where the rough surfaces and irregular shapes can be observed (B).

The product yield after size fractionation was calculated using **Equation 2.2 and Equation 2.3**. In general, the production time was comparably high for the extremely low quantity of product produced **(Table 2.3)**. From a single batch, only one vial with 1 mg PP MPs/g glycerol was obtained which is significantly lower than the desired 40 mg/g defined in the TPP. It has to be noted that further refinement of the particle size distribution (*via* filtration and centrifugation) contributed to yield reduction. However, there are no references for mass yield values of similar materials described in the literature. For comparison of mass yields, the PSD characteristics need to match because large particles contribute disproportionately to the overall mass compared to small particles. Ultimately, this low product yield is a significant barrier in the development of reference materials, since large quantities are typically required.

Table 2.3: Product yield and production time (n = 5 independent batches).

Mean yield per batch:	0.91 ± 0.34 mg (RSD: 38%)
Percentage of starting material:	0.005 ± 0.002%
Mean production time:	2 ± 1 days

Dispersibility from ethanol and glycerol

To assess the influence of the medium on the PSD, the QC dispersion protocol was used to redisperse particles from the same batch before and after exchanging the medium. This protocol uses harsh conditions (i.e. high energy input *via* bath sonication) to obtain either the primary particle size, or the size of irreversible agglomerates. **Figure 2.5** shows representative PSD curves of 1-10 µm MPs dispersed from ethanol or glycerol. While the 10th percentile stayed unchanged, an increase from 6.1 µm to 6.3 µm, and from 14.4 µm to 16.1 µm of the 50th, and 90th percentile, respectively, can be observed. Agglomerates in the ethanolic suspension are usually redispersible when the QC dispersion protocol is applied. However, agglomerates that formed during the medium exchange (e.g. by particles that dried on the glass wall during ethanol evaporation) are often not redispersible. This is most likely the cause of the D_{90} increase. However, the overall excellent colloidal stability in glycerol was reflected in the low RSD% of all D-values: D_{10}: 1.01%, D_{50}: 2.72%, D_{90}: 8.04%. This ideal case needed further verification through a batch-to-batch comparison study.

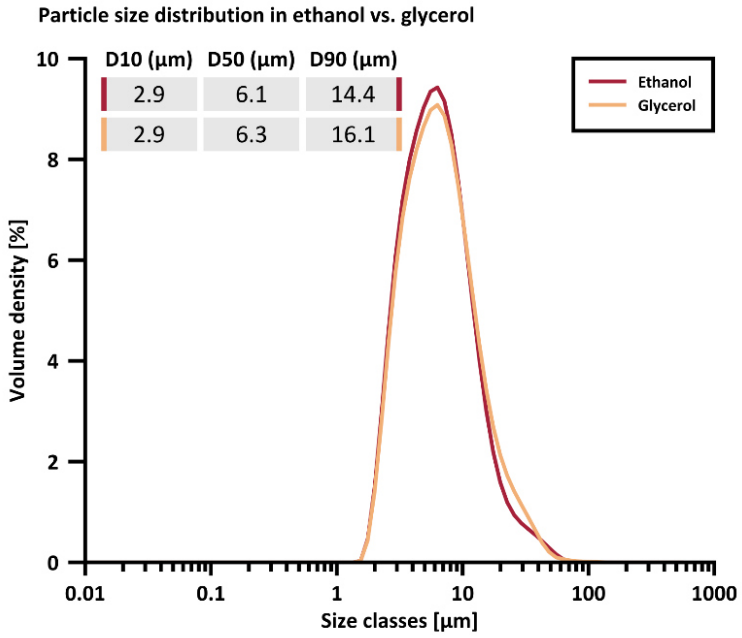

Figure 2.5: Comparison of the particle size characteristics following exchange of ethanol with glycerol. The red trace shows the particle size distribution of an ethanolic PP microplastic suspension (batch 032), whereas the orange trace shows the size distribution of the same material following subsequent medium exchange to glycerol.

Batch-to-batch variability

The robustness of combined milling, fractionation and dispersion procedures was determined through size distribution analysis of intermediate ethanolic suspensions (n = 16 batches) and the final product in glycerol (n = 5 batches; **Figure 2.6**). Evaluation of the size distribution characteristics of the ethanolic intermediate of sixteen batches produced by four different operators showed a highly reproducible median particle size (D_{50}) of 6.84 ± 1.12 µm **(Figure 2.6A)**. Data variability was highest in the D_{90} values, as demonstrated by the increasing RSD% of the PSD quantiles: D_{10}: 8.4%, D_{50}: 16.4%, D_{90}: 26.0%. The higher variation in the D_{90} values was attributed to differences in the way the four different operators performed critical operating steps, such as handling the unstable pellets when centrifugation was applied for size separation. **Figure 2.6B** shows n = 5 batches in ethanol and glycerol of the same operator. It can be observed that the PSD values for the final product in glycerol were shifted slightly towards larger sizes compared to ethanolic suspensions when multiple batches were characterized. The RSD% values for the glycerol products reflect this as well: D_{10}: 19.2%, D_{50}: 36.7%, D_{90}: 56.5%. A paired t-test showed a statistically significant increase in the D_{10} ($p = 0.005$) and D_{50} ($p = 0.02$) but not for the D_{90} ($p = 0.06$) due to its larger variability. The larger sizes and higher variation of the glycerol product was attributed to the slightly more complex dispersion process required for glycerol suspensions (e.g. addition of an extra heating step to reduce glycerol viscosity prior to dispersion in aqueous media). In some instances, the PSD quantiles were nearly identical between the ethanol and glycerol suspensions, whereas in other cases, the glycerol suspensions led to substantially higher D_{90} values, highlighting the importance of robust dispersion protocols. The small sample sizes due to the limited yield per batch and the emphasis of larger particles when measuring PSDs *via* laser diffraction contributed to higher D_{90} values.

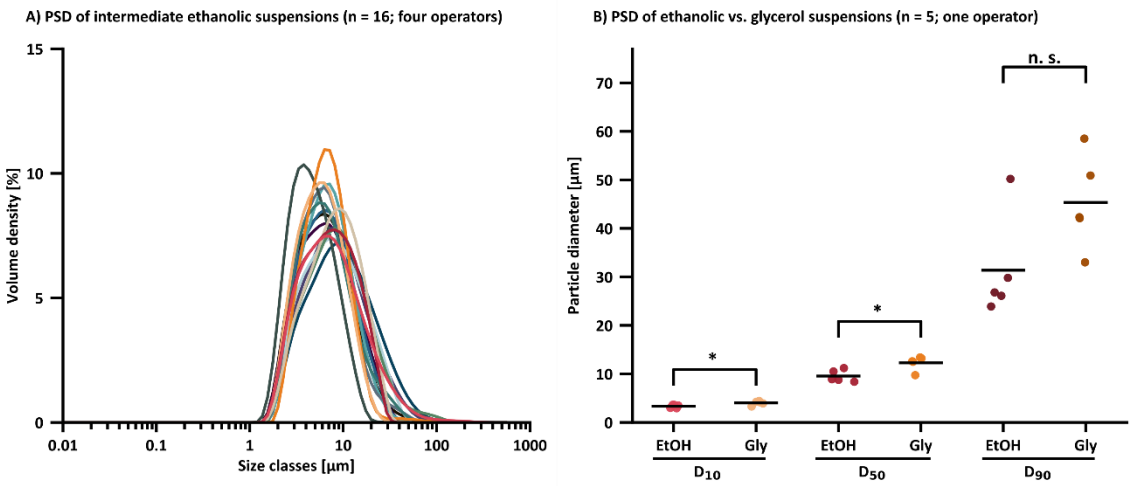

Figure 2.6: Particle size distribution curves of the intermediate ethanolic suspensions of n = 16 batches produced by four different operators (A). Comparison of the 10th, 50th, and 90th percentile of the intermediate ethanolic suspensions of n = 5 batches produced by one operator and the same five batches after exchange of ethanol for glycerol (B). Statistical significance was tested using a paired t-test (CI: 95%) where n.s. = p > 0.05, * = p < 0.05, ** = p < 0.01, and *** = p < 0.001.

The final important discussion point regarding the PSD data is the observation that only 41 ± 5% of the test material is within the desired range of 1-10 µm. In contrast, 70 ± 4% is between 1-20 µm. Strictly speaking, the current version of the test material would be considered out-of-specification and may not be suitable for the intended use. Further analysis would be required to determine whether it would be appropriate to modify the target particle size range of the intended product or perform further optimization work to narrow the PSD even further. Since the latter approach is likely to result in a further decrease in product yield, this may not be a practical or feasible option.

Size stability during long-time storage

To gain reference material status, a critical material attribute (CMA) should be defined and its stability of over longer periods (shelf-life) needs to be demonstrated, typically for one year before materials are tested again and eventually re-certified[179]. Stability of the PSD, as one of the defined CMAs, was monitored through a real-time long-term stability study using a non-optimized protocol (optimization started later). The material was stored under

light exclusion at room temperature for 32 months (~2.5 y) and for the remeasurement, the same non-optimized dispersion protocol was applied to ensure comparability. The overlay of the obtained PSD curves shows that the PSD curve of the stored material shifted towards larger sizes, which indicates agglomeration **(Figure 2.7)**. Due to the density difference (glycerol: 1.26 g/cm^3 and PP: 0.90 g/cm^3 according to their datasheets) PP MPs will float over time. However, this can be minimized when the material is regularly used or redispersed. Furthermore, it is expected that RSD% values can be reduced (below the desired 15% threshold) by using the optimized dispersion protocol in future studies.

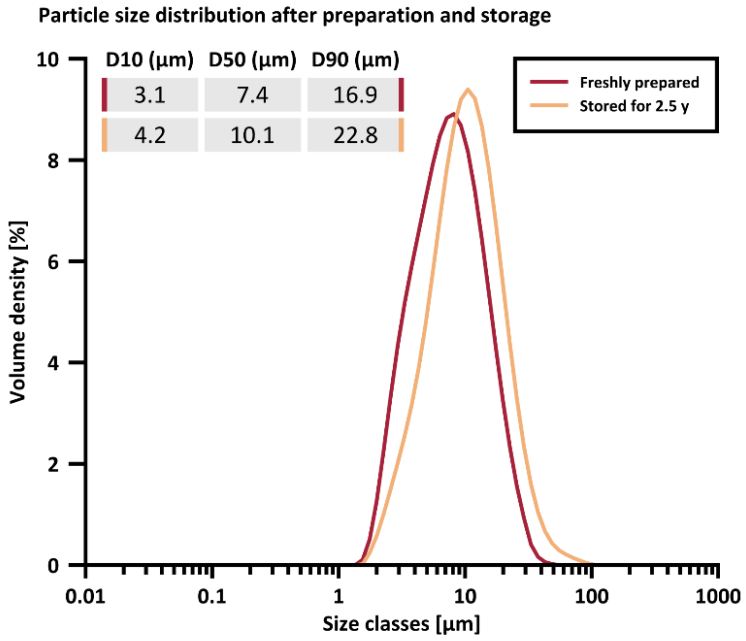

Figure 2.7: Particle size distribution (PSD) curves of PP microplastic glycerol stocks. The red trace shows the PSD of the freshly prepared glycerol suspension (batch 005), whereas the orange trace shows the PSD of the same material remeasured after 2.5 years of storage at room temperature.

Dispersion in biorelevant media

To assess the suitability for use *in vitro* and *in vivo*, full dispersibility in biorelevant isotonic media needs to be demonstrated. Two dispersion protocols were developed, where one is for i) quality control (QC, **see Chapter 0**) of the produced materials and the

second one for ii) assessment of the PSD in biorelevant media (BRM, **see Chapter 0**). In contrast to the QC protocol where Tween®80 is used to obtain good dispersibility and the PSD is measured in water, the BRM dispersion protocol utilizes bovine serum albumin (BSA) as biocompatible dispersion aid, which can stabilize MP suspensions[130], and the PSD is determined in cell culture medium (DMEM/F-12 without FBS). In **Figure 2.8**, the PSD curves of the same batch (batch 005 stored for 2.5 y) dispersed in water (QC) and DMEM (BRM) are shown to overlap, indicating that the material is fully dispersible in both cases and does not change its size characteristics, as indicated by the percentiles in the inset. It has to be noted that previous studies utilized an Elmasonic P 30 H sonication bath (Elma Schmidbauer GmbH, Singen, Germany) operated at 37 kHz (120 W nominal power). During optimization of the dispersion protocols, the sonication bath was replaced (Sonocool SC 255, Bandelin electronic GmbH & Co. KG, Berlin, Germany) which operated at 35 kHz and had higher energy inputs (180 W nominal power) over the same sonication time. Hence, the peak in the submicron region can be attributed to the breakdown of previously non-dispersible agglomerates. This highlights that the effectiveness of a dispersion protocol is highly dependent on the sonication bath used and that the frequency and nominal power are important factors besides sonication time.

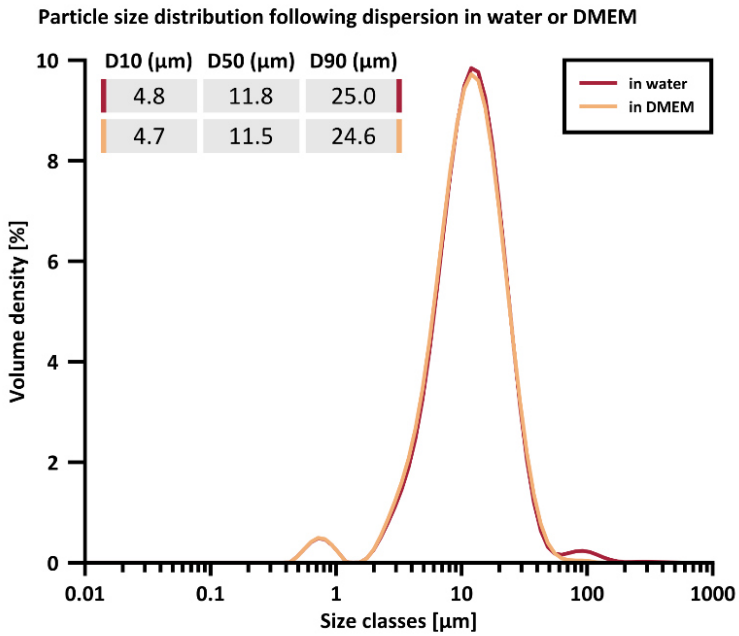

Figure 2.8: Particle size distribution (PSD) curves of microplastic particles following different dispersion protocols. The red trace shows the PSD of a PP microplastic suspension (batch 005) dispersed with Tween®80 in water (QC), whereas the orange trace shows the PSD of the same material dispersed with BSA and measured in DMEM (BRM).

Effects of the production process on microbial contamination rate

Sterility of the material is important for *in vitro* and, especially *in vivo,* toxicology studies since contamination can contribute to measured effects and lead to misinterpretation of results

(Swierczewska Magdalenaand Crist, 2018)

. Fourteen batches of PP MPs were assessed for growth of viable microorganisms. Eleven batches were produced as dry powders representing comparator materials with a larger size range and three batches were dispersed in glycerol representing materials produced using the method described above **(Table 2.4)**. Contamination only occurred in dry powder batches (028 and 048) which showed fungal growth at all three concentrations tested. An effective way of avoiding contamination *via* air would be to conduct all production steps in a controlled environment like a clean room or laboratory scale safety bench with HEPA filter system. However, this was not applicable during this study and all

steps were carried out in a clean but not controlled environment resulting in a contamination rate of 18% for dry powders. Interestingly, none of the glycerol stocks tested were contaminated even after prolonged storage. It has to be noted that only a limited number of glycerol batches were tested and that increasing the number of batches tested might result in a higher contamination rate.

Table 2.4: Produced dry powder and glycerol batches tested for bacterial (LB agar) and fungal (SAB agar) contamination. Each batch was tested at three different concentrations (200, 50 and 10 µg microplastics per mL).

Storage medium	Batch	LB Agar (CFU/mL)			SAB Agar (CFU/mL)		
		Concentration of microplastics tested (µg/mL)					
		200	50	10	200	50	10
Dry powder	027	0	0	0	0	0	0
	028	0	0	0	140	2	15
	044	0	0	0	0	0	0
	045	0	0	0	0	0	0
	048	0	0	0	143	44	9
	052	0	0	0	0	0	0
	053	0	0	0	0	0	0
	059	0	0	0	0	0	0
	061	0	0	0	0	0	0
	062	0	0	0	0	0	0
	Mixed batches	0	0	0	0	0	0
Glycerol	072	0	0	0	0	0	0
	005 (2.5 y)	0	0	0	0	0	0
	008 (2.5 y)	0	0	0	0	0	0

Osmolarity

The advantages of using glycerol as matrix have already been discussed. However, the osmolarity of relevant vehicles for *in vitro* (DMEM, DMEM + 10% FBS) or *in vivo* (0.9% NaCl) applications increases when glycerol is added. Thus, the freezing point depression of the vehicles with and without the addition of glycerol concentrations up to 6.1% (w/v) were measured and the osmolarity was calculated **(Table 2.5)**. Depending on the cell type, the

tolerance to hypo- or hyperosmotic stress can vary and is usually lower *in vivo*. This is why - compared to DMEM - sterile saline solution has a lower osmolarity but still allows lower amounts of glycerol. I*n vivo* applications require isotonicity (300–312 mOsmol)[181] which is achieved between 0.2-0.4% glycerol content, whereas *in vitro* tests allow higher osmolarity. Scherließ (2011) reported that the highest viability of the Calu-3 cell line was maintained between 290-390 mOsmol at pH 6-7[182], which corresponds to glycerol concentrations up to 0.8% (< 400 mOsmol). It was confirmed that this concentration had no effects on cell viability or stress markers depending on the cell type (**see Chapter 0**). Unfortunately, the low particle concentration in the glycerol stock (1 mg/g) reduced the administrable dose considerably, to about 8 µg/mL, which is impractical for dose escalation studies that generally recommend testing concentrations up to 100 µg/mL. Therefore, the concentration of the PP MP stock solution in glycerol needs to be increased by at least one order of magnitude to be useful in *in vitro* toxicity assays.

Table 2.5: Mean osmolarity of different glycerol concentrations (%w/v) added to DMEM + 10% FBS and 0.9% saline solution. Values represent the mean and standard deviation of n = 3 experiments.

Amount of glycerol added (% w/v)	Vehicle	Osmolarity (mOsmol)	Vehicle	Osmolarity (mOsmol)
0%	DMEM	314 ± 2	-	-
0%	DMEM + 10% FBS	319 ± 3	0.9% NaCl	284 ± 1
0.05%	DMEM + 10% FBS	323 ± 1	0.9% NaCl	289 ± 2
0.1%	DMEM + 10% FBS	326 ± 1	0.9% NaCl	293 ± 2
0.2%	DMEM + 10% FBS	336 ± 2	0.9% NaCl	299 ± 0
0.4%	DMEM + 10% FBS	351 ± 12	0.9% NaCl	319 ± 3
0.8%	DMEM + 10% FBS	394 ± 2	0.9% NaCl	356 ± 4
1.6%	DMEM + 10% FBS	485 ± 4	0.9% NaCl	436 ± 3
3.1%	DMEM + 10% FBS	656 ± 4	0.9% NaCl	602 ± 1
6.2%	DMEM + 10% FBS	1009 ± 12	0.9% NaCl	952 ± 1

2.4 Study limitations and future perspectives

All the obtained results were subjected to critical evaluation based on the defined critical and desired quality attributes. **Table 2.6** summarizes the current state of development (achieved, achieved with limitations, and not achieved), where only two out

of ten critical and desired quality attributes were achieved. The low yield is particularly decisive, as it influences many other critical and desired quality attributes (production time, isotonicity only at low particle concentrations, limited mass concentration of the glycerol stock) or precludes their evaluation (homogeneity and stability controls as defined by ISO 33401[114] and 33405[115] guidelines, testing for endotoxins, or chemical stability e.g. *via* ATR-FTIR). Therefore, future optimization efforts should primarily focus on increasing the product yield.

Table 2.6: Development status of pristine PP test materials 1-10 µm. The performance of the current materials is compared to the mandatory and desired quality attributes derived from the TPP.

CQAs	Status description	Status
Must contain no viable microorganisms and a sufficiently low endotoxin content	Sterility achieved Endotoxins were not tested.	±
Must be sufficiently concentrated to enable dilution to relevant test concentrations with a biocompatible osmolarity	Full dispersibility achieved. Isotonicity achievable when < 0.8% residual glycerol in sample.	±
Must not contain exogenous dispersing agents, such as Tween® surfactants or serum albumin (required for protein corona studies).	Achieved.	✓
Must show sufficiently high batch-to-batch reproducibility within the 1-10 µm size range (RSDs < 25%).	D_{90} values are associated with a high variability and may be dependent not only on the primary particle size but also on the dispersion quality.	✗
Must be dispersible in various media so that > 90% of the test material is < 10 µm in size.	After production, only 41 ± 5% of the particles lie between 1-10 µm but no difference between QC and BRM dispersions.	±
DQAs	**Status description**	**Status**
Should be irregularly shaped in the form of fragments.	Achieved.	✓
Should have a high particle concentration per unit product to allow for flexible planning of dose escalation studies.	Low product yield values limited the mass concentration to 1 mg PP / g glycerol, whereas the target concentration would be 40 mg/g.	✗
Should be packaged in a "multi-dose" container to reduce the need for multiple single-unit containers.	Achieved but only at low concentrations.	±
Should maintain chemical, physical and microbial stability over at least one year shelf life and in-use life span.	Chemical stability not tested. Physical stability out-of-specification (RSD > 15%). Microbial stability achieved.	±
Should have an acceptable product yield per batch (> 10%) and manufacturing time (< 2 days).	Production yield < 0.005%, production time > 2 days.	✗

2.5 Conclusions and contributions to the field of research

Ultimately, the method of comminution and extensive size fractionation was not fit for purpose. Despite all optimization efforts for large scale production of PP MPs between 1-10 µm, the production was discontinued for the IMPTOX program due to low yields. The knowledge generated (e.g. regarding milling, size fractionation, dispersibility, or stability) is nonetheless useful as it can be transferred to other milling procedures and aids the development of materials targeting larger size ranges or other polymer types.

Chapter 3

Down in scale: Method development to produce polyethylene terephthalate and polypropylene nanoplastics for study in biological assays

3 Test material development – Polyethylene terephthalate and polypropylene nanoplastics

Parts of this chapter were first published on the 1st of April 2025 in Environmental Science: Nano (https://doi.org/10.1039/D4EN01186D) and reproduced with permission from the Royal Society of Chemistry[2].

3.1 Introduction and background

The need for nanoplastic test materials

For MPs, the number of studies investigating their environmental concentrations and faith, as well as their effects on cells and whole organisms is growing fast. The production of larger plastic particles is comparably easy and for analyzation fast tools like light microscopy, FTIR or Raman are widely available[183]. Reports on MPs in various organs of the human body like lungs[83,159], the heart[184] or placenta[185] showed that there is reason for concern. However, smaller NPs remain understudied because i) highly sophisticated analytical tools are needed for their detection in environmental or tissue samples, and ii) suitable test materials designed for biological testing are often not available. Providing pristine NP test materials comprised of a single polymer would enable the evaluation of the material's intrinsic toxicity, potential synergistic effects with adsorbed cargo and the validation of new analytical tools. Such materials are urgently needed because smaller particles generally pose a higher toxicity risk. They can cross biological barriers more easily and accumulate in different organs. This has been shown for the blood-brain-barrier in fish[186], or *via* computer modelling[187,188]. Furthermore, *in vitro* studies demonstrated that NPs caused dose dependent inflammatory, genotoxic, and cytotoxic responses in human keratinocytes[189], or oxidative destruction of intestinal epithelial cell lines[108]. As described in **Chapter 1** , most of the studies were conducted using PS but a wider variety of relevant polymers need to be evaluated. Thus, it was aimed at producing NPs comprised of PET and PP suitable for *in vitro* and *in vivo* assays. To obtain high quality materials, the same QbD inspired approach for the development of MPs **(Chapter 2)** was employed, starting with the definition of a TPP.

Development of a TPP for nanoplastics

When applied to the development of NP test materials for use in biological assays, the QbD approach starts with the development of a target product profile (TPP) which describes the intended use and the desired product characteristics. In the current project, we would like to design test materials in the submicron size range suitable for use in cell-based assays and *in vivo* toxicity tests. To be suitable for such applications, the test materials must be i) reproducibly dispersible in a range of aqueous media with physiological osmolarity, ii) free of additives, such as exogenous surfactants, which could confound test assay results, iii) free of process-derived contaminants, endotoxins, and microorganisms, iv) stable in terms of size and sterility for at least one year, preferably at room temperature, v) packaged in such a manner to allow for dosing across a wide range of concentrations to enable dose-escalation studies, vi) producible in quantities realistic for distribution to multiple labs, and vii) reproducible in terms of low batch-to-batch variation for key product characteristics **(Figure 3.1)**.

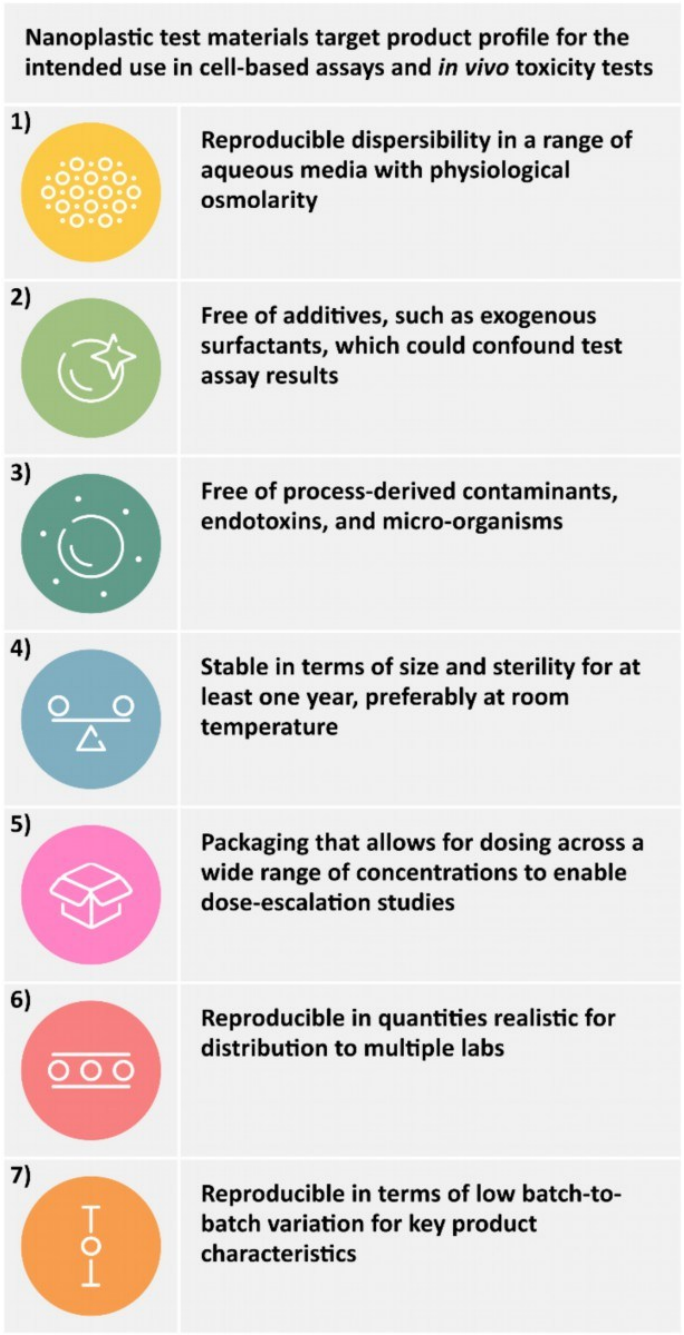

Figure 3.1: Target product profile (TPP) of nanoplastic test materials for in vitro and in vivo use.

From this TPP, CQAs for the desired test material were defined along with their target values or acceptable ranges and are listed in **Table 3.1**.

Table 3.1: Proposed list of CQAs (i.e. properties of interest) and their corresponding specifications recommended for reference nanoplastics intended for use in biological assays.

CQAs	Specification	Recommended methods/comments
Homogeneity of particle concentration (uniformity of nanoplastic content across several units)	Guidelines do not provide a recommendation for a maximal allowable variability. We suggest 85-115% of the target value[190].	For batches with > 100 units, a minimum of 10 units measured in duplicates. For batches with < 100 units, at least 3 units or 10% of the batch size measured with four technical replicates[190].
Homogeneity of the particle size distribution profile	> 85% of the particles are < 1 µm using the validated QC dispersion protocol.	Particle size distribution data should be determined using a validated QC dispersion protocol combined with LD analysis.
Stability of the particle size distribution profile	D_{10} and D_{50} measured after 12 months storage at ambient room temperature should not differ > 15% from the original values. The % < 1 µm should not drop below 85%.	Particle size distribution data should be determined using a validated QC dispersion protocol combined with LD analysis.
Sterility after manufacture and storage	0 CFU/mL after production and 12 months storage of unopened containers at ambient room temperature.	Sterility should be tested using a validated method following dispersion using a validated biorelevant dispersion protocol with sterile cell culture media.
Endotoxin content measured after manufacture	< 0.1 EU/mL[191]	Endotoxin content should be tested using a validated method following dispersion using a validated biorelevant dispersion protocol with sterile, low-endotoxin grade cell culture media.
Residual solvents from the production process	Residual solvents < 1%	GC-MS. If no biological effect is expected, higher amounts of residuals could be acceptable.

Very few production methodologies described in the literature are able to satisfy these requirements. NPs in dry powder form produced either through top-down or bottom-up approaches are typically difficult to fully disperse in aqueous media, unless they are chemically modified or aged to contain sufficient hydrophilic surface modifications for acceptable aqueous dispersibility. NPs produced as aqueous dispersions often require the addition of exogenous surfactants to maintain colloidal stability, preservatives for microbial stability, and are often only colloidally stable at low concentrations, which do not enable dose-escalation studies[72,73,107,121]. As described in **Chapter 2** , we explored glycerol as a

biocompatible storage medium to overcome these limitations in our PET and PP research grade test materials. The rationale for our choice of glycerol as a non-aqueous storage medium included the following points:

- Glycerol is a non-volatile, natural preservative, maintaining microbial stability during storage at room temperature[192].
- The high viscosity of glycerol prevents agglomeration over long storage periods, even at high concentrations without exogenous surfactants.
- Glycerol is commonly used to help disperse highly cohesive powders in aqueous liquids[193,194]. Therefore, it promotes homogenous dilution into aqueous media, such as cell culture medium.
- It is well-tolerated at relatively high concentrations[195,196] (up to 1.5 g/kg oral and 1 g/kg intravenous administration). Further administration routes for products containing glycerol include e.g., buccal, intradermal, intravenous, dermal, nasal, inhalation, auricular, and ocular[197,198].
- In diluted form, glycerol is highly biocompatible in both cell-based assays[182] and *in vivo* models[195].

Study design and hypotheses

Milling experiments described in **Chapter 2** showed that the top-down procedures investigated are not effective in producing PET and PP NPs. Hence, a more pragmatic approach was needed even when it would not fulfill all desired quality attributes (e.g. irregularly shaped fragments). A promising alternative was found in nanoprecipitation where the polymer is first solubilized in an appropriate solvent and subsequently precipitated into a non-solvent. Lee *at al.* (2022) showed that this method can produce PP NPs (562 ± 118 nm) with high yields (> 84%) but several key aspects for a future reference material like long-term stability, reproducibility, and dispersing issues were not discussed[69]. Based on findings from Tanaka *et al.* (2023)[199], the procedure was further optimized to meet the TPP specifications. Simultaneously, the method was adapted for PET with additional input (e.g. the used solvent, temperature, and solvent/non-solvent ratio) from Achilias *et al.* (2009)[126] with subsequent optimization. To test the hypothesis that PET and PP NP test

materials stored in a glycerol medium fulfill the requirements outlined in the TPP, a comprehensive study was conducted to characterize their performance in a model *in vitro* cell culture assay system. Five batches of pristine, highly concentrated PET and PP nanosuspensions in glycerol (40 mg/g) were prepared and all pre-defined quality parameters characterized including size distribution profiles following dispersion into different aqueous media, dispersion uniformity, size stability over one year storage, bulk chemistry, surface hydrophobicity, residual solvent content, endotoxin content, sterility, osmolarity, and biocompatibility.

3.2 Materials and methods

Materials

Polypropylene (PP, CAS: 9003-07-0) and polyethylene terephthalate (PET, CAS: 25038-59-9) granules were kindly provided by PlasticsEurope. Tween®80 (Polysorbate 80, P1754), glycerol (≥ 99%, anhydrous for synthesis, 8.18709), xylene (IUPAC dimethylbenzene, isomeric mixture for analysis, 1.08297) and benzyl alcohol (IUPAC phenylmethanol, ReagentPlus®, 108006) were obtained from Sigma-Aldrich (Merck KGaA, Darmstadt, Germany). Filters were purchased from Whatman (0.8 µm, membrane filters, WHA7408004, Whatman plc, Maidstone, UK) and Merck Millipore (2 µm, PC membrane, TTTP04700 and 0.45 µm, PVDF membrane, SLHVR33RS, Merck Millipore KGaA, Billerica, USA). Ethanol (96%, v/v) was sourced from Brenntag (Brenntag Austria GmbH, Vienna, Austria). For vacuum filtration, a glass filter holder system was provided by VWR (511-0666, VWR International LLC., Radnor, USA). LB-agar and Sabouraud 4% glucose-agar were purchased from Carl Roth (X932.1, Carl Roth GmbH & Co. KG, Karlsruhe, Germany). Dulbecco's Modified Eagle Medium/Nutrient Mixture F-12 (DMEM/F-12, [+]L-Glutamine, no phenol red, 21041-025) was ordered from Thermo-Fisher (Fisher Scientific GmbH, Schwerte, Germany), whereas fetal bovine serum (FBS Superior, S0615) was obtained from Sigma-Aldrich (Merck KGaA, Darmstadt, Germany).

Preparation of nanoplastics

For the preparation of NPs, methods from Achilias *et al.* (2009)[126], Lee *et al.* (2022)[69], and Tanaka *et al.* (2023)[199] were adapted and optimized (SOP available at DOI; 10.5281/zenodo.14881493). Briefly, PET (260 mg) was dissolved in benzyl alcohol (10 mL) while heated to 215 ± 0.2°C in a silicone oil bath and stirred at 250 rpm for 45 min. The hot PET/benzyl alcohol solution (215 ± 0.2°C) was transferred with a glass pipette into 15 min pre-cooled ethanol (125 mL, placed in an ice bath) while stirred at 400 rpm. The precipitated suspension was stirred for 3 min until cool and subsequently washed 5 times with ethanol (100 mL) by filtering. A polycarbonate membrane with a pore size of 2 µm was employed to retain NPs, made possible by their rapid agglomeration during filtration. The particles on the filter were resuspended in fresh ethanol (26 mL) in a pre-weighed flask (m_{flask}) and subsequently sonicated in a temperature-controlled sonication bath (Sonocool SC 255, Bandelin electronic GmbH & Co. KG, Berlin, Germany) for 2 h at 21 ± 1°C and 100% intensity. All sonication steps in this study were carried out with the same instrument and intensity (35 kHz, 180 W nominal power). Finally, the weight of the flask with suspension was determined (m_{susp}).

To prepare PP NPs, the same procedure was performed with the following adaptations: PP granules (165 mg) were dissolved in xylene (80 mL) at 185 ± 0.2°C. The hot solution (185 ± 0.2°C) was added to ethanol (240 mL) as described above and the suspension was filtered through a 0.8 µm nylon membrane, undergoing the same rigorous washing protocol with ethanol to remove residual xylene. The washed material retained on the filter membrane was resuspended in ethanol (16 mL) and subsequently bath sonicated for 45 min at 21 ± 1°C prior to weighing.

Concentration and product yield

Concentrations of NPs in ethanol after washing were determined gravimetrically by transferring 0.5-1 mL suspension into a pre-weighed Eppendorf tube (2 mL, m_{empty}) and determining the fill weight (m_{filled}). The sample was then dried with a rotary evaporator (water bath at 50°C, pressure 20 mbar, reduced incrementally) and the dry mass (m_{dry}) was

determined. When the mass loss was < 1%, the concentration and percent yield were calculated with **Equation 3.1 and Equation 3.2**.

Equation 3.1: The concentration (c) of the washed nanosuspension calculated in mg/g.

$$c\ (mg/g) = \frac{\left(m_{dry} - m_{empty}\right) \times 1000}{\left(m_{filled} - m_{empty}\right)} \quad (3.1)$$

Equation 3.2: Percentage yield of the washed nanosuspension.

$$Y\ (\%) = \frac{c \times m_{susp}}{m_{granules}} \quad (3.2)$$

Transfer into glycerol

Glycerol stock suspensions (40 mg nanoplastics/g glycerol) were heated to 60 ± 1°C and was mixed with the appropriate mass of ethanolic nanosuspension to achieve a final concentration of 40 mg nanoplastic per 1 g glycerol. The mixture was immediately vortexed and bath sonicated for 5 min to ensure even distribution. Ethanol was evaporated with a rotary evaporator at 50°C by reducing the pressure in a stepwise manner to 20 mbar and the process was deemed completed when no more than 1% of mass loss was measured gravimetrically. Aliquots of the final suspension (1 g) were transferred into HPLC glass vials (1.5 mL), sealed and stored under exclusion of light in a cardboard box.

Determination of residual solvents

Samples of ethanolic NP suspensions (PET and PP) were drawn, vortexed and bath sonicated for 1 min before 1.8 mL were transferred into a 2 mL Eppendorf tube and centrifuged twice at 21,380 × g for 2.5 min at room temperature. Subsequently, 1.5 mL of the supernatant was transferred into amber HPLC vials (2 mL) and analyzed with GC-MS (Trace1300/ISQ7000, Thermo Scientific Inc., Waltham, USA). Samples (1 µL) were injected directly and measured in triplicates. A CP-SIL-5 column (30 m, 0.25 µm, 0.25 mm, Agilent Technologies Inc., Santa Clara, USA) was employed with Helium as the carrier gas. The

solutions were run through the separation column using an autosampler in split mode (1:50) at an injection temperature of 260°C. After the injection, the GC oven with the separation column was operated with the following temperature program: Temperature: 50°C, Time: 15 min. At the end of the column, the gas flow from the separation column was transferred into the mass spectrometer at 250°C. The MS spectra were recorded in the retention time range of 2 to 15 min, with the molecular fragments being detected in the range of 50 m/z (mass-to-charge ratio) to 200 m/z to exclude the solvent.

Contact angle measurements

To assess the surface hydrophobicity of the used materials, PET granules were melted onto a glass slide (200°C, 5 min) and PP granules were cut with a scalpel to obtain flat surfaces (reference starting material). A subset of the prepared PET and PP granules were heat treated for 128 h at 180°C and 20 h at 140°C, respectively (oxidized control). Ethanolic NPs (intermediate product) were dried by vacuum filtration through a 0.8 µm nylon membrane. Dry NP powders and the prepared granules were fixed onto a slide with double-sided tape. Caution was taken to cover the whole surface with powder and compress it with a spatula before taking measurements. Compression was also necessary to prevent absorption of the water drop into the powder bed. Contact angles were measured with a drop shape analyzer (DSA30S, Krüss GmbH, Hamburg, Germany) using the sessile drop technique with de-ionized water as a test liquid. Individual measurements (n = 30) were taken for each sample, except heat treated (heat) PP (n = 9). The baseline was set manually and only measurements were included, where the software could correctly detect the droplet shape. Every measurement was performed at a new dry position. The droplet volume was set to 2 µL at a rate of 0.16 µL/min and after a 5 sec pause 6 measurements were taken with 1 frame per second. Individual measurement values are shown and the mean value calculated for statistical comparison.

Attenuated total reflection–Fourier transform infrared spectroscopy (ATR-FTIR)

Spectra were obtained with the Alpha II FTIR-spectrometer (Bruker Optics GmbH & Co. KG, Ettlingen, Germany) equipped with an ATR module (Platinum-ATR, single reflection ATR with a monolithic diamond). Before each measurement, blanks were recorded and automatically subtracted from the averaged spectrums. The dried NPs and PET granules were transferred directly onto the ATR crystal, while PP granules were cut to obtain best contact with the ATR crystal. Five different batches of dried NPs or starting material granules were tested with three technical replicates, each consisting of 32 scans and an optical resolution of 4 cm^{-1} between 4000 and 400 cm^{-1}. For processing (baseline correction and peak normalization) and analysis of the spectra, the SpectraGryph software (v1.2.16.1) was employed and averages are presented. To determine the carbonyl index (CI) of PP with **Equation 3.3**, the area of the peak of interest ($A_{C=O}$) from 1820-1650 cm^{-1} was divided by the area of the reference peak ($A_{ref.}$) from 1500-1420 cm^{-1}.

Equation 3.3: Determination of the carbonyl-index (CI).

$$CI = \frac{A_{C=O}}{A_{ref.}} \tag{3.3}$$

Dispersion in aqueous media for quality control (QC)

For assessment of the particle size distribution characteristics of the test materials, a QC dispersion protocol was developed using the non-ionic, synthetic surfactant, Tween®80. The aim was to maximize particle deagglomeration to gain accurate information on the primary particle size distribution characteristics of the product.

Dispersion from ethanol

When dispersing NPs from the intermediate product (ethanolic suspension), 200 µL suspension were mixed with 800 µL of 5%, w/w Tween®80 in high purity water (HPW; step 1 dilution) followed by bath sonication at 21 ± 1°C (15 min for PET and 40 min for PP, respectively). This suspension (typically 1 mg/mL plastic content) was subsequently further

diluted to the desired concentration in a 0.3% Tween®80/HPW (step 2 dilution), whereby the final Tween®80 content typically ranged from 0.35-0.39%.

Dispersion from glycerol

For the dispersion of NPs from the glycerol suspension, the content of the vial was first homogenized by applying the protocol outlined in **Table 3.2**. Briefly, the glycerol stock was heated to 60°C to reduce its viscosity and ease handling. Alternating cycles of vortex and heating, combined with a sonication step, ensured an evenly distributed sample. The sample was used immediately, and the desired amounts were weighed-in while the sample was still hot.

Table 3.2: Homogenization protocol for nanoplastic test materials stored in glycerol.

Step	Protocol	Duration
1)	Heat the suspension to 60°C in a water bath	2 min at 60°C
2)	Vortex	30 sec.
3-6)	Repeat steps 1 and 2 twice	2 min at 60°C / 30 sec.
7)	Sonicate at 60°C and 100% intensity at 32 kHz	3 min
8-13)	Repeat steps 1 and 2 three more times	2 min at 60°C / 30 sec.
14)	Use immediately	

A sample was then removed using a glass Pasteur pipette and 1 drop (~25 mg suspension containing ~1 mg NP) was added to a pre-weighed glass vial. The weight of the sample was determined and the mass of NPs calculated. An appropriate volume of 5% w/w Tween®80 in HPW was added to the sample to achieve a NP concentration of 1 mg/mL and bath sonicated at 21 ± 1°C (15 min for PET and 40 min for PP, respectively). This suspension (step 1 dilution) was further diluted to the desired concentration in 0.3% Tween®80/HPW (step 2 dilution), whereby the final Tween®80 content typically ranged from 0.37-0.48%.

Dispersion in biorelevant media (BRM)

When performing cell culture studies, or investigations of the bio-/ecocorona formed on the particle surface[66,200], it can be necessary to avoid the use of a synthetic surfactant as a dispersing agent. Therefore, a dispersion protocol using bovine serum albumin (BSA) and serum-supplemented cell culture medium as the dispersing agent was developed (SOP available at DOI: 10.5281/zenodo.14881493). Briefly, glycerol suspensions were heated, homogenized and one drop dispensed into a clean glass vial as described above. The PET sample (25 ± 0.25 mg) was mixed with 1000 µL of a 10% m/v aqueous BSA solution prepared in HPW (filtered through a 0.45 µm PVDF membrane, Millex®-HV, Low Protein Binding Durapore®) to achieve a NP concentration of 1 mg/mL (step 1 dilution). The mixture was shaken gently to avoid air bubble formation and subsequently bath sonicated for 1 min at 21 ± 1°C. Thereafter, distilled water or serum-supplemented cell culture medium was added (step 2 dilution) to achieve the final desired concentration and bath sonicated 15 min prior to further use. The more hydrophobic PP NPs required a modified approach with 40 min of bath sonication at 21 ± 1°C. The theoretical BSA concentration is typically 1.5% for a NP concentration of 150 µg/mL.

Scanning electron microscopy (SEM)

Samples of glycerol suspensions were washed by vacuum filtration and residues were resuspended in ethanol. These ethanolic suspensions were dropcast onto a glass slide, fixed onto a sample holder with double-sided conductive adhesive tape and dried overnight. On the following day, the samples were gold-sputtered and imaged with an EVO MA 10 (Zeiss, Oberkochen, Germany) using secondary electron contrast mode with voltages of 10 kV.

Particle size distribution and size stability after 12 months storage

The particle size distribution was measured using laser diffraction (LD) to detect the presence of agglomerates in the suspension. Dynamic light scattering (DLS) was also used to characterize batches where the majority of particles were in the submicron size range.

LD

Samples were dispersed either according to the QC or biorelevant dispersion protocols described above. After the step 1 dilution, QC samples were added stepwise into 6 mL 0.3% Tween®80 solution until an optical density value of 3-5% was achieved. The instrument (Mastersizer3000, Malvern Panalytical Ltd., Malvern, UK) performed 10 consecutive measurements and calculated the average PSD. When using the biorelevant dispersion protocol, samples were added dropwise to 6 mL degassed cell culture medium (DMEM/F12 without phenol red) immediately after bath sonication until an optical density value of 3-5% was achieved (typically ~33 µg NPs per mL) and the PSD could be measured. Mie-Theory was applied using the following parameters for PET (RI: 1.636, absorption: 0.01) and PP (RI: 1.490, absorption: 0.01) at room temperature.

DLS

Samples were dispersed using the QC dispersion protocol and the step 1 diluted suspension was further diluted in distilled water to a concentration of 66 µg/mL. This was necessary to avoid turbidity and the measurement of Tween®80 micelles **(Figure 3.7)**. These samples (700 µL) were then measured in a disposable PS cuvette (semi-micro, 67.742, Sarstedt AG & Co. KG, Nümbrecht, Germany) with the Zetasizer Nano ZS (Malvern Panalytical Ltd., Malvern, UK). Measurements were conducted at 25°C in backscatter mode (NIBS, 173°) and the "general purpose" analysis model using the same material properties as for laser diffraction and the built-in values for water as medium (RI: 1.330, Viscosity: 0.8872 cp).

Determination of viable microorganisms

Determination of viable microorganisms was tested using the pour-plate method[171,172], employing Lysogeny broth (LB) agar for evaluation of aerobic bacteria and Sabouraud 4% glucose agar for fungi detection. NPs in glycerol were dispersed using the biorelevant dispersion protocol to achieve final concentrations of 10, 50 and 200 µg/mL. Sterile glycerol mixed with cell culture media in the same amounts as used for the NP dispersion was used as a vehicle control. Dispersions (1000 µL) were then added to the agar

plates and incubated for 3 days at 30°C (LB plates) or 7 days at 20°C (Sabouraud plates). The number of colony forming units (CFU) were counted and reported as CFU/mL. *Escherichia coli* and *Saccaromyces cerevisiae* were used as positive controls employing 10^{-9} and 10^{-5} serial dilutions, respectively.

Endotoxin content

Endotoxin content was assessed according to the STE-1.1 protocol issued by the Nanotechnology Characterization Laboratory using a limulus amebocyte lysate (LAL) assay (Pierce™ Chromogenic Endotoxin Quant Kit, Thermo Fisher Scientific Inc., Waltham, USA), including inhibition/enhancement controls with the same batches[201]. Briefly, samples were dispersed using the biorelevant dispersion protocol and diluted to a final concentration of 50 µg/mL in Dulbeccos Modified Eagle Medium with fetal bovine serum (DMEM/F12+10% FBS). Each sample (50 µL) was transferred into a pre-equilibrated (37°C) 96-well plate. Reconstituted amebocyte lysate (50 µL) was added and the mixture was incubated for 20 min. Subsequently, a reconstituted chromogenic substrate solution (100 µL) was added and incubated for another 6 min. The reaction was stopped with acetic acid solution (25%, 50 µL). The absorbance was read at 405 nm using a UV/Vis spectrophotometer (Epoch 2, Biotek Instruments Inc., Winooski, USA). Three technical replicates were measured per batch and the endotoxin level was calculated using standard curves ($R^2 > 0.980$). The mean limit of detection (LOD) and limit of quantification (LOQ) values for n = 5 calibration curves were 0.024 ± 0.009 EU/mL and 0.073 ± 0.028 EU/mL which corresponds to 0.002 ± 0.001 ng/mL and 0.007 ± 0.003 ng/mL, respectively[191,202] and are suitable for this study.

Osmolarity

DMEM and serial dilutions of DMEM + 10% FBS + penicillin/streptomycin ($DMEM_{compl.}$) with glycerol were prepared in triplicate ranging from 6.2 to 0.05% (w/v) glycerol. The freezing point depression was measured using a K-7400S Semi-Micro Osmometer (Knauer Wissenschaftliche Geräte GmbH, Berlin, Germany) and the average osmolarity values (mOsmol) were calculated from n = 3 replicates.

Cytotoxicity

The human bronchial cell line, Calu-3 (ATCC-HTB-55, LGC Standards Ltd., Teddington, UK) was used for determining the cytotoxicity of glycerol and NP dilutions in media. A 3-[4,5-dimethylthiazol-2-yl]-2,5 diphenyl tetrazolium bromide (MTT) assay was employed with passage numbers 11-36 (n = 11 biological replicate experiments). Glycerol concentrations ranged from 0.04 to 20% (w/w) which equated to 0.05 to 25% (w/v) based on the density of glycerol at 60°C (1.234 g/cm^3)[203] as heating is required by the dispersion protocol. Nanoplastic concentrations of 10 to 150 µg/mL were investigated. Cells were seeded at a density of 3 x 10^5 cells/mL and incubated overnight. Cells were then incubated with the samples for 24 h (37°C, 5% CO_2), after which the MTT stock solution (20 µL, 5 mg/mL) was added. After 3.5 h, formazan crystals were dissolved in dimethyl sulfoxide (100 µL) and the absorbance was measured at 570 nm. As positive control (0% viability), cells were incubated with Triton®-X100 (0.25%), whereas untreated cells served as negative control (100% viability). The cell viability was calculated by using the following equation:

Equation 3.4: Calculation of cell viability in %. ODsample = optical density of the treated cells; ODpos.ctrl = optical density of the positive control (0.25% Triton®-X100); ODneg.ctrl = optical density of untreated cells.

$$CV\ (\%) = \frac{OD_{sample} - OD_{pos.ctrl}}{OD_{neg.ctrl} - OD_{pos.ctrl}} \times 100 \quad \textbf{(3.4)}$$

Following guidance from the Nanotechnology Characterization Lab, the data is considered acceptable when the CV% was less than 50% for both control and sample replicates[204]. In our study, untreated cell controls exhibited a CV% of 12%, while CV% values of the treatment groups (when all test concentrations were pooled together) were 14%, 17% and 20% for nanoPET, nanoPP and glycerol samples, respectively. We therefore concluded that the data variability met standard acceptance criteria.

Data visualization and statistics

Raw data from laser diffraction (LD), dynamic light scattering (DLS) and ATR-FTIR measurements was exported with the respective software (Malvern's Mastersizer and Zetasizer software and SpectraGryph) and plotted with Python (3.11.0) using the Matplotlib library (3.6.3). Statistical tests were performed using a CI of 95% with Microsoft Excel (1808, Built 10415.20025) and the Numpy library (1.23.4) for Python.

3.3 Results and discussion

Statement of transparency

SEM images and the quantification of residual solvents (in particular benzyl alcohol and xylene) were kindly provided by Dipl.-Ing. (FH) Christiane Weimann from the Federal Institute for Materials Research and Testing in Berlin (BAM) and Dr. Gisbert Rieß from the Montanunivesität Leoben, respectively. Interpretation of the FTIR spectra was supported by Dr. Tassilo Waniek from the BAM. Toxicity testing of glycerol was performed by my colleague Jacqueline Schwarzinger. Tests for assessing microbial contamination, endotoxin content, and toxicity of the produced NPs were conducted by my colleague My Vanessa Ngyuen Hoang. Data on batch-to-batch reproducibility was obtained with help from Dr. Vesna Jovanovic from the University of Belgrade.

Shape and yields

The production of PET and PP NPs was based on a combination of the methods reported by Achilias *et al.* (2009)[126], Lee *et al.* (2022)[69], and Tanaka *et al.* (2023)[199]. These approaches used elevated temperatures to dissolve PET in benzyl alcohol (180°C; 50 mg/mL) and PP in xylene (140°C; 50 mg/mL) and injected the hot solutions into n-hexane (60 mL), methanol (60 mL), ethanol (100 mL) or DMSO (100 mL) at room temperature under stirring conditions. The solvents (benzyl alcohol and xylene) were subsequently removed by rinsing the nanosuspensions with acetone or hexane using a 0.2 µm PTFE or polyester filter. In order to avoid complications with high concentrations of DMSO, we chose to precipitate the PET and PP into ethanol as an anti-solvent and rinsing agent. In the final step, we used rotary evaporation to exchange ethanol with glycerol, a non-volatile, biocompatible storage medium with preservative properties **(Figure 3.2A-B)**[192].

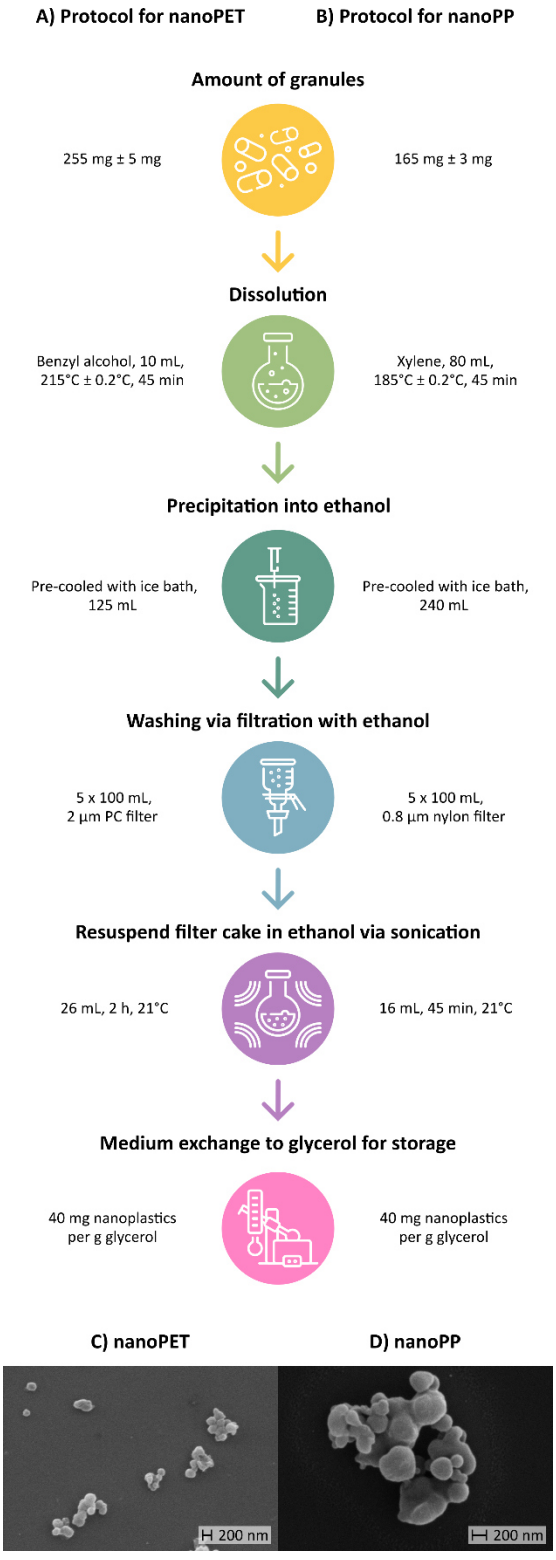

Figure 3.2: Production scheme of PET (A) and PP (B) nanoplastic suspensions. Overview of controlled parameters and the experimental settings used. Representative SEM micrographs of PET (C) and PP (D) nanoplastics.

SEM images of the nanomaterials produced in this manner revealed their roughly spherical shape **(Figure 3.2C-D)**. Primary particle sizes also correspond to the PSD profile obtained with complementary techniques **(see Chapter 0)**. Product yields for a typical batch size of 255 ± 5 mg and 165 ± 3 mg were 90.6 ± 3.3% and 91.2 ± 1.5% for PET and PP NPs, respectively **(Table 3.3, Table 3.4)**. Thus, 230 mg of PET and 150 mg of PP NPs can be produced with this method per day. This represents 5 (PET) and 3 (PP) vials containing 1 g of a 40 mg/g NP suspension in glycerol.

Table 3.3: Relative (%) and absolute (mg) yields of five individually produced PET nanoplastics. Means ± SDs are presented in the last row.

Sample	Yield % (absolute mg)
nanoPET_140	92.4 (237.1)
nanoPET_141	86.9 (223.6)
nanoPET_142	90.6 (230.1)
nanoPET_144	95.8 (247.8)
nanoPET_145	87.4 (225.9)
nanoPET_mean	90.6 ± 3.3 (232.9 ± 8.8)

Table 3.4: Relative (%) and absolute (mg) yields of five individually produced PP nanoplastics. Means ± SDs are presented in the last row.

Sample	Yield % (absolute in mg)
nanoPP_078	90.4 (153.5)
nanoPP_079	90.3 (151.8)
nanoPP_080	89.4 (149.0)
nanoPP_081	93.5 (156.3)
nanoPP_082	92.6 (152.1)
nanoPP_mean	91.2 ± 1.5 (152.5 ± 2.4)

Residual solvents, contact angles, and FTIR

Residual solvents (in particular benzyl alcohol and xylene) were quantified for a single batch of PET (#118) and PP (#077) NPs using GC-MS. Benzyl alcohol was not detected in either sample. Unquantifiable traces of xylene were only found in the PP sample.

The surface hydrophobicity was investigated with contact angle measurements and revealed larger contact angles (thus higher hydrophobicity) for PP compared to PET, which is expected based on the polymer structures **(Figure 3.3A)**. Heat treatment (heatPET: 128 h at 180°C; heatPP: 20 h at 140°C) was used to induce surface oxidation and act as a positive control resulting in smaller contact angles as expected. Surprisingly, both NPs (nanoPET/PP) showed significantly higher contact angles compared to the starting materials (nativePET/PP, native polymer granules), indicating an increase in surface hydrophobicity. This observation is likely an effect of the nanostructured topography of the compacted NP samples[205], commonly referred to as the lotus effect, which is known to increase surface hydrophobicity and water repellency[206].

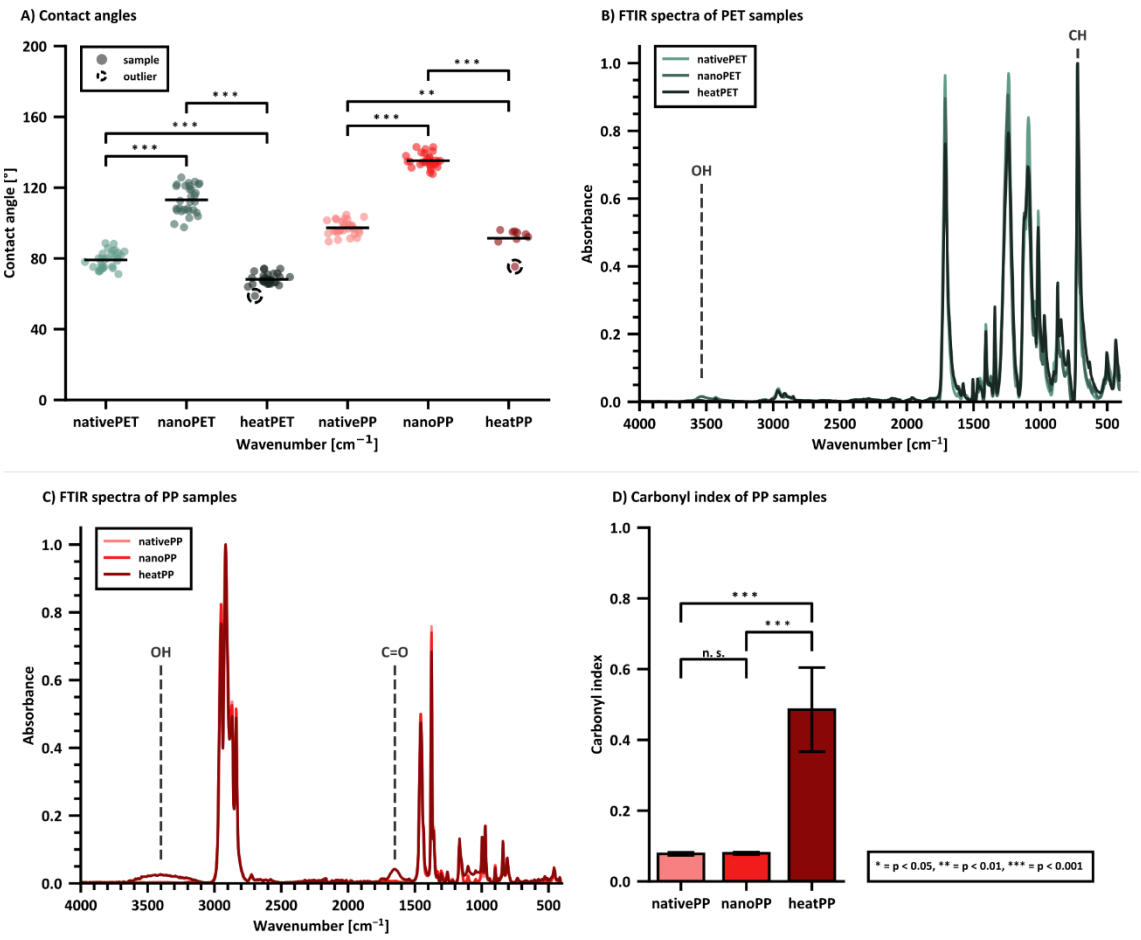

Figure 3.3: Surface hydrophobicity and bulk chemical composition of dried PET and PP nanoplastics (prepared from the intermediate ethanolic suspension) compared to the respective starting material was assessed *via* contact angle measurements (A) and ATR-FTIR spectra (B-C). The respective carbonyl index value of PP (D) was calculated from its ATR-FTIR spectrum. Contact angle measurements (30 droplets per material except heatPET with 9 droplets) were collected for one representative nanomaterial batch (PET: batch 118, PP: batch 077), while ATR-FTIR spectra were collected from five batches of nanoPET and nanoPP (measured in three technical replicates). Statistical significance was tested with a one-way ANOVA, where n.s. = $p > 0.05$, * = $p < 0.05$, ** = $p < 0.01$, and *** = $p < 0.001$.

ATR-FTIR was used to characterize the chemical composition of the nanomaterials. Bulk information on the entire particle is obtained since the penetration depth of ATR-FTIR is generally larger than the primary diameter. The PET/PP nanomaterials are compared to the starting materials as well as the native materials after heat treatment. Heat treatment did not affect both polymer types equally. Except for a slight colour change, PET did not show any other visual signs of degradation. PP turned intensively yellow and showed

surface cracks, hence oxygen was able to penetrate deeper layers of the material. As reported in literature, the IR spectrum of heat-treated PET (heatPET, **Figure 3.3B**) shows a broadening between 550-650 cm^{-1} of the peak at 720 cm^{-1} compared to the starting material (nativePET), which is attributable to aromatic C–H out of plane bending[207]. The spectrum of PET nanoplastic (nanoPET) mostly overlaps with nativePET and does not show the additional peaks of heatPET. Therefore, a chemical change due to the production process can be excluded. However, nanoPET shows an additional OH stretching vibration at 3200-3500 cm^{-1} which is likely a sign of residual solvent that could not be fully removed. It is hypothesized that the higher polarity of PET favors polar interaction with ethanol and hinders its complete evaporation, which may account for the absence of this band in the PP nanoplastic (nanoPP) spectrum. Another possibility is that this band originates from residual benzyl alcohol, which shows features in this area, although other stronger benzyl alcohol peaks are missing in the nanoPET spectrum.

The heat-treated PP (heatPP, **Figure 3.3C**) shows a pronounced carbonyl peak at 1650 cm^{-1}, smaller signals at 1550 cm^{-1} and 1750 cm^{-1}, and a broad absorption band between 3100-3650 cm^{-1} corresponding to formed hydroxyl bonds[208]. The overlay of the starting material (nativePP) and the PP nanoplastic (nanoPP) spectra did not show relevant differences, especially in the carbonyl region where heatPP did exhibit additional signals. It was therefore concluded that the production process did not alter the chemical profile of the PP and no residual solvents remained in the nanoPP. Additionally, the carbonyl index (CI) value can be calculated for aliphatic polymers like PP using **Equation 3.3** and provides information about the oxidation status of the material. The CI of nanoPP was similar to the nativePP but significantly lower than heatPP **(Figure 3.3D)**. ATR-FTIR spectra of five batches of both PET and PP nanoplastics also revealed a very low batch-to-batch variability **(Figure 3.4A-E, Figure 3.5A-E)**.

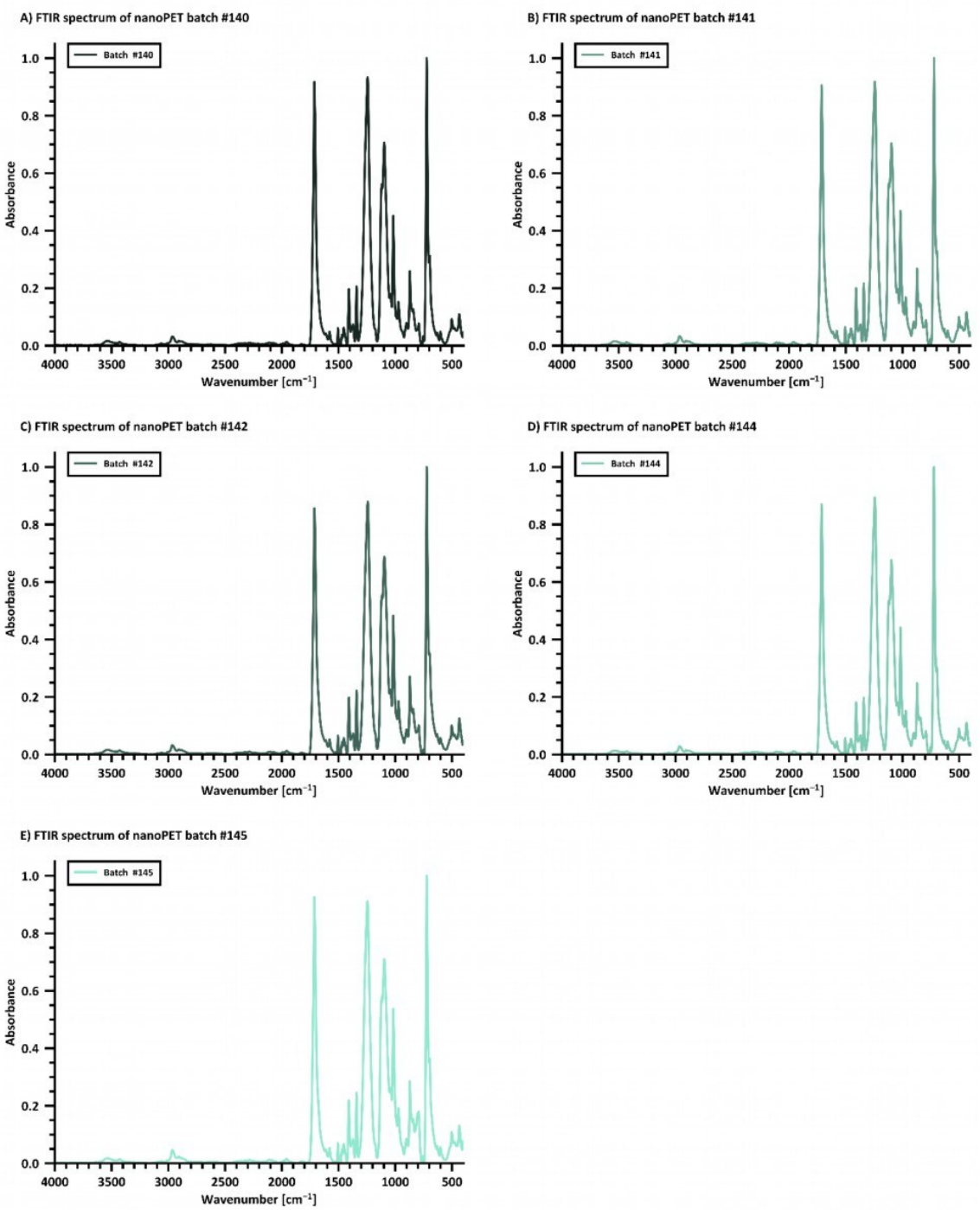

Figure 3.4: Individual ATR-FTIR spectra of the five discussed nanoPET batches (#140, #141, #142, #144, #145; A-E).

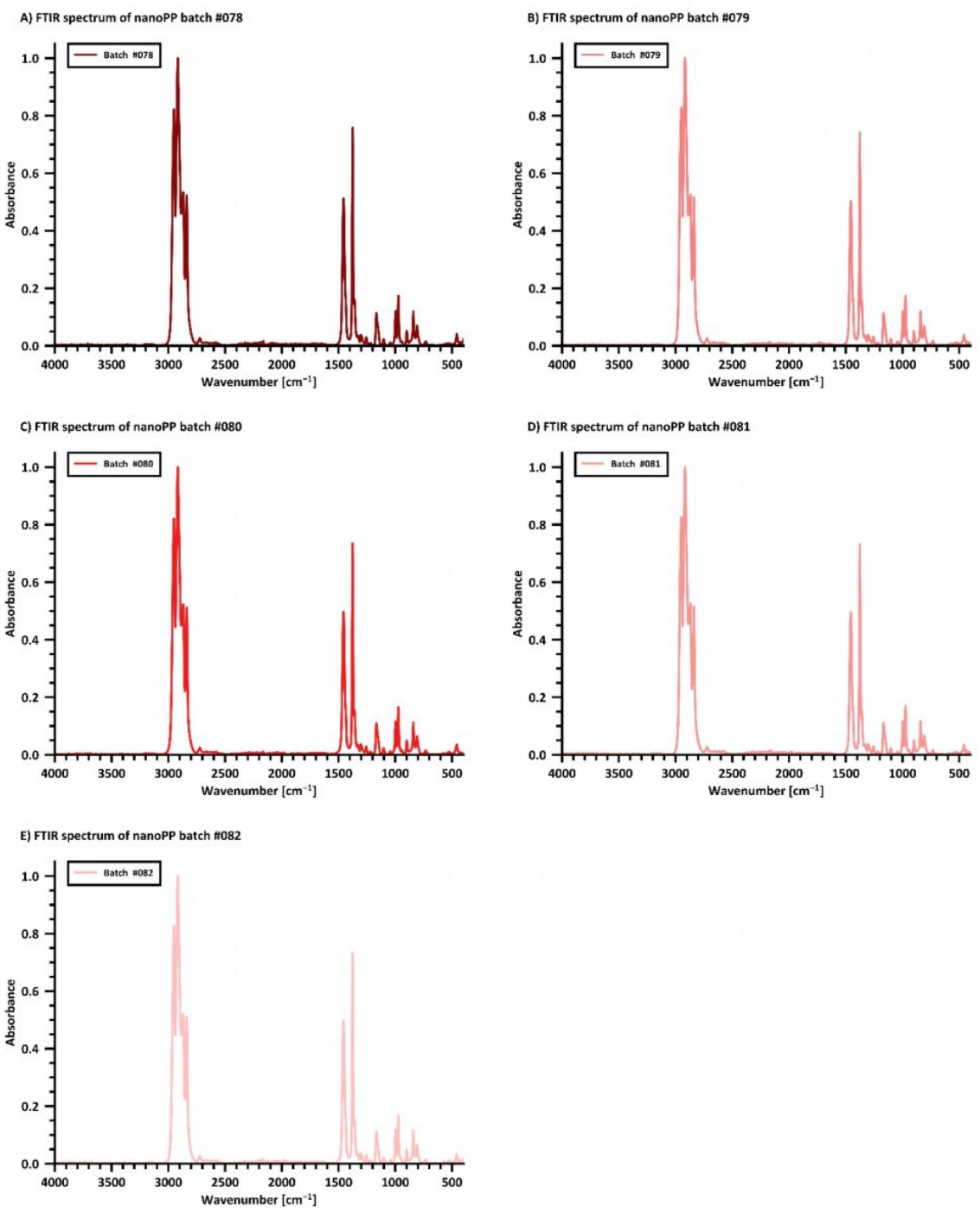

Figure 3.5: Individual ATR-FTIR spectra of the five discussed nanoPP batches (#078-#082; A-E).

Size distribution and reproducibility

The high surface hydrophobicity of the relatively pristine PET and PP NPs makes dispersion into aqueous media challenging. Pilot experiments indicated that high surfactant concentrations, high energy inputs *via* sonication and long sonication times were required to reliably deagglomerate as much of the nanosuspension as possible to reflect the primary PSD. An optimized QC dispersion protocol using a relatively high content of the non-ionic surfactant Tween®80 was developed specifically for determination of the PSD characteristics of the materials **(Figure 3.6A-B)**.

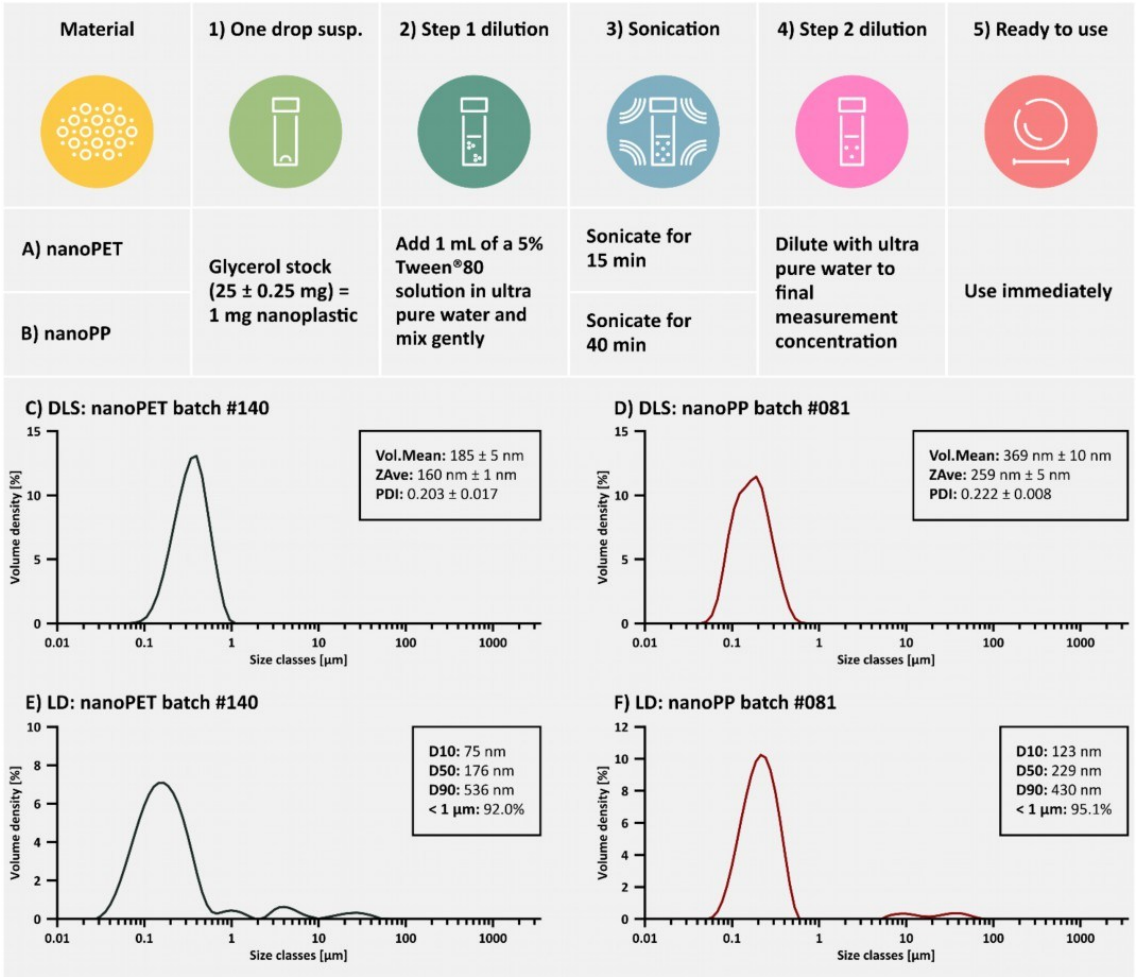

Figure 3.6: Comparison of DLS and LD particle size distribution curves for matched PET (C, E; batch 140) and PP (D, F; batch 081) nanoplastic samples dispersed from glycerol using the QC dispersion protocol (A-B). Common size descriptors from each measurement technique are provided in the insets.

Although DLS is considered the more appropriate method for determination of submicron-sized materials, this technique presented three major challenges for QC size measurements of the NPs: i) DLS does not cope well with the presence of micron-sized agglomerates in the system, ii) it has difficulties with very low or high density materials, which exhibit flotation or sedimentation during the relatively short DLS measurement times and iii) the final concentration of Tween®80 used in our QC dispersion standard operating procedure (SOP) is above the critical micelle concentration (CMC, 0.0014%, m/v)[209], resulting in the detection of Tween®80 micelles in the 10 nm range which has been reported previously[209,210]. **Figure 3.7** shows micelles of 7.3 ± 0.15 nm in a volume-based size distribution (8.4 ± 0.06 nm intensity-based distribution) of the used Tween®80 solution (5%, w/w) when measured with DLS. When larger particles are measured with Tween®80 above the CMC as dispersant, those micelles introduce a shift of the Z-Ave even when the micelle peak is not visible in the obtained graph.

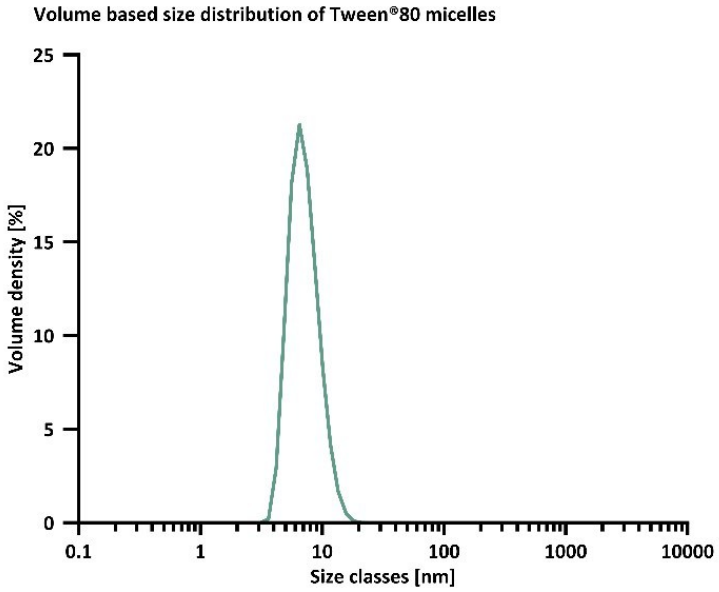

Figure 3.7: Volume based size distribution of Tween®80 micelles above the critical micelle concentration.

We therefore explored LD as a complementary technique for QC size measurements, which was not as sensitive to these issues. In fact, we found that the LD-generated PSD curves were more informative for QC studies of the NPs under a variety of conditions. Comparisons of DLS and LD measurements on the same batch of materials also show roughly similar values, demonstrating that size distribution profiles generated by LD can provide a fairly accurate depiction of the material size characteristics, dispersibility and batch-to-batch variability **(Figure 3.6C-F)**. It should be noted that the sizes generated by the respective scattering techniques are calculated hydrodynamic diameters of hypothetical spheres with the equivalent volume as the measured particle and are therefore less accurate for irregularly shaped particles[211]. This explains the differences between the observed diameters on SEM images and the hydrodynamic diameters.

Batch-to-batch variability of the ethanolic intermediate product

QC measurements of the ethanolic intermediate product revealed that particles < 1 µm were produced with high yields (> 90%) and low variability (< 5%) for both polymer types **(Figure 3.8, Table 3.5)**. The batch-to-batch variation, represented by D_{10} and D_{50}, was higher for PET than for PP but stayed below 13%. In this study, the use of surfactants was limited to QC measurements and avoided during production, which led to spontaneous agglomeration and a higher degree of variability, especially of the D_{90}. Furthermore, the pronunciation of larger particles in light scattering techniques (higher scattering intensity) also drives the variability in this size range[212]. However, the overlays of the size distribution curves of five produced batches show excellent similarity, especially in the desired size fraction < 1 µm.

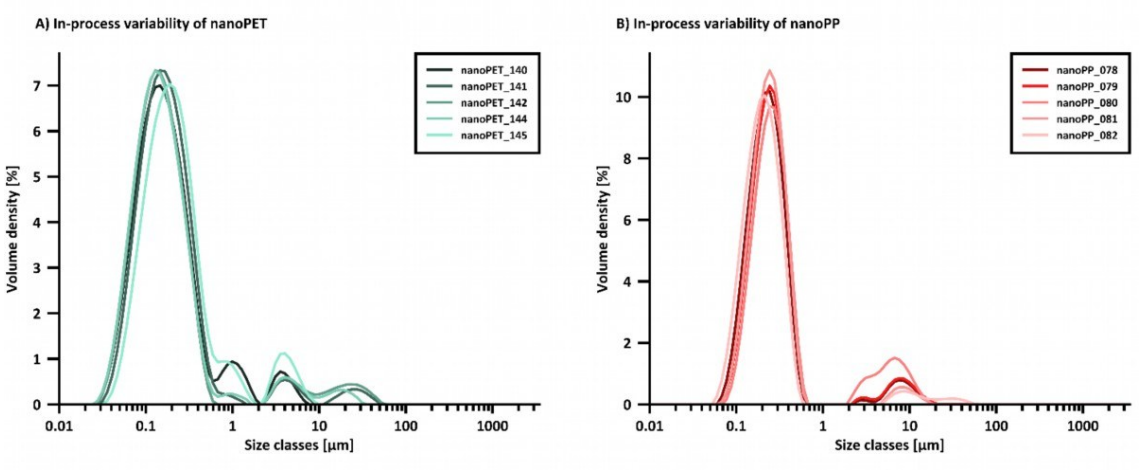

Figure 3.8: Comparison of in-process LD particle size distribution curves for five individually produced nanoPET (A) and nanoPP (B) batches dispersed in ethanol using the QC dispersion protocol.

Table 3.5: Size distribution data and % < 1 µm of nanoPET and nanoPP batches in-process controls of the intermediate product (in ethanol). Batch-to-batch variability is represented by mean ± SD (RSD%) of n = 5 batches per polymer type.

Polymer	Batch in ethanol	D_{10} [µm] (RSD%)	D_{50} [µm] (RSD%)	D_{90} [µm] (RSD%)	% < 1 µm (RSD%)
PET	#140	0.070	0.165	0.589	93.9
	#141	0.077	0.175	0.456	90.7
	#142	0.069	0.157	0.456	92.8
	#144	0.068	0.154	0.439	93.1
	#145	0.089	0.212	0.906	91.5
	Mean	0.0747 ± 0.008 (10.6%)	0.173 ± 0.021 (12.2%)	0.569 ± 0.177 (31.1%)	92.4 ± 1.1 (1.2%)
PP	#078	0.130	0.242	0.461	94.1
	#079	0.141	0.261	0.508	93.0
	#080	0.153	0.288	4.950	85.1
	#081	0.139	0.253	0.450	96.3
	#082	0.115	0.217	0.406	95.7
	Mean	0.136 ± 0.013 (9.3%)	0.252 ± 0.023 (9.2%)	1.36 ± 1.798 (132.7%)	92.8 ± 4.0 (4.3%)

Intra-batch variability (ethanol vs. glycerol)

To assess the difference between the size distribution of PET NPs before and after the medium exchange from ethanol to glycerol, a one-way ANOVA of the 10^{th}, 50^{th}, and 90^{th} percentile and the % < 1 µm was performed with a CI of 95%. No statistically significant difference between n = 5 individually produced batches of nanoPET was detected (D_{10}: p = 0.39, D_{50}: p = 0.33, D_{90}: p = 0.19, % < 1 µm: p = 0.25). In **Figure 3.9A-E**, the distribution curves of all five batches are depicted in ethanol (light color) and glycerol (dark color). Similarly, the five individually produced batches of nanoPP were assessed and no statistically significant difference between the abovementioned properties could be detected (D_{10}: p = 0.97, D_{50}: p = 0.91, D_{90}: p = 0.93, % < 1 µm: p = 0.95). The size distribution curves of the suspensions in ethanol (light color) and glycerol (dark color) are shown in **Figure 3.10A-E**.

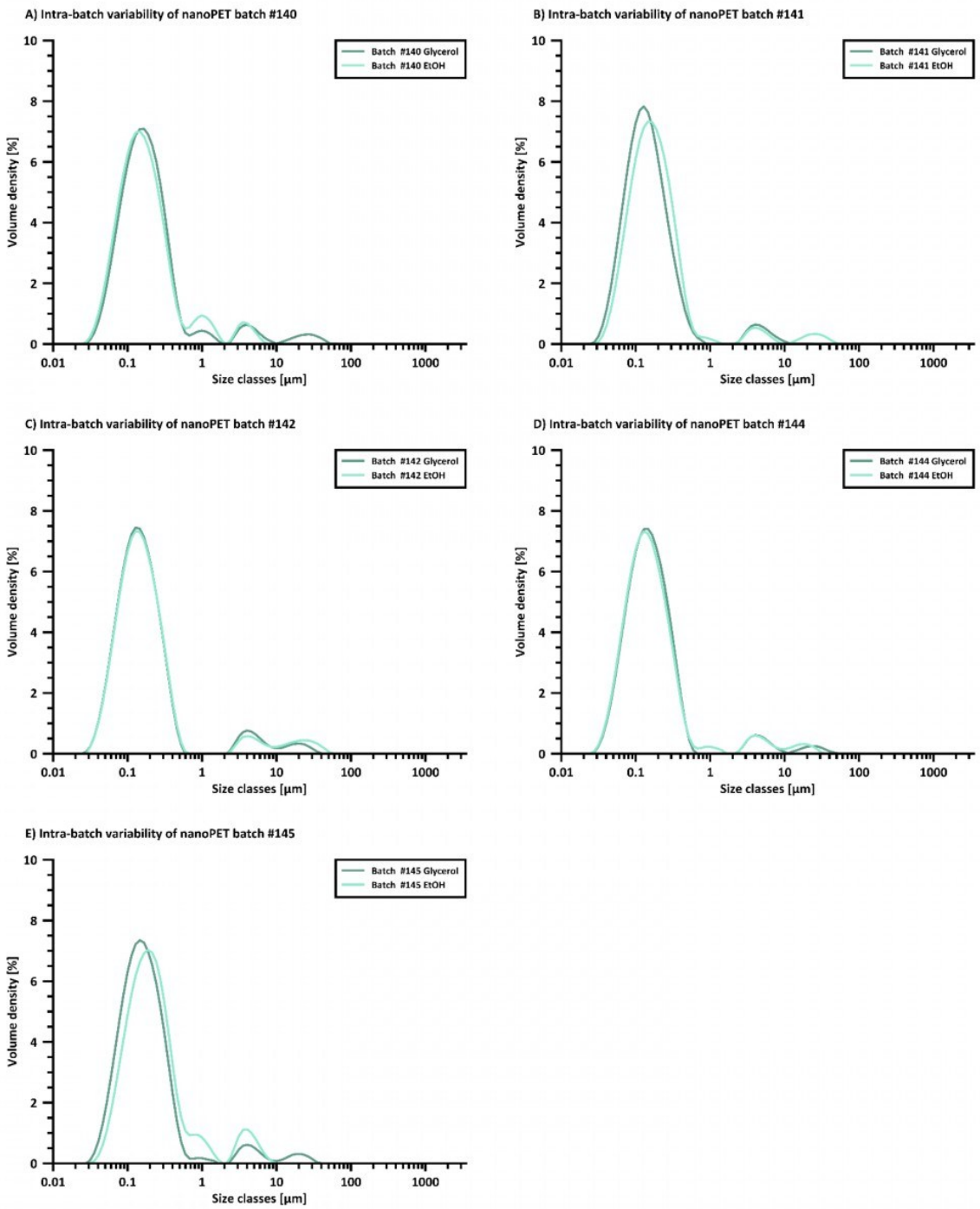

Figure 3.9: Intra-batch variability for nanoPET through medium exchange from ethanol to glycerol (A-E). A one-way ANOVA of the 10th, 50th, and 90th percentile and % < 1 µm did not show a statistically significant difference between ethanol and glycerol (CI: 95%).

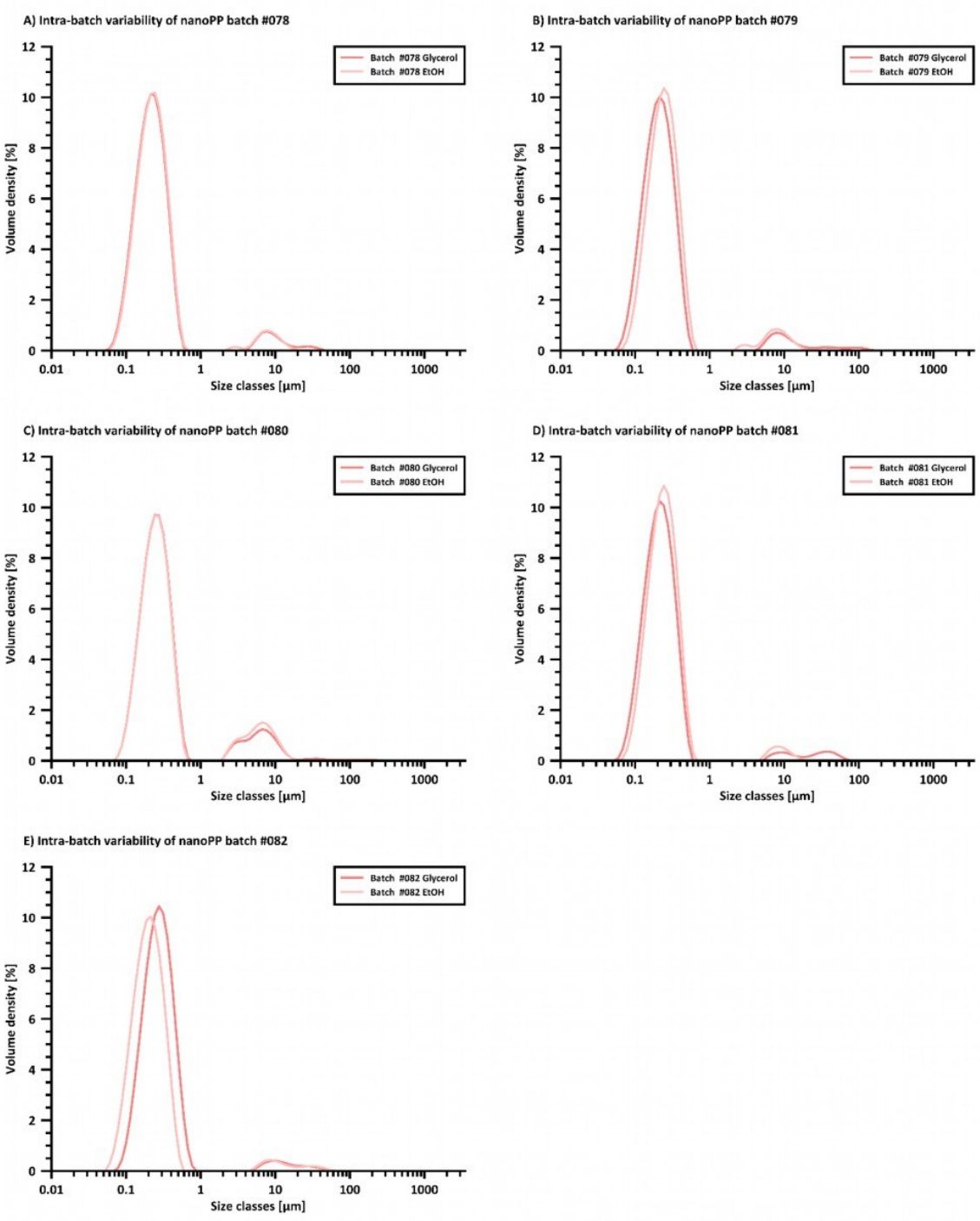

Figure 3.10: Intra-batch variability for nanoPP through medium exchange from ethanol to glycerol (A-E). A one-way ANOVA of the 10th, 50th, and 90th percentile and % < 1 µm did not show a statistically significant difference between ethanol and glycerol (CI: 95%).

Batch-to-batch variability of the final glycerol product

Batch-to-batch variability was evaluated using key particle size descriptors derived from LD measurements (D_{10}, D_{50}, D_{90}, and % < 1 µm). From the overlayed size distribution curves in **Figure 3.11A-B** it can be seen that each batch contains a small fraction of larger agglomerates in the micron size range, which cannot be fully dispersed despite the aggressive conditions of the QC dispersion procedure. During SEM imaging, no primary particles above 1 µm were detected. Although more images would be necessary for representative size analysis, only agglomerates were larger than 1 µm. Further, multiple measurements showed a higher variability of the D_{90} values (90% of the particle population has a particle size smaller than this diameter), but has less of an impact on the median particle size (D_{50}). Interestingly, the most stable and informative PSD descriptor is the percentage of particles in the submicron size range (% < 1 µm).

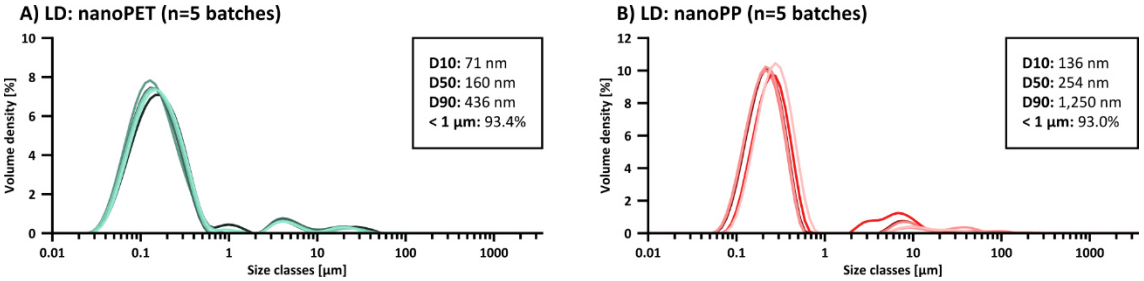

Figure 3.11: Batch-to-batch reproducibility of the particle size distribution is shown for n = 5 independent batches of PET (A) and PP (B). Common size descriptors from each measurement technique are provided in the insets.

It is worthwhile to mention that early batches (#100-107) of the PET NPs showed a higher prevalence of non-dispersible agglomerates. Investigations revealed that a slightly higher solution temperature (215°C) and tight control over temperature variations during the precipitation process (± 0.2°C) effectively increased the % of particles < 1 µm from 69 ± 6% (9% RSD) to 92 ± 1% (1% RSD) once a stricter temperature control was implemented.

Long-term stability of the final glycerol product

One batch of nanoPET and nanoPP was subjected to long-term storage at room temperature. The glycerol stocks were stored for 12 months in their primary package (1 mL glass HPLC vials) under light exclusion in a cardboard box. Samples were drawn immediately after production and after 6, 9, and 12 months. The QC dispersion protocol was applied and size distribution stability was assessed. The size distribution overlay of nanoPET **(Figure 3.12A)** shows that non-dispersible agglomerates form and shift from the 5 µm to the 20 µm region. However, changes of the properties of interest are negligibly small **(Table 3.6)**. RSDs of D_{10} and D_{50} are < 15% and therefore considered stable. The high RSD of D_{90} (121.9%) illustrates the formation of non-dispersible agglomerates and the % < 1 µm decreased by 1% but stayed high at 89.9%, thus meeting the specification of the TPP. The nanoPP size distribution curve shows a slight shift after 6 months but stayed unchanged thereafter **(Figure 3.12B)**. During 12 months, RSDs of D_{10} and D_{50} stayed below 15%, the % < 1 µm decreased by 6.3% but stayed high at 89.5% and was therefore also considered stable.

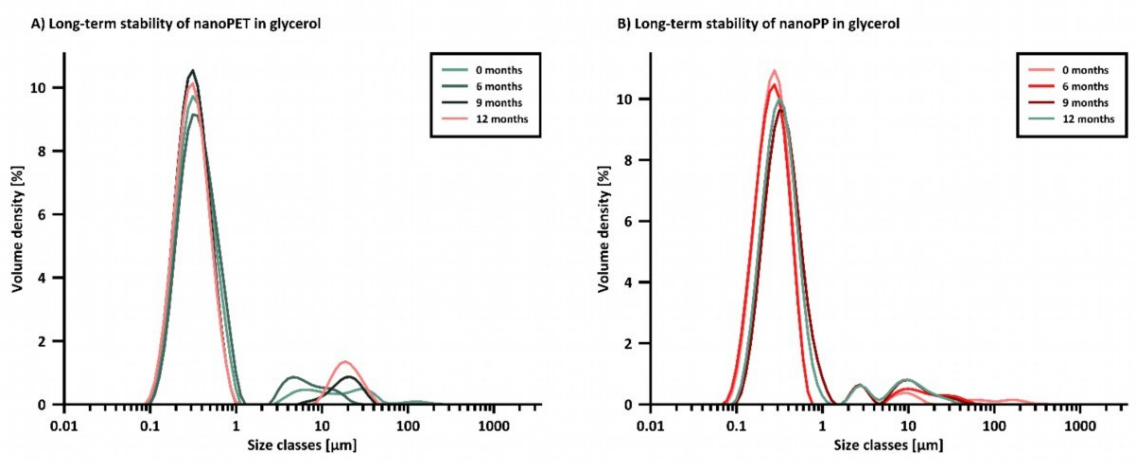

Figure 3.12: Size distribution curves of nanoPET (A) and nanoPP (B) stored for 0, 6, 9, and 12 months in glycerol. Stocks were dispersed according to the QC dispersion protocol.

Table 3.6: Size distribution data and % < 1 µm of nanoPET and nanoPP batches stored in glycerol at room temperature for 12 months. Variability is represented by mean ± SD (RSD%) of n = 4 sampling time points per polymer type.

Polymer	Sampling point	D_{10} [µm] (RSD%)	D_{50} [µm] (RSD%)	D_{90} [µm] (RSD%)	% < 1 µm (RSD%)
PET	0 M	0.202	0.374	0.917	90.9
	6 M	0.211	0.399	1.06	89.5
	9 M	0.191	0.343	0.714	93.1
	12 M	0.191	0.348	9.41	89.9
	Mean	0.199 ± 0.008 (4.2%)	0.366 ± 0.022 (6.1%)	3.03 ± 3.69 (121.9%)	90.8 ± 1.4 (1.5%)
PP	0 M	0.159	0.288	0.517	95.8
	6 M	0.155	0.286	0.546	94.0
	9 M	0.205	0.383	1.300	88.7
	12 M	0.193	0.356	2.160	89.5
	Mean	0.178 ± 0.021 (12.1%)	0.328 ± 0.042 (12.9%)	1.131 ± 0.672 (59.4%)	92.0 ± 3.0 (3.2%)

Dispersibility

To assess the PSD under conditions suitable for cell culture studies or indeed when studying the formation of an eco-corona on the NP surface[66,200], a dispersion protocol in biorelevant media is necessary. In the current study, we devised an exemplary biorelevant dispersion protocol suitable for cell culture studies using the protein, bovine serum albumin (BSA), as a primary dispersing agent. In this particular SOP, a two-step dispersion procedure was employed, in which the nanoPET or nanoPP test materials in glycerol were first dispersed in concentrated BSA (10%), followed by a second dilution (step 2 dilution) into complete cell culture medium (cDMEM = DMEM supplemented with 10% FBS and 1% penicillin/streptomycin) **(Figure 3.13A-B)**.

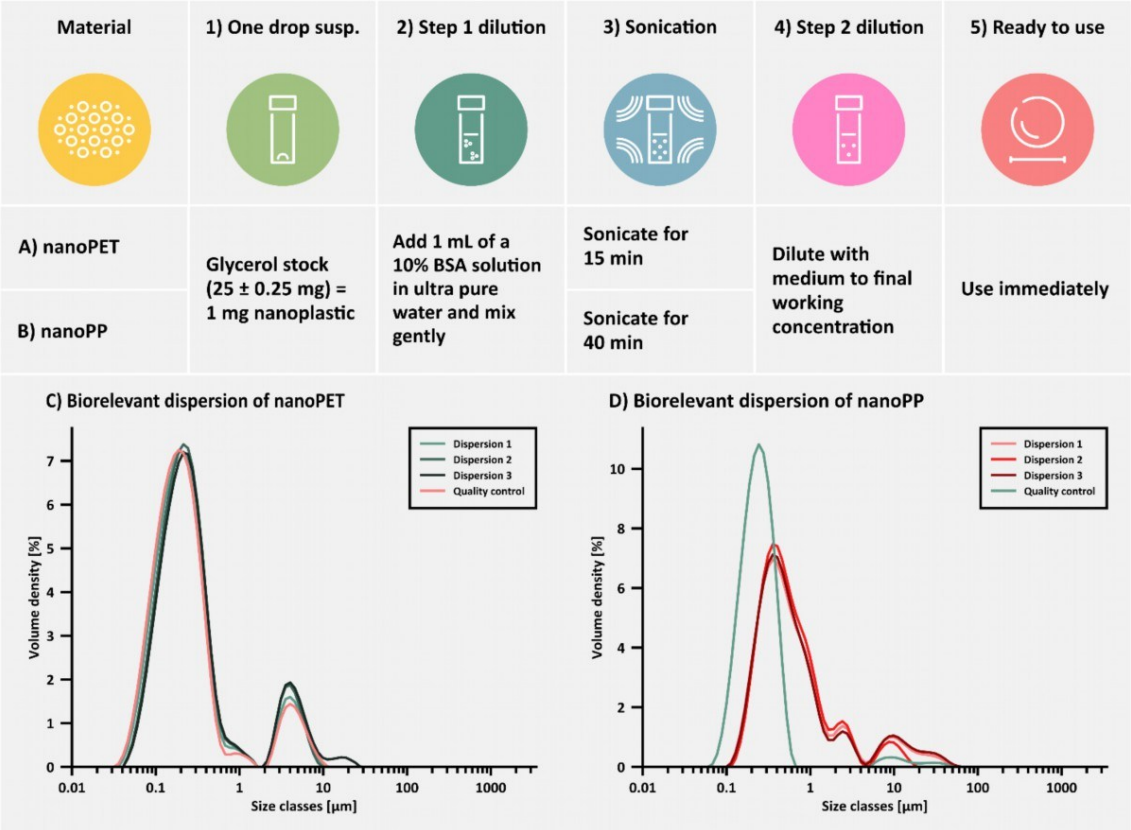

Figure 3.13: LD particle size distribution curves for PET (C; batch #121) and PP (D; batch #081) nanoplastic samples dispersed from glycerol using the biorelevant dispersion protocol (A-B; n = 3 dispersion events). The light red (PET) and light blue (PP) traces show the same batch of nanoplastics dispersed using the quality control protocol for comparison.

It was hypothesized that such a biorelevant dispersion protocol might not be as effective in preventing NP agglomeration compared to high concentrations of the synthetic surfactant, Tween®80 (QC dispersion). Fortunately, the more hydrophilic PET NPs could be fully dispersed using the biorelevant dispersion protocol showing no relevant differences to the QC dispersion protocol **(Figure 3.13C)** when applied to the same batch. In contrast, the more hydrophobic PP NPs showed a reproducible shift towards larger particle sizes using the biorelevant dispersion protocol **(Figure 3.13D)**. The % < 1 µm was slightly lower than the average dispersion using the QC protocol in both cases **(Table 3.7)**. Studies on the binding capacity and affinity of proteins (specifically BSA) to the PP and PET NP surface are scarce. We hypothesize that the experienced difference in redispersibility between PET and PP in

biologically relevant medium is mainly driven by their different physicochemical properties. A study on PS showed that surface hydrophilization *via* aging alters protein adsorption and increases the adsorption of hydrophilic proteins[213]. Notably, pristine (more hydrophobic) PS particles showed only minor protein adsorption, while aged (hydrophilized) PS particles were entirely covered[213]. This study was carried out with bronchoalveolar lavage fluid, which another study used to determine the protein binding capacity of PET (0.224 ± 0.005 mg/g)[107]. Further, the binding of BSA on PET MPs and its stabilizing effect hast been described[214]. Unfortunately, no such experimental data exists for PP NPs. Computational models showed that hydrophobic interactions with hydrophobic and aromatic amino acids are highly relevant in the protein adsorption process for PP[215]. Studies on PP MPs showed binding of BSA to some extent with stronger binding of a pure protein (BSA) than a protein mixture (yeast extract in this example)[130]. This is in line with our observations, that pure proteins (BSA, OVA) are more effective than mixtures (like FBS). Based on those findings, we hypothesize that BSA has a higher affinity towards the more hydrophilic PET and, thus, disperses PET NPs more effectively than PP NPs. However, this has to be confirmed by measuring the binding affinity and capacity of BSA on our PET and PP NPs. A range of different biorelevant proteins and ecologically relevant surfactants[66,73] are currently under investigation for their ability to homogenously disperse the PET and PP NPs studied here but preliminary results indicate that each dispersing agent behaves differently, therefore requiring the development of bespoke dispersion protocols for every new system.

Table 3.7: Size uniformity of PET and PP nanoplastic glycerol batches following dispersion using the biorelevant dispersion protocol (n = 3 separate dispersion events from a single batch). Particle size distribution descriptors were derived from LD measurements. D_{10}: 10% of the particle population has a particle size smaller than this diameter, D_{50}: median, D_{90}: 90% of the particle population has a particle size smaller than this diameter. Values depict the mean ± standard deviation values with the relative standard deviation (%) provided in parentheses. Please note, diameters are reported in µm.

System	Dispersion SOP	D_{10} ± SD [µm] (RSD%)	D_{50} ± SD [µm] (RSD%)	D_{90} ± SD [µm] (RSD%)	% < 1 µm ± SD (RSD%)
PET	Biorelevant (n = 3 dispersions from batch #121)	0.101 ± 0.005 (5.1%)	0.236 ± 0.012 (5.2%)	3.33 ± 0.45 (13.4%)	86.5 ± 1.7 (1.9%)
PP	Biorelevant (n = 3 dispersions from batch #081)	0.241 ± 0.005 (1.9%)	0.528 ± 0.004 (0.7%)	4.64 ± 1.93 (41.7%)	74.5 ± 1.3 (1.8%)

Determination of viable microorganisms & endotoxin content

Due to the usage of volatile solvents and elevated temperatures, it was not possible to produce PET and PP NPs under fully aseptic conditions. However, the utilization of organic solvents in clean fume hoods combined with minimal handling steps should theoretically minimize accidental contamination with viable microorganisms as well as fungal spores from the ambient lab environment. Testing of 22 batches of PET and PP NPs for microbial growth was performed with materials diluted to 10, 50 and 200 µg/mL using the biorelevant dispersion protocol. None of the batches tested showed evidence of microbial contamination (0 CFU/mL). Positive controls with *Escherichia coli* (641 ± 187 CFU/mL) and *Saccharomyces cerevisiae* (452 ± 51 CFU/mL) were performed to verify assay functionality. Negative controls with glycerol diluted in cell culture medium and sterile water (0 CFU/mL) were also carried out. Additionally, an unopened vial of the PET batch #025 and PP batch #026 was tested after 10 and 12 months storage at ambient room temperature. Neither sample showed any indication of microbial growth.

Endotoxin content of cell culture medium controls, and NPs diluted to 50 µg/mL using the biorelevant dispersion protocol (n = 13 batches) did not reveal any values above the LOD (0.024 ± 0.009 EU/mL). Thus, we conclude that the respective NP preparation methods did not result in measurable endotoxin contamination. The results demonstrate that the material also does not exceed the suggested maximal contamination value of 0.1 EU/mL

recommended by Li *et al*. for *in vitro* experiments[164–166]. It must be noted that non-endotoxin pyrogens or other bacterial/fungal or viral contaminants can also influence *in vitro* and *in vivo* tests[216]. The Ph. Eu. 11 (Chapter 5.1.10) approves the monocyte activation test to assess for non-endotoxin pyrogens and should be employed in future studies, especially when larger batches are produced.

Osmolarity and cytotoxicity

When diluted directly into cell culture medium, residual glycerol can contribute to an increase in osmolarity **(Table 3.8)**. The osmolarity of the test system is important for cytotoxicity studies, since both hypo- and hypertonic samples can stress cells causing artefactual cellular responses [217–220], which could be mistakenly attributed to the test material. Many cell types can tolerate deviations from physiological osmolarity from approximately 290 – 390 mOsmol, although certain cell types can be more sensitive than others[221,222]. Therefore, testing of vehicle controls (including glycerol in this case) is always recommended. **Table 3.8** provides an overview of the respective amounts of glycerol and NPs present in a series of dilutions prepared with the biorelevant dispersion protocol. The corresponding osmolarity values from three replicate measurements are provided showing that dilutions exceeding 0.8% (w/v) glycerol exhibit hyperosmotic characteristics, i.e. an osmolarity > 400 mOsmol.

Table 3.8: Mean osmolarity values of different amounts of glycerol (% w/v) added to DMEM + 10% FBS. Values represent the mean and standard deviation of n = 3 experiments. *Nanoplastic concentrations in each dilution are calculated based on application of the biorelevant dispersion protocol for a nanoplastic sample in glycerol (40 mg plastic/g glycerol).

Vehicle	Amount of glycerol (%, w/v) added	Nanoplastic concentration (µg/mL) in dilution*	Osmolarity (mOsmol)
DMEM	0	-	314 ± 2
DMEM + 10% FBS	0	-	319 ± 3
	0.05	20	323 ± 1
	0.1	40	326 ± 1
	0.2	80	336 ± 2
	0.4	160	351 ± 12
	0.8	320	394 ± 2
	1.6	640	485 ± 4
	3.1	1240	656 ± 4
	6.2	2480	1009 ± 12

To characterize the effects of the PET and PP NP test materials (and their possible content on residual components) on cell viability, *in vitro* cytotoxicity experiments were performed. First, the effects of pure glycerol added to cell culture medium in concentrations ranging from 0.05-25% w/v were assessed **(Figure 3.14A)** followed by experiments evaluating the effects of NPs diluted in cell culture medium (nominal particle concentration: 10-150 µg/mL; **Figure 3.14B-C**) which corresponds to a glycerol concentration of 0.025-0.38% (w/v). The MTT assay, which measures the metabolic activity of cells, was performed using a human bronchial cell line (Calu-3). Cells were incubated with the test systems for 24 h and the cell viability compared to the untreated control group was determined. When comparing the cytotoxicity results of the nanoPET (density: 1.38 g/cm^3)[223] with the nanoPP (density: 0.90 g/cm^3 according to the material data sheet) data, it should be noted that a higher concentration of the nanoPET is expected to reach the Calu-3 cell layer *via* sedimentation and diffusion processes[224–226] compared to the low-density nanoPP, which will be prone to flotation. At the highest concentration of nanoPP tested, the cell viability appeared to decrease but not significantly. Ongoing studies using an expanded concentration range are underway to determine whether this is a real sample-induced

effect, an effect of the vehicle, which might include residual production components or a particle-induced effect.

As described above, the optimal osmolarity for Calu-3 cells ranges from 290-390 mOsmol. This corresponds well with our observations that glycerol is well-tolerated up to 0.8% (w/v) (394 ± 2 mOsmol) over a 24 h period **(Figure 3.14A)**. At higher glycerol concentrations, the cell viability drops below the 70% cytotoxicity threshold defined by ISO 10993[227]. Shorter incubation times will enable the use of a higher glycerol content. For example, R. Scherließ (2011) reported that Calu-3 cells exposed to increasing concentrations of glycerol for only 4 h exhibited a half-maximal cytotoxic concentration (CC_{50}) of 2.8 mol/L (3457 ± 12 mOsmol), i.e. nearly 10-fold higher than the CC_{50} value determined for a 24 h incubation[182]. Presence of the NPs up to concentrations of 150 µg/mL (containing ~0.4% w/v glycerol), showed no reduction in cell viability over 24 h **(Figure 3.14B-C)**. The tested plastic concentration range corresponds to the most commonly used concentration range for *in vitro* cytotoxicity experiments in this field of study[228–230] supporting the conclusion that the amount of glycerol used as a storage medium should not negatively impact cytotoxicity studies up to these NP concentrations. However, further studies with a wider range of cell types, including different cell lines and primary cells, are underway to determine the wider applicability of this conclusion. It is also important to highlight that the impact of glycerol on the function of a wider range of biological assays should be assessed.

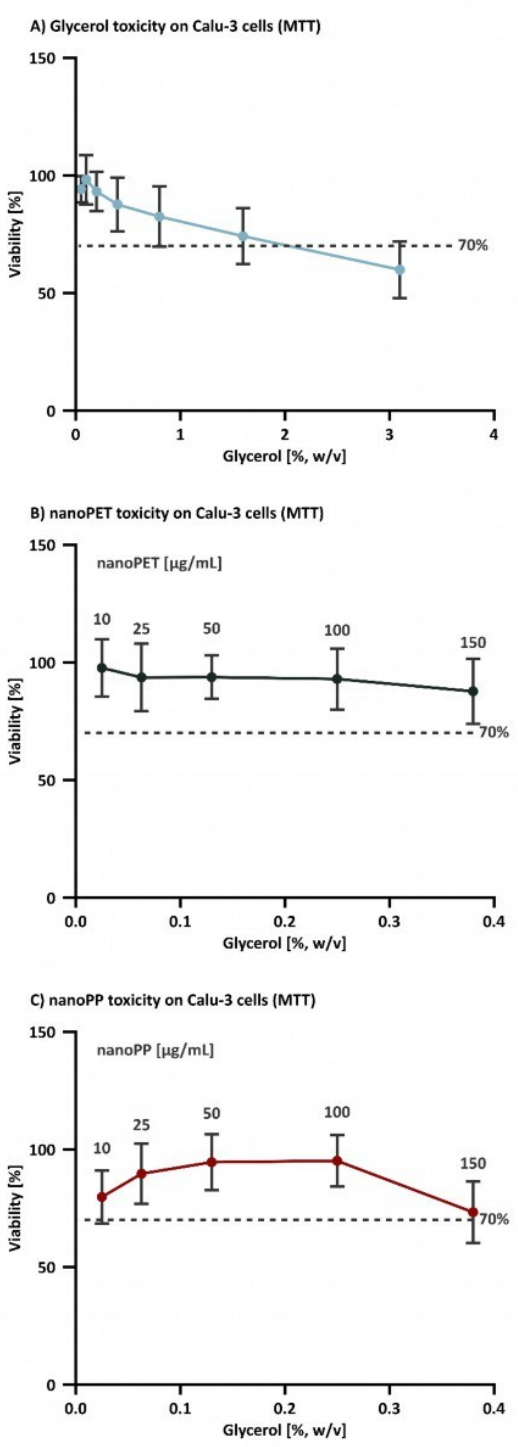

Figure 3.14: Viability of Calu-3 cells after 24 h exposure to different test systems: (A) Glycerol in concentrations of 0.05; 0.1; 0.2; 0.4; 0.8; 1.6; 3.1% (w/v). Values presented are the mean and standard deviation from n = 11 replicate experiments with different cell passage numbers. The viability of Calu-3 cells incubated 24 h with PET (B) and PP (C) nanoplastics diluted to 10-150 µg/mL (containing 0.025; 0.063; 0.13; 0.25; 0.38% (w/v) glycerol). Values presented are from n = 5 replicate experiments.

Study limitations and future perspectives

The encouraging results regarding yield, reproducibility, dispersibility, and stability demonstrated the potential of the PET and PP NPs as viable test materials. However, there are some points to consider on the way to gain reference or certified reference material status. Non-solvent nanoprecipitation in ethanol enables rapid NP generation, but particles are always spherical with a smooth surface structure – although not perfectly spherical like PS beads. Particle morphology is an important point to consider because it can affect colloidal stability[231], biological interactions[232], and toxicity of NPs[233]. Lee *et al*. (2022) showed that by using water as non-solvent, alternative surface structures can be obtained[69]. Thus, investigation of other non-solvents could further broaden the spectrum of available test materials that resemble the environmental situation.

Relative yields were high compared to other methods, but absolute yields were still limited and one of the reasons that content homogeneity studies were not performed in the current work. However, scale-up from tens to hundreds of milligrams was possible without much optimization effort when ratios were kept constant. Future investigations should focus on switching from manual towards automated methods. For example, if a temperature controlled automated pump system could be employed for the precipitation step, yields up to gram amounts per batch are feasible and even a continuous precipitation process could be developed. After large-scale production, homogeneity according to the ISO 33405:2024 standard[115] needs to be demonstrated before gaining reference material status. Independent confirmation of CQAs such as PSD, sterility and endotoxin content should also be performed *via* an inter-lab comparison study.

It was notable that dispersion of the nanoPP in biorelevant media could not achieve the original PSD requiring further development work. Further aspects which require additional investigation include storage stability over longer time periods and in-use shelf-life. Glycerol is known to be hygroscopic when used in high concentrations[192]. Although no noticeable change in PSD, microbial growth or endotoxin content was observed within 12 months in unopened containers, we have not yet extensively investigated these parameters under in-use conditions, i.e. multiple openings of the vials. It is recommended to assess long-term stability complying with the ISO 33405:2024 standard[115] in further studies and

whether the glycerol storage medium does not interfere with a wider panel of commonly used biological assays at concentrations present following dilution. Finally, a broad discussion including international organizations, policy makers and the research community is needed to refine the proposed TPP and provide guidelines for reference material producers of NPs for intended use in biological assays.

3.4 Conclusions and contributions to the field of research

To our knowledge, there are currently no NP reference materials certified specifically for use in *in vitro* and *in vivo* biological assays. Therefore, there is also no precedence for the development of this type of reference material. On the other hand, the research community has reported an urgent need for well-defined NPs for an intended use in biological and toxicology studies[68,70–74], thus, there is a strong rationale for exploring the boundaries of reference material development. Based on the more complex requirements for intended uses in biological systems, it may be necessary to expand the certification criteria and include further CQAs, such as colloidal stability in complex aqueous media, sterility and endotoxin content.

Using a QbD inspired approach to product development, PET and PP NP research grade test materials were developed in this study for intended use in biological assays. Encouragingly, the data generated here indicates that these prototype NPs are suitable in terms of PSD, uniform dispersibility, size stability over 12 months storage, sterility, low endotoxin content and biocompatibility for their intended use. Compared to other published test systems, CQAs for biological assays were considered (sterility, endotoxins, solvent residues), material and study comparability were assured (batch-to-batch variability, storage stability) and practicality through transparent reporting of production time and yield has been shown. With the current approach, five out of six requirements of the proposed TPP **(Table 3.1)** could be fulfilled for both nanomaterials **(Table 3.9)**.

Table 3.9: Development status of PET and PP nanoplastic test materials > 1 µm. The performance of the current materials is compared to the critical quality attributes (CQAs) derived from the target product profile.

CQAs	Status description	Status
Homogeneity of particle concentration (uniformity of NP content across several units).	Not tested but a range of 85-115% of the target value is proposed.	☒
Homogeneity of the particle size distribution profile.	After production, it was achieved that > 85% of the particles are < 1 µm using the validated QC dispersion protocol.	☑
Stability of the particle size distribution profile.	It was achieved that the D_{10} and D_{50} measured after 12 months storage at ambient room temperature did not differ > 15% from the original values and the % < 1 µm did not drop below 85%.	☑
Sterility after manufacture and storage.	Sterility (0 CFU/mL) after production and 12 months storage of unopened containers at ambient room temperature was achieved.	☑
Low endotoxin content measured after manufacture.	Endotoxin levels below the recommended threshold (< 0.1 EU/mL[191]) were achieved.	☑
Minimal residual solvents from the production process.	This was achieved, as only unquantifiable trace amounts of xylene were measured (< 1%).	☑

In the course of this investigation, the importance of optimized, bespoke dispersion protocols for NPs in biorelevant media became increasingly evident. For potential users of these test materials this would mean that the responsibility of optimizing and validating biorelevant dispersion protocols for different dispersion media would fall to individual laboratories. With the help of a validated QC dispersion protocol and an example of a bespoke biorelevant dispersion protocol, we have provided a workflow which users can adopt to assess the impact of their own dispersion process on the NP size distribution profile, which is one of the most important variables tested in studies on particle toxicity. In conclusion, research grade test materials comprised of PET and PP NPs were developed with promising perspectives to achieve wider spread use in biological assays examining the impact of NPs on human health.

Chapter 4

Micro- and nanoplastics in aerosols: Method development and validation for the use of a glass liquid impinger as a sampling device

4 Exposure assessment: MNPs in sea spray aerosols

4.1 Introduction and background

This study was part of the IMPTOX project, with the aim of quantifying MNP exposure levels through inhalation of sea spray aerosols (SSA). As described in **Chapter 1** , Allen *et al*. (2020) showed that SSA can contain MPs from the ocean, but due to methodological limitations (filter mesh sizes and µ-FTIR imaging method), only particles > 10 µm could be sampled and detected[62]. Particles < 10 µm however, are of particular interest for inhalation exposure assessment as the aerodynamic diameter of a particle determines its deposition pattern and penetration depth into the respiratory system, with nanoparticles even reaching alveoli[234]. This nano fraction is of concern as it has been shown that NPs can cross biological barriers and potentially cause inflammation and cell death[235]. Information on environmental concentrations of MNPs is scarce but crucial to estimate health risks.

Why use a glass liquid impinger for aerosol collection?

There are various devices used to sample air but the desire to work with plastic free devices drastically reduces the available options. In a WHO report on inhalation exposure to MNPs, liquid impingers are explicitly mentioned as options for suitable sampling devices[25]. The European Pharmacopoeia (Ph.Eur.) describes devices for the characterization of fine particulates in aerosols. Among the described devices, a two stage glass liquid impinger (GLI) with high volume airflow is described[236]. The rationale for choosing this device included the following points: i) the device is entirely made of glass which prevents contamination through plastic parts, ii) particulates are divided into upper airway and lower airway depositing particles based on their aerodynamic diameter, and iii) the particulates are captured in a liquid matrix, which is easy to remove for further analysis. Although this device is standardized and easily available, it is not a standard method for environmental air sampling.

Glass liquid impinger characteristics

Aerosol particulate matter (PM) is a complex mixture of airborne particles. Particles are classified by their aerodynamic diameter, which takes the size, shape and density of the particles into account and therefore describes possible deposition patterns of airborne particles in different regions of the lung[137,142]. The WHO differentiates between inhalable particles (aerodynamic diameter < 100 µm) – which usually deposit in the nose and upper airways and are subsequently swallowed[237,238] – and respirable particles (aerodynamic diameter < 10 µm), where the probability of particle deposition in the peripheral lung is dependent on the aerodynamic diameter[239,240]. WHO guidelines focus on $PM_{2.5}$ and PM_{10} which are defined as particles with an aerodynamic diameter below 2.5 µm and 10 µm respectively[142]. They are of special interest because associations between short- and long-term exposure and adverse health effects have been shown[241–243].

First described by Hallworth & Westmoreland[244], the GLI geometry and constant airflow of 60 ± 5 L/min, within the range of human respiration rates, leads to the separation of particles by their aerodynamic diameter. Particles above an aerodynamic diameter of 6.4 µm will impact at the mouth and throat piece (MTP) or upper compartment (UC) and represent the upper respiratory tract fraction, whereas particles below that size will deposit in the lower compartment and account for the lower respiratory tract fraction **(Figure 4.1)**. Although impingers are commonly used to collect bioaerosols[245], the collecting efficiencies for aerosolized PS particles < 1 µm was found to be less than 20%[246]. This highlighted the need for optimizing the method to be suitable for collecting both MPs and NPs from air.

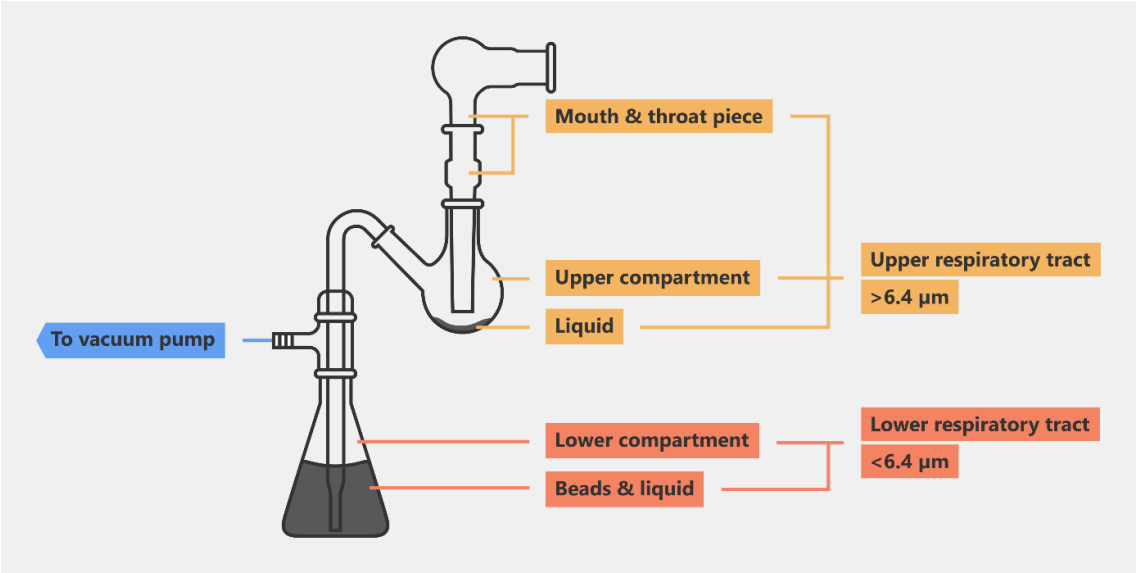

Figure 4.1: Scheme of the glass liquid impinger (GLI). Samples from the mouth and throat piece (MTP) and upper compartment (UC) are combined and separated from samples from the lower compartment (LC).

Use of granular bed filtration to increase ultrafine collection efficiency

Depending on the particle size, studies from Spanne *et al.* (1999) and Hogan *et al.* (2005) found that the collection efficiency of liquid impingers for particles between 20-700 nm and 30-100 nm were < 20% and < 10% respectively[246,247]. Modifications like the use of frits increased the collecting efficiency for particles < 220 nm to 30-95% but complicate particle harvest for further analysis, similar to filters[248]. Yu *et al.* (2016) reported that the poor collection efficiency of commonly used impingers for ultrafine particles can be drastically enhanced when employing so called granular bed filtration. They showed that through the introduction of glass beads (d = 3 mm) into the collection chamber collecting efficiencies up to 99% were achieved for particles from 20-400 nm. Factors like the sample liquid volume, depth of the packed beads, and flow rate played a role, where larger sample liquid volumes and higher depth of beads showed higher collection efficiencies[249]. Changing the flow rate was not feasible for this study since it would change the particle size cut-off between the two compartments and possibly not reflect human respiration rates anymore. Based on the findings from Yu *et al.* (2016), we used ceramic beads of a similar size (ZrO_2, d = 2.6-3.3 mm) to optimize the standard GLI method and increase the collecting

efficiency for submicron-sized particles when using the GLI as sampling device to capture MNPs from aerosols.

Why use TED-GC-MS for MNP identification and quantification?

Analysis of the captured aerosol samples is challenging due to overall low expected concentrations of MNPs in air and the small size of the fractions of interest (**see Chapter 0**). As described in **Chapter 0**, especially particles < 10 µm are relevant for the inhalation exposure route due to their ability to reach deeper regions of the lung where they eventually accumulate and cause adverse effects like inflammation through activation of macrophages[159], or cellular senescence that can cumulate in pulmonary fibrosis[250]. Indeed, a recent study found that PS MNPs (80 nm and 1 µm) triggered fibrotic responses in the lung of mice after 60 days of whole-body inhalation exposure. Ultimately, exposed mice developed pulmonary fibrosis where the larger 1 µm particles caused more severe lung toxicity than the 80 nm particles[251]. However, number-based methods like spectroscopy (FTIR, Raman) or microscopy (SEM, TEM) are either not sensitive enough to detect such small particles or time-consuming sample preparation is necessary (e.g. removal of the matrix and interfering compounds). Mass-based thermoanalytical methods like pyrolysis gas chromatography coupled with mass spectrometry (Py-GC-MS) present a viable alternative because they provide qualitative (sample chemistry) and quantitative (sample mass) information and are not limited to a specific particle size[251]. Classical Py-GC-MS, however, has two disadvantages: i) only small sample volumes can be measured (sample mass < 1 µg), and ii) sample preparation is needed to remove interfering matrix compounds.

Goedecke *et al.* (2022)[252] used thermal extraction-desorption GC-MS (TED-GC-MS) for the analysis of MNPs in wastewater treatment plant effluents. With this method, comparably high sample masses of 10-50 mg can be measured. The sample is decomposed *via* heating (600°C) in a thermobalance, providing information on mass loss as a function of temperature and time, and the volatile compounds are then collected on a solid phase. After transfer into the GC-MS unit, the compounds are thermally desorbed, separated by GC, and analyzed *via* mass spectrometry. This enables sample analysis without complex sample pre-treatment with LOD between 0.21-6.99 µg for relevant

polymers like PS, PP, PET, or PE[252,253]. It was concluded that TED-GC-MS is the method of choice for analysis of aerosol samples captured with the GLI due to the large measurable sample mass, low LOD, and minimal sample preparation.

Design of method validation studies

Since the combination of a novel impinger device with granular bed filtration and TED-GC-MS analysis is wholly new in the field of environmental air quality assessment, an in-depth validation study of performance, recovery rate, and limits of detection and quantification were required for the entire system. Since multiple washing steps were also involved in sample collection and analysis, these procedures were analyzed using a tiered approach to method validation. Both unlabeled and fluorescently labeled PET and PP test materials were employed in validation studies to determine the recovery rate and detection limits for the entire procedure. Thus, the following research questions were investigated in a preliminary validation study:

- If a known amount of labeled PET and PP test material is spiked into the liquid in the impinger at both stages, is the washing procedure suitable for a high recovery rate (> 85% recovered mass from each individual compartment)?
- If a known amount of fluorescently labeled PET and PP test materials is aerosolized into the liquid impinger under the air flow conditions chosen for field studies and deposits throughout the device, is the washing procedure suitable for a high recovery rate and mass balance (> 85% total recovered mass)?
- If a known amount of a NP mixture containing equal masses of unlabeled PET, PP and PS nanomaterials is aerosolized into the device, the washing and processing protocol completed, samples transported to the BAM and analyzed with TED-GC-MS, can the analytical method identify and quantify the different materials in sufficiently low amounts? Can the entire procedure provide evidence of a suitable recovery rate and mass balance (> 85% total recovered mass)?

- Is it possible to determine a limit of detection and quantification relevant for subsequent field studies?

To answer these questions, three experimental setups were used. In method validation study #1 **(Figure 4.2A)**, NPs with the fluorescent label F8BT were used for spiking the system with either PET or PP NPs. Subsequently, the recovery rate of the developed washing and sample collection procedure was determined. In a second approach **(Figure 4.2B)**, the same NPs were utilized to nebulize PET or PP NPs and collect them with the GLI to establish a deposition profile. Validation study #3 investigated the collection efficiency of a nebulized mixture of unlabeled PET, PP, and PS NPs *via* TED-GC-MS **(Figure 4.2C)**.

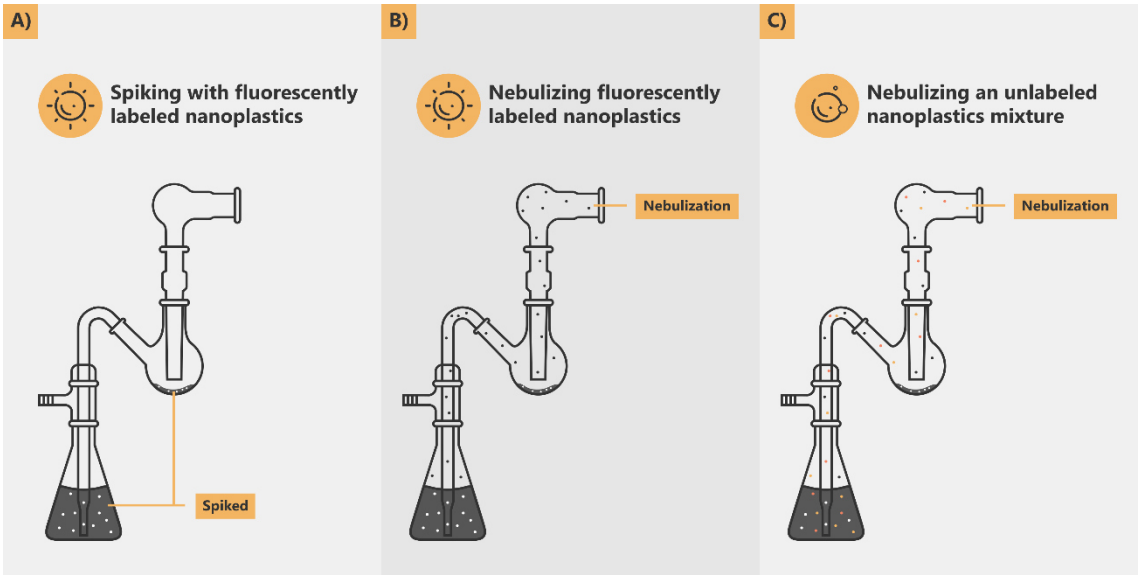

Figure 4.2: Overview of the conducted method validation studies with known amounts of nanoplastics. In validation study #1, both compartments were spiked with a single type of fluorescently labeled nanoplastics and the recovery rate after the washing and sample collection procedure was determined (A). For validation study #2, the same fluorescently labeled nanoplastics were nebulized into the system and their deposition profile was assessed (B). Validation study #3 used a mixture of unlabeled polymers, nebulized this mixture into the system and the mass of the captured nanoplastics was determined *via* TED-GC-MS to establish the limit of detection and limit of quantification for this method.

Design of field studies

The main research questions and hypothesis were outlined in **Chapter 1.3** together with their rationale. Briefly, it was hypothesized that increasing levels of plastic debris in the ocean leads to increased levels of MNPs in SSA. This hypothesis was based on a study from Allen *et al*. (2020) that showed that MPs are part of SSA and that the sea also acts as a source for MPs[62]. The second hypothesis was developed from the same idea that the waterbody close to the aerosol sampling side determines the MNP concentration in the air. It has been reported that lakes can contain considerable amounts of plastic debris and that they also generate aerosols[85,86]. Therefore, it was hypothesized that lakeside aerosols collected at the Neusiedler Lake can contain MNPs but much lower concentrations are expected due to the lower expected plastic pollution. The use of filters by Allen *et al*. limited their investigations to particles > 5 µm, excluding NPs entirely[62]. The GLI has no theoretical lower size limit and can fractionate inhalable PM by aerodynamic diameter. We thus hypothesized that our novel sampling device combined with TED-GC-MS analysis can fill the knowledge gaps by capturing both micro- and nanoplastics and determining the polymer type and mass in both fractions (inhalable, and respirable fraction).

Two distinct sampling sites were chosen to test the postulated hypotheses. For baseline measurements with low expected MNP abundance in lakeside aerosols, the Neusiedler Lake in Podersdorf, Austria (47°51'57.6"N, 16°50'03.8"E) was chosen due to its rural location and status as protected national park and UNESCO World Heritage Site. The first sampling campaign was carried out between the 8th-12th of August 2022 and designed to test the developed protocol in the field. Analysis of the obtained samples revealed that all the factory-sealed vials used for sample collection were contaminated with fibrous material **(Figure 4.3)**. Contamination must have occurred during production before the vials were sealed with their respective lids and packaged. Thereafter, the preparation protocol was extended by a thorough washing protocol where all vials were washed with distilled water and filtered ethanol inside a laminar flow cabinet. The second campaign at the same site was conducted between the 15th-17th October 2022, using the optimized protocol **(Figure 4.4A-B)**.

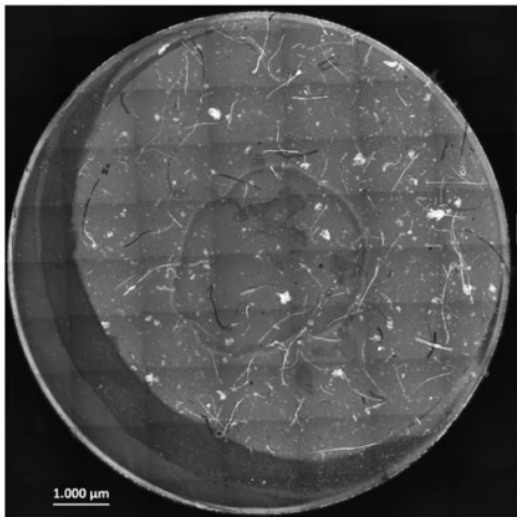

Figure 4.3: SEM image of fibrous material of unknown origin (possibly paper packaging) present within unopened glass vials used for sample collection.

The second sampling site was located on the island Brač in Croatia (43°32’29.0”N°16°41’20.2”E) **(Figure 4.4C-E)**. This site was chosen for testing the hypothesis that SSA represents a source of elevated plastic exposure due to higher plastic pollution of the Adriatic Sea[158] compared to the Neusiedler Lake[157] **(see Chapter 1.3.3)**. Sampling was carried out between the 27th-29th of September 2022 on two measurement sites to test whether SSA collected directly at the shoreline (sea spray aerosols, 43°19'20.7"N, 16°24'41.8"E, **Figure 4.4E**) and aerosols collected 100 m inland (seaside aerosols, 43°19'23.1"N, 16°24'43.4"E, **Figure 4.4D**) show differences in their MNP composition. It was hypothesized that sampling at the shoreline will capture SSA almost exclusively, while sampling inland can contain aerosols of mixed origin depending on the wind direction. Meteorological data (time, temperature, relative humidity, wind speed and direction) was recorded during all field sampling campaigns and each individual collection run. To account for possible plastic contamination, procedural blanks were collected at all sites in between sampling replicates. This involved filling the GLI with liquid in the field, then immediately performing the washing and processing steps according to the collection protocol.

Figure 4.4: Aerosol sampling locations in Austria (A-B) and Croatia (C-E) showing the GLI device with respect to a lake (Austria) and coastal (Croatia) shoreline. The weather station used provided real time meteorological data during the measurement. Maps were used from Lencer (https://commons.wikimedia.org/wiki/File:Austria_location_map.svg), „Austria location map“, and NordNordWest (https://commons.wikimedia.org/wiki/File:Croatia_location_map.svg), „Croatia location map“, Marker added by Lukas Wimmer, https://creativecommons.org/licenses/by-sa/3.0/legalcode.

4.2 Materials and methods

Materials

The fluorescent dye F8BT (Poly-[(9,9-di-n-octylfluorenyl-2,7-diyl)-alt-(benzo[2,1,3]thiadiazol-4,8-diyl)], 698687, average Mn ≤25000) was sources from Sigma-Aldrich (Merck KGaA, Darmstadt, Germany). All liquids were filtered through a 0.22 µm filter membrane (GSWP04700, MCE, MF-Millipore) and were used for washing, rinsing and sampling. The liquids were stored in glass vessels with all plastic parts removed and sealed with glass stoppers or aluminum foil. All sample glass vials (20 mL) were rinsed with distilled water (5 mL) followed by ethanol (5 mL, 50%, v/v) and sealed in a laminar flow cabinet to avoid contamination through ambient air. All other glassware used (e.g. pipettes and funnels) were rinsed generously with distilled water after each collection and covered in aluminum foil when not in use. The reference to ethanol (50%) always implies a 50% mixture (v/v) of pre-filtered ethanol with distilled water, unless specifically described otherwise. Materials that are not mentioned in this section are described in the materials sections of **Chapters 2 and 3** .

Preparation of F8BT-labeled nanoplastics

The same methods for NP preparation were used as described in **Chapter 0**with the following modifications: The polymer of interest (PET or PP) was solubilized in 2 mL less than described in the standard protocol. The fluorescent polymer F8BT (0.8 w% of the used starting material, typically 2 mg or 1.2 mg F8BT for 260 mg or 160 mg of PET or PP respectively) was solubilized separately in a glass vial (4 mL) containing 1 mL of the respective solvent *via* heating and bath sonication. After 30 min of heating, the solubilized F8BT was added to the polymer/solvent mixture, the vial was rinsed once with 1 mL fresh solvent and the wash was also added to the mixture. After 15 more minutes of heating, the polymer of interest and F8BT were co-precipitated into ethanol (96%, w/w). Further processing was done the same as described in **Chapter 0**but in a darkened fume hood to protect the labeled plastics from light.

Characterization of F8BT labeled nanoplastics: Size and optical properties

A QC dispersion protocol similar to the one used in **Chapter 0**was employed to disperse the labeled test materials and create fluorescence calibration curves needed for the impinger validation studies. The working stock (a 1 mg/mL suspension) was prepared by transferring 25 mg of the homogenized glycerol stock (40 mg/g) into a glass vial (4 mL) and by subsequently adding 3.3% (instead of the usually used 5% for easier subsequent dilution to the final Tween®80 concentration of 0.33%) Tween®80 solution (1 mL) into the same vial (step 1 dilution). Pre-mixing was achieved by vigorous pipetting, followed by sonication in a water bath for 15 (PET) to 40 min (PP) at 22 ± 1°C. A serial dilution from 100 µg/mL to 0.20 µg/mL was then produced in 0.33% Tween®80 (step 2 dilution). For the first concentration, the working stock (100 µL, 3.3% Tween®80) was mixed with distilled water (900 µL), resulting in 100 µg/mL NPs in 0.33% Tween®80. The mixture was vortexed (10 sec) and sonicated (30 sec) before proceeding to the next dilution. All subsequent dilution steps were produced by mixing the current concentration (500 µL) with 0.33% Tween®80 (500 µL) with subsequent vortex and sonication. In total, three individual serial dilutions with ten dilution steps were produced and samples of each step (100 µL) were transferred in triplicates into a 96-well plate. The fluorescent intensity of all samples and blanks (Tween®80 solution, 0.33%) was measured with a Tecan infinite 200Pro (Tecan Group Ltd., Männedorf, Switzerland) with Ex: 460 nm, Ex bandwidth: 9 nm, Em: 541, Em bandwidth: 20 nm. Blank values were subtracted from the measured sample absorption values and averaged before creating a regression curve. The calibration curve was deemed acceptable when $r^2 > 0.980$[201]. The obtained calibration curve was analyzed with the linear regression algorithm of Excel, to obtain the standard deviation of the y-intercept (SD_y). Thereafter, the LOD and LOQ were calculated according to **Equation 4.1** and **Equation 4.2**.

Equation 4.1: The limit of detection (LOD) is calculated in µg/mL based on the standard deviation of the y-intercept (SDy) and the slope (s).

$$LOD = 3.3 \times \frac{SD_y}{s} \quad (4.1)$$

Equation 4.2: The limit of detection (LOD) is calculated in µg/mL based on the standard deviation of the y-intercept (SDy) and the slope (s).

$$LOQ = 10 \times \frac{SD_y}{s} \quad (4.2)$$

Optimal excitation and emission wavelengths of F8BT-labeled NPs were established using the same instrument but in scanning mode. The obtained fluorescence intensities were normalized by setting the highest peak to 1 and the excitation spectra were plotted from 300 510 nm, whereas emission spectra were plotted from 490 to 650 nm to avoid interferences through overlapping signals.

Calibration curves for the quantification of fluorescein

Sodium fluorescein was weighed into a glass vial and solubilized in a Tween®80 solution (0.33%) and subsequently mixed by vortexing (10 sec) to obtain a stock solution (1 mg/mL). This stock was further diluted with the same Tween®80 solution to create the working solution (50 µg/mL in 0.33% Tween®80). From this working solution, a serial dilution was prepared by mixing the appropriate amount of working solution with Tween®80 solution (0.33%). The following concentrations and Tween®80 (0.33%) as blank were prepared: 10 µg/mL, 8 µg/mL, 6 µg/mL, 4 µg/mL, 2 µg/mL, 1 µg/mL, 0.5 µg/mL. The absorption of all samples was measured in triplicates with a spectrophotometer (Biotek Epoch 2, Agilent Technologies Inc., Santa Clara, USA) at 490 nm. Blank values were subtracted from the measured sample absorption values before calculating means and creating a regression curve. The calibration curve was deemed acceptable when $r^2 > 0.980$[201].

Validation study #1: Assessment of F8BT-labeled nanoplastic recovery rate from different sections of the GLI

As described in the introduction, it is important to determine whether the washing procedure used to collect materials deposited in the different compartments of the GLI provides an acceptable recovery rate. The Ph. Eur. specifies limits for the mass balance recovery between 75-125% when using the GLI for collection of the emitted dose[236]. Since there are no other regulations for the recovery rate of impingers measured *via* fluorescence intensity, the same limits were deemed acceptable for the conducted validation experiment. To determine this, F8BT-labeled PET and PP were dispersed in 2% FBS (Tween®80 was avoided due to foam generation in the GLI). Briefly, homogenization of the F8BT-labeled NP glycerol stock suspensions was carried out as described in **Chapter 0**. Working stocks (1 mg/mL, 2% FBS) were prepared as described in **Chapter 0**but using FBS instead of Tween®80 (step 1 dilution) and working suspensions (50 mL; 10 µg/mL) were obtained by subsequently diluting the required amount of stock suspension (500 µL) with FBS solution (2%, 49.5 mL) and sonicating the final suspension for 3 min directly before spiking. A 2% FBS solution was also prepared for use as background control.

F8BT-labeled NPs or the FBS vehicle were added to the upper (7 mL) and lower (30 mL) compartments (UC and LC) of the GLI, respectively, at a final concentration of 10 µg/mL in each compartment (spiking). The LC also contained 475 g (= 130 mL) pre-washed ceramic beads (9730, ZY-P, 2.6-3.3 mm, SiLibeads, Sigmund Lindner GmbH, Warmensteinach, Germany). The vacuum pump was then switched on for 30 min (flow rate: 60 ± 2 L/min) to create turbulence mimicking in-use conditions. Afterwards the liquid in the UC was collected in a volumetric flask (25 mL). The empty UC was then rinsed three times with 6 mL ethanol (50%, v/v) and each rinsing was added to the same flask (UC flask). The liquid from the UC that evaporated during the experiment was replaced by filling the volumetric flask to the mark with distilled water. The liquid in the LC (~20 mL) was transferred into a separate volumetric flask (50 mL, LC flasks) by pouring the LC contents into a glass funnel fitted with a coarse frit to separate the ceramic beads from the liquid, which was allowed to drip into the flask. The empty LC was subsequently washed three times with 6 mL ethanol (50%, v/v), then the wash liquid poured over the ceramic beads and allowed to drip into the flask. Subsequently, the ceramic beads were washed once with ethanol (10 mL, 50%, v/v)

and the wash was collected into the same flask. Distilled water was then used to fill the flask to the mark.

Fluorescence measurement

Prior to fluorescence intensity measurements, the flasks were mixed by bath sonication (1 min). Immediately, three samples were withdrawn (100 µL) and transferred into a 96-well plate. The fluorescent intensity of all samples and blanks (FBS solution, 2%) was measured with a Tecan infinite 200Pro (Tecan Group Ltd., Männedorf, Switzerland) with Ex: 460 nm, Ex bandwidth: 9 nm, Em: 541, Em bandwidth: 20 nm. Fluorescence intensity (arbitrary units) of the blanks was averaged and the mean blank value subtracted from the sample fluorescence. The fluorescence recovered in compartments representing the upper respiratory tract (UC flask) and the lower respiratory tract (LC flask) was reported as a percentage of the intensity of the spiked sample containing 10 µg labeled NPs per mL liquid. This experiment was carried out n = 3 times with both PET and PP NPs in order to determine whether NP surface properties impacted their recovery rate.

Validation study #2: Assessment of F8BT-labeled nanoplastic recovery rate from different sections of the GLI after aerosolization into the device

In this second validation experiment, the aim was to determine whether aerosolization of a known amount of F8BT-labeled NPs into the GLI follows the same deposition profile as a nebulized reference solution, i.e. if the NPs are carried through the system in the nebulized droplets. This experiment increases the complexity and mimics environmental sampling conditions, since it is unknown which fraction of NPs will deposit in each compartment. Therefore, 2 mL of a fluorescein solution (500 µg/mL) in Tween®80 (0.33%) were nebulized to establish the deposition profile of a nebulized liquid without NPs. Sample collection was performed as described in **Chapter 0**but with water as rinsing agent instead of ethanol (50%). Fluorescein and blank (0.33% Tween®80 solution) absorptions were subsequently measured as outlined in **Chapter 0**before calculating the deposited mass in the different compartments using the fluorescein calibration curve. The fluorescein

deposited in each part was expressed as a percentage of the total fluorescein loaded into the nebulizer.

Thereafter, labeled NPs were used for nebulization as comparator materials. Homogenization of the F8BT-labeled NP glycerol stock suspensions was carried out as described in **Chapter 0**. Working stocks (1 mg/mL) were prepared as described in **Chapter 0** with Tween®80 (3.3%, w/w) and working suspensions (3 mL; 10 µg/mL) were obtained by subsequently diluting the required amount of stock suspension (30 µL) with distilled water (2970 µL) and sonicating the final suspension for 3 min directly before nebulization. A 0.33% Tween®80 solution was also prepared for use as a background control. Before adding the sample (2-2.5 mL NP suspension or 0.33% Tween®80 blank), the weight of the dry, empty nebulizer reservoir equipped with the red nozzle (PARI LC SPRINT Nebulizer, with 2.8 µm mass median aerodynamic diameter, MMAD) was determined (NR_D). The filled reservoir was weighed again (NR_F), and the GLI was fully assembled and the aerosolizer (PARI BOY® Classic, PARI GmbH, Starnberg, Germany) and the vacuum pump (LCP6, Copley Scientific Ltd., Nottingham, UK) were connected. The pump was switched on and the flow was adjusted to 60 ± 2 L/min and monitored throughout the experiment using a flowmeter (5300-1, TSI Inc., Shoreview, USA). When the air flow stabilized, the sample was aerosolized for 4.5 min. The reservoir was weighed again (NR_N) and the nebulization efficiency (NE%) and total nebulized liquid (TNL) was calculated according to **Equation 4.3** and **Equation 4.4**.

Equation 4.3: Nebulization efficiency (NE) in %, where NRN = mass of the nebulizer reservoir after nebulization, NRD = mass of the nebulizer reservoir dry, and NRF = mass of the nebulizer reservoir filled.

$$NE(\%) = 100 - \frac{(NR_N - NR_D) \times 100}{(NR_F - NR_D)} \quad (4.3)$$

Equation 4.4: Total nebulized liquid (TNL) in g, where NRD = mass of the nebulizer reservoir dry, NRF = mass of the nebulizer reservoir filled, and NRN = mass of the nebulizer reservoir after nebulization.

$$TNL\ (g) = (NR_F - NR_D) - (NR_N - NR_D) \quad (4.4)$$

Sample collection was carried out as described in **Chapter 0**with the following adaptations: All liquids were collected in pre-washed amber glass vials (30 mL) with metal lids, and the MTP was also rinsed three times with 6 mL ethanol (50%, v/v) where the liquid was collected in a separate vial (MTP vial). **Figure 4.5A-B** outlines the sample collection process, with all washing and subsequent processing steps performed until samples were ready for measurement. Briefly, all glass vials were placed into a desiccator and the lids opened sufficiently to allow evaporation of a majority of the ethanol. After 2-3 days, the samples were freeze-dried **(Figure 4.5A)**. The content of each 30 mL vial was re-dispersed by rinsing three times with 3 mL ethanol (50%, v/v) and sonicating each rinse sample for 1 min prior to transfer **(Figure 4.5B)**. The rinse liquid from the MTP vial was then transferred to UC vial (representing the upper respiratory tract = URT), while the rinse liquid from the LC2 vial was transferred to the LC1 vial (representing the lower respiratory tract = LRT). The ethanol of the two remaining vials (UC, LC1) was then removed with a rotary evaporator (water bath 45°C) by slowly decreasing the pressure to 80 mbar. When no more liquid was visible, the pressure was reduced to 40 mbar and dried for 5 more min. Residual NPs in the nebulizer were collected and dried similarly. Tween®80 blank samples and a sample of the suspension used for nebulization were dried in the same manner. Those samples were used directly after drying.

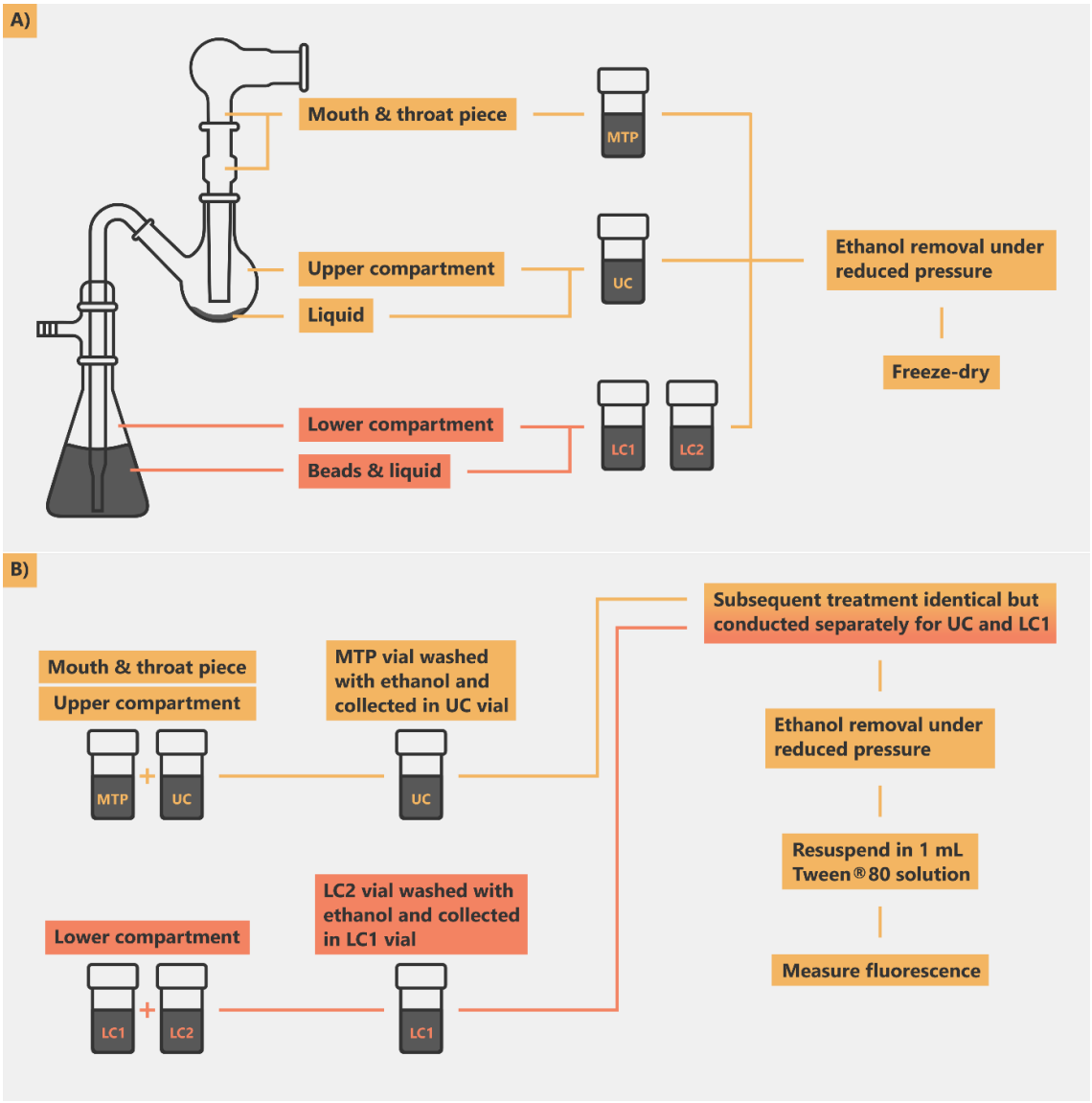

Figure 4.5: Scheme of the sample collection and drying process (A). Samples from the mouth and throat piece (MTP) and upper compartment (UC) were pooled and represented the upper respiratory tract (URT), whereas samples from the lower compartment (LC1 and LC2) were pooled and represented the lower respiratory tract (LRT). Fluorescent intensity was measured and the NPs content quantified using pre-established calibration curves (B).

Nanoplastic fluorescence measurement

Prior to fluorescence intensity measurements, a 0.33% Tween®80 solution (1 mL) was added to the dried vials and sonicated for 1 min. Immediately, three samples were withdrawn (100 µL) and transferred into a 96-well plate. The fluorescent intensity of all F8BT-

labeled NP samples and blanks (Tween®80 solution, 0.33%) was measured as described in **Chapter 0**, prior to quantification using the calibration curves reported in the same chapter. The mass of NP depositing in each fraction (URT, LRT, nebulizer reservoir) was then calculated. Total mass recovered was calculated by adding the content from these three fractions and dividing by the amount in the nebulizer prior to aerosolization (expressed as a percentage).

Validation study #3: Assessment of unlabeled nanoplastic recovery rate from different sections of the GLI after aerosolization into the device and TED-GC-MS analysis

In this third validation experiment, the aim was to determine whether aerosolization of a mixture of known amounts of unlabeled PET, PP and PS NPs into the GLI can be quantified accurately using TED-GC-MS. This experiment increases the complexity of the system even further and mimics the final procedure to be used in field studies. The unlabeled PET and PP NP stock suspensions (1 mg/mL) were prepared as described in **Chapter 0**. The mixture working suspensions (10 mL) were prepared by diluting the correct amount of stock suspension into Tween®80 (0.33%, w/w) so that a final concentration of 10 µg/mL for each polymer (PET, PP and PS) was achieved. Nebulization of the mixture, sample collection, and drying was conducted as described in **Chapter 0**. **Figure 4.5A** outlines the sample collection process, with all washing and subsequent processing steps performed until samples were in a dry storage state, suitable for storage and transport to collaboration partners at the BAM, Germany. **Figure 4.6** outlines the washing and processing steps performed at the BAM to fully collect MNPs from the storage containers and transfer collected materials to the TED-GC-MS for analysis. Briefly, the vials were washed three times with 1.5 mL dichloromethane (DCM) and transferred into a glass beaker (10 mL). The DCM was then reduced to < 1 mL by evaporation in a temperature-controlled chamber (36°C) within 3-4 h. The remaining DCM was then poured into an Al_2O_3 pan and brought to dryness (30 min) inside the pan. The beaker was then washed with DCM (0.7 mL), the wash was poured into the Al_2O_3 pan, and the DCM was evaporated. After complete evaporation, this washing process was repeated four times (conducted five times in total) and the sample was finally dried overnight at 50°C before TED-GC-MS measurements were

conducted. Before starting the washing procedure, the UC vials of one procedural blank and one aerosol sample were spiked with a 13C labeled PS standard (8 µL) to monitor the collection efficiency.

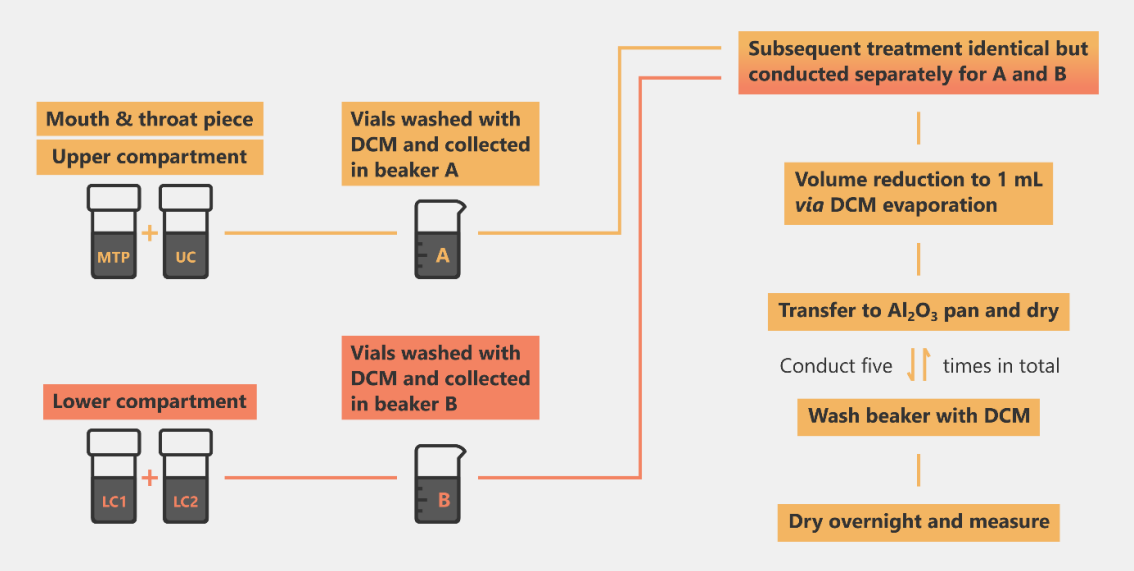

Figure 4.6: Processing protocol for collection and transfer of MNPs from the storage vials to the TED-GC-MS pans for analysis. Samples from the mouth and throat piece (MTP) and upper compartment (UC) were pooled and represented the upper respiratory tract (URT), whereas samples from the lower compartment (LC1 and LC2) were pooled and represented the lower respiratory tract (LRT).

Field studies: Air sampling in Podersdorf, Austria and Brač, Croatia

The preparation of materials used for air sampling, and the sampling and sample collection procedure were identical for both campaigns. Divergences between the Austrian and Croatian campaign are described below and concern sample pooling before TED-GC-MS analysis. For aerosol sampling, the GLI was positioned in a way that the mouthpiece was 120 cm above ground level and faced the shoreline. The ceramic beads (475 g =130 mL) and distilled water (20-30 mL) were introduced into the LC. Thereafter, all parts were assembled and distilled water (7 mL) was transferred into the UC. The flow controller and vacuum pump were connected and switched on. Finally, the flow was adjusted to 60 ± 2 L/min and a timer was started. During the aerosol sampling, wind and weather conditions (temperature, rel. humidity, wind direction, and wind speed) were continuously recorded

using a Bresser 5-in-1 Wetter Center (Cat.Nr. 7002511, Bresser GmbH, Rhede, Germany). Evaporated liquids in the UC and LC were replenished occasionally, during which the timer and vacuum pump were stopped for 1-5 min. After 167 min (2.78 h) runtime, all instruments were switched off and the samples were collected immediately as described in **Chapter 0**. Vials were stored at -20°C until prepared for further analysis according to **Figure 4.5B**. The dry samples were shipped to our collaborators at BAM, where they were processed as outlined in **Chapter 0** and **Figure 4.6**. Procedural blanks were taken under field conditions before the very first measurement and at the end of each sampling day to assess background levels and potential sample carry over. A procedural blank followed the same procedure as an aerosol sample but without switching on the vacuum pump. Briefly, the GLI was assembled and distilled water was introduced into the UC (7 mL) and LC (20 mL) including the ceramic beads. The device was disassembled again, the liquids were collected, all glass parts were rinsed with ethanol (50%), and the washing fluids were likewise collected in the respective vials. Subsequent processing was identical to aerosol samples. Vials from individual sampling runs were pooled according to **Figure 4.6**. They represented the upper respiratory tract (beaker A) and the lower respiratory tract (beaker B) fractions and were measured together as one sample *via* TED-GC-MS.

The sampling campaign at the Neusiedler Lake in Podersdorf, Austria (47°51'57.6"N, 16°50'03.8"E) was carried out between the 15th-17th October 2022. It is a popular recreation area and known among windsurfers due to continuous and sufficiently strong winds, mainly blowing from the northwest, hence across the lake towards the chosen sampling location in Podersdorf. The lake is located in an overall rural area and despite the agricultural sector, no big industrial facilities are in the vicinity of the lake. Further, it is a protected national park (2.5-5 km around the lake) and UNESCO World Heritage Site. Considering those factors, it was hypothesized that captured aerosols originating from or travelling across the lake will carry low or non-detectable amounts of MNPs in 10 m^3 sampled air. However, the plastic content of lakeside aerosols in rural areas is not well described and background levels can, therefore, not completely be excluded. Sample collection was conducted between 8:00-20:00 (n = 8 with 10 m^3 air per sample) at periods without precipitation. Mainly southwestern winds occurred during sampling with one exception (sample #3) where solely eastern winds were blowing, hence coming from inland **(Table 4.1)**.

Table 4.1: Sampling runs from the Neusiedler Lake campaign and the associated weather data. Weather conditions with ≥ 3 observations were averaged and presented alongside with the standard deviation (SD). Wind directions are given as ranges from all observations.

Sample # – date (weather data points)	Temperature ± SD (°C)	Rel. humidity ± SD (%)	Wind direction	Wind strength ± SD (m/s)
#1 – 15.10.22 (n = 3)	14.9 ± 0.4	86 ± 3	S-WSW	1.6 ± 0.6
#2 – 15.10.22 (n = 2)*	14.9	92	E-SW	0.7
#3 – 16.10.22 (n = 2)	15.2	87	E	0.9
#4 – 16.10.22 (n = 4)	19.8 ± 0.7	69 ± 4	ESE -SSW	1.3 ± 0.5
#5 – 16.10.22 (n = 4)*	22.1 ± 0.4	58 ± 2	ESE	1.5 ± 0.6
#6 – 17.10.22 (n = 3)	16.5 ± 3.3	73 ± 9	SW	1.6 ± 0.3
#7 – 17.10.22 (n = 3)	21.3 ± 0.7	57 ± 3	SE-SSW	1.3 ± 0.3
#8 – 17.10.22 (n = 5)	23.3 ± 0.4	43 ± 2	ESE-WSW	1.0 ± 0.4

**Samples #2 und #5 were used for filtration and microscopic examination.*

Aerosol samples of the Croatian campaign were taken on three consecutive days between the 27th-29th of September 2022 **(Table 4.2)**. In total, 12 samples from two distinct sites were collected (n = 6 collections of 10 m^3 air at each site). Site #1 was about 30 m above sea level and 100 m inland from the shoreline (43°19'23.1"N, 16°24'43.4"E) and winds were typically weak (0-0.9 m/s) and from various directions. The collected aerosols were therefore likely of mixed origin and further referred to as “seaside aerosols”. Site #2 was around 2 m above sea level and 5 m from the shoreline (43°19'20.7"N, 16°24'41.8"E) and the slightly stronger winds (1-4 m/s) came almost exclusively from the sea (westerly to south westerly). It was postulated, that from this site all collected aerosols originated from sea spray and the samples were therefore referred to as “sea spray aerosols”. Although samples #6 and #12 experienced northwestern winds, they did not come entirely from inland (N-NE).

Table 4.2: Sampling runs from the Brač island campaign and the associated weather data. Weather conditions with ≥ 3 observations were averaged and presented alongside with the standard deviation (SD). Wind directions are given as ranges from all observations.

Sample # – date (weather data points)	Temperature ± SD (°C)	Rel. humidity ± SD (%)	Wind direction	Wind strength ± SD (m/s)
#1 – 26.09.22 (n = 2)	21.2	83	WNW	0.7
#2 – 27.09.22 (n = 2)	19.6	82	SSE-WSW	0.9
#3 – 27.09.22 (n = 3)	21.6 ± 0.3	76 ± 4	W-WSW	3.2 ± 0.7
#4 – 27.09.22 (n = 4)	23.5 ± 0.9	66 ± 5	WSW	1.4 ± 0.4
#5 – 27.09.22 (n = 3)	22.2 ± 2.7	60 ± 7	SSW-WNW	0.3 ± 0.2
#6 – 28.09.22 (n = 2)	21.0	77	WNW-NW	0.3
#7 – 28.09.22 (n = 2)	20.9	78	WSW	2.6
#8 – 28.09.22 (n = 3)	23.0 ± 1.6	64 ± 6	WSW	1.5 ± 0.5
#9 – 28.09.22 (n = 3)	22.1 ± 0.7	63 ± 1	SE-E	0.6 ± 0.2
#10 – 29.09.22 (n = 3)	21.0 ± 0.4	74 ± 2	SE-WNW	0.4 ± 0.2
#11 – 29.09.22 (n = 3)	24.0 ± 0.7	62 ± 2	ESE-W	1.0 ± 0.1
#12 – 29.09.22 (n = 4)	26.9 ± 0.5	52 ± 1	W-NW	1.3 ± 0.5

Data processing

If not stated otherwise, experiments were carried out at least three times. Blank controls were averaged and the mean blank value subtracted from individual sample values before sample means and SDs were calculated.

Statistical testing and plotting

To test for statistically significant differences between the detected PP masses in blank controls and aerosol samples, an independent t-test was applied (CI: 95%) using the SciPy (1.14.1), NumPy (2.1.1), and Pandas (2.2.3) libraries in Python (3.11.0). Figures were plotted with Matplotlib (3.9.2).

4.3 Results and discussion

Statement of transparency

SEM images of samples from the first sampling campaign were provided by Dr. Paul-Tiberiu Miclea from the Fraunhofer Institute for Microstructure of Materials and Systems (IMWS). Air samples from the field sampling campaigns and nebulization experiments with unlabeled materials were kindly prepared by Frank Milczewski for TED-GC-MS measurements and analyzed by Dr. Korinna Altmann, both from the Federal Institute for Materials Research and Testing in Berlin (BAM). Excitation and emission spectra of the produced labeled PET and PP NPs were obtained by My Vanessa Nguyen Hoang. Fluorescein nebulization experiments were performed together with Dr. Gabriela Hädrich.

Characterization of fluorescently labeled nanoplastics

Unlabeled NPs are hard to visualize and track, due to their simple structure (mainly hydrocarbons) and size. One commonly used approach to quantify such small structures is to label these materials fluorescently with Nile Red or other similar small molecules. Although dyes like Nile Red are very accessible and easy to use, they tend to leach over time and reduce the limit of detection (LOD) and limit of quantification (LOQ). To overcome these flaws, the polymeric fluorescent dye, poly-[(9,9-di-n-octylfluorenyl-2,7-diyl)-alt-(benzo[2,1,3]thiadiazol-4,8-diyl)] (F8BT) was used, which is known for its high photoluminescence. Because of its polymeric structure (M_n: ≤ 25,000 g/mol), it is hypothesized that the molecule is too large and too hydrophobic to leach out of the precipitated NPs providing stability and reliability. This hypothesis is under investigation by a collaborator but not yet completed. Its hydrophobic nature allows solubilization in the same solvents used for PET (benzyl alcohol) and PP (xylene) and its co-precipitation into ethanol. PET and PP NPs were labeled with 0.8% (w/w) F8BT and used for method validation. Spectral scans of F8BT-labeled PET and PP NPs (50 µg/mL) dispersed in 10% FBS revealed maxima at 460 and 541 nm for excitation and emission, respectively **(Figure 4.7)**.

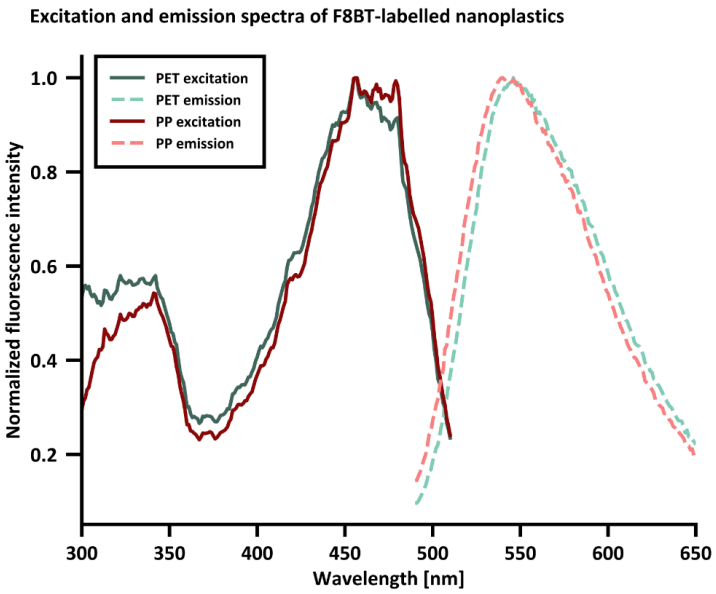

Figure 4.7: Absorbance and emission spectra of F8BT labeled PET (blue) and PP (red) nanoparticles dispersed in 10% FBS.

Calibration curves for both polymers were produced as described in **Chapter 0**and their characteristics and LOD and LOQ are listed in **Table 4.3**.

Table 4.3: Calibration curve characteristics of a fluorescein solution and F8BT labeled PET and PP nanoparticles dispersed in 0.33% Tween®80. LOD = limit of detection; LOQ = limit of quantification.

Sample	Equation	r^2	LOD (µg/mL)	LOQ (µg/mL)
Fluorescein	Y = 0.1444x – 0.0228	0.9972	0.06	0.19
PET-lb	y = 531.35x – 141.5	0.9999	0.50	1.51
PP-lb	y = 741.49x – 54.723	1.0000	0.05	0.15

Particle size distributions of F8BT-labeled PET and PP NPs (100 µg/mL) following dispersion in Tween®80 (0.33%) were characterized *via* DLS. LD could not be employed due to the low concentrations used for nebulization in validation study #2. Interestingly, the QC dispersion protocol failed to fully disperse the labeled PP NPs as indicated by the broad size distribution profile with agglomerates of up to 7 µm **(Figure 4.8)**. Nevertheless, the majority

of the particles were below the mass median aerodynamic diameter (2.8 µm) of the nebulizer used in the validation study **(see Chapter 0)** and, thus, deemed acceptable.

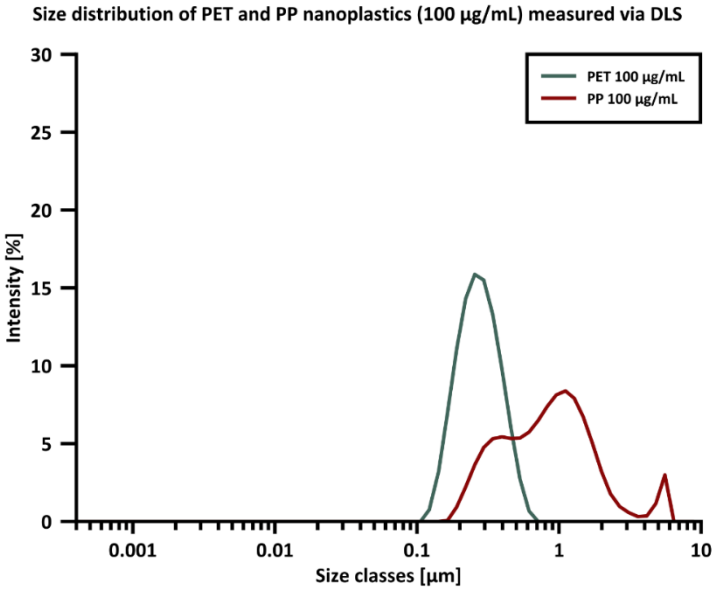

Figure 4.8: Intensity-based particle size distribution of labeled PET and PP nanoplastics measured via DLS. This 100 µg/mL step 1 dilution was used to create the final 10 µg/mL step 2 dilution for nebulization.

Validation study #1: Assessment of F8BT-labeled nanoplastic recovery rate from different sections of the GLI

The washing and sample collection procedures are key elements of the sampling method. To assess whether the recovery of samples is quantitatively robust (75-125%), known amounts of fluorescently labeled NPs (PET-lb, PP-lb) were dispersed using a biorelevant dispersion protocol and spiked into the UC and LC of the GLI and the recovery rate determined. The recovery rate of all samples except the LC spiked with PP NPs was above 95% **(Figure 4.9)**. Unsurprisingly, the recovery rate was generally lower for PP, especially in the LC. It is hypothesized that the higher hydrophobicity of PP makes it more difficult to recover with the washing protocol, which is also reflected by the larger SD. Additionally, although the high surface area of the granule bed in the LC could increase the ultrafine aerosol collection efficiency in the impinger, it may contribute to the reduced

recovery rate of the NPs in the LC. Thus, thorough washing of the granule bed is mandatory for materials with high hydrophobicity. The recovery rates of both polymer types were within the acceptable range of 75-125% of the theoretical concentration and it was therefore concluded that the washing and collection protocol is sufficiently robust. However, it has to be noted that the recovery rate of PP from the LC (86 ± 5%) is close to the aimed 85% threshold formulated in **Chapter 0**.

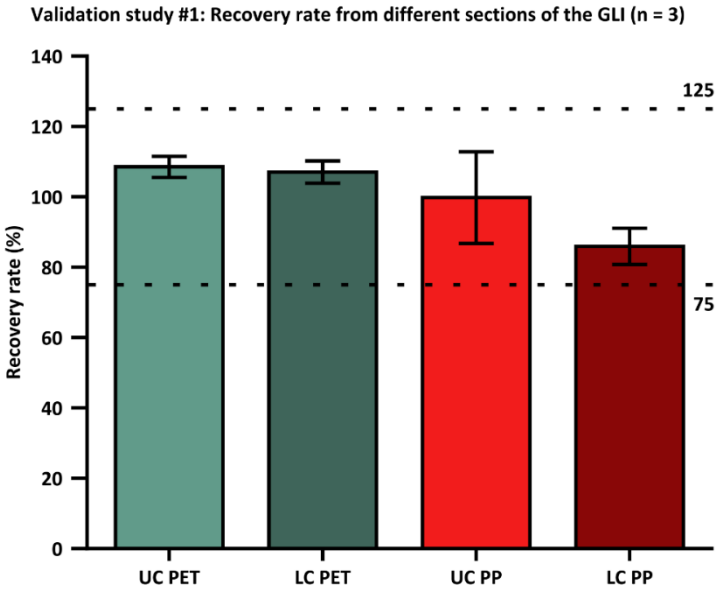

Figure 4.9: Method validation #1. Recovery rates of fluorescent materials from the UC and LC after running the instrument for 30 min (n = 3).

Validation study #2: Assessment of F8BT-labeled nanoplastic recovery rate from different sections of the GLI after aerosolization into the device

Prior to the nebulization experiment, it was expected that 10% of the NPs would stay in the nebulizer reservoir (NR), 10% would deposit in the UC and the remaining 80% would deposit in the LC. This assumption was based on the nebulizer datasheet, and cutoff size of the GLI which determines whether particles deposit in the UC or the LC (above, or below the cutoff size respectively). The nebulizer manufacturer stated that 80% of the produced droplets are < 5 µm (mass-based fraction) and the cutoff size of the GLI is given with 6.4 µm aerodynamic diameter. However, uncertainty existed through the addition of 0.33% Tween®80 since surfactants are known to lower the dynamic surface tension of a liquid which leads to smaller droplet sizes when sprayed[254].

In the first part of this study, fluoresceine in 0.33% Tween®80 was nebulized into the GLI to establish the distribution pattern **(see Chapter 0)**. Surprisingly, 39% of the fluorescein was not nebulized and stayed in the reservoir **(Figure 4.10A)**. The deposited fraction in the UC (5%) was considerably lower than in the LC (21%) as expected. However, the low mass balance (65%) revealed that a significant amount of fluorescein could not be recovered. It is hypothesized that fluorescein was retained on the ceramic beads facilitated through their large surface area, as well as in other sections of the GLI device. This was supported by an observation where fluorescence was detected in blanks of the following experiment after thorough washing of the entire GLI.

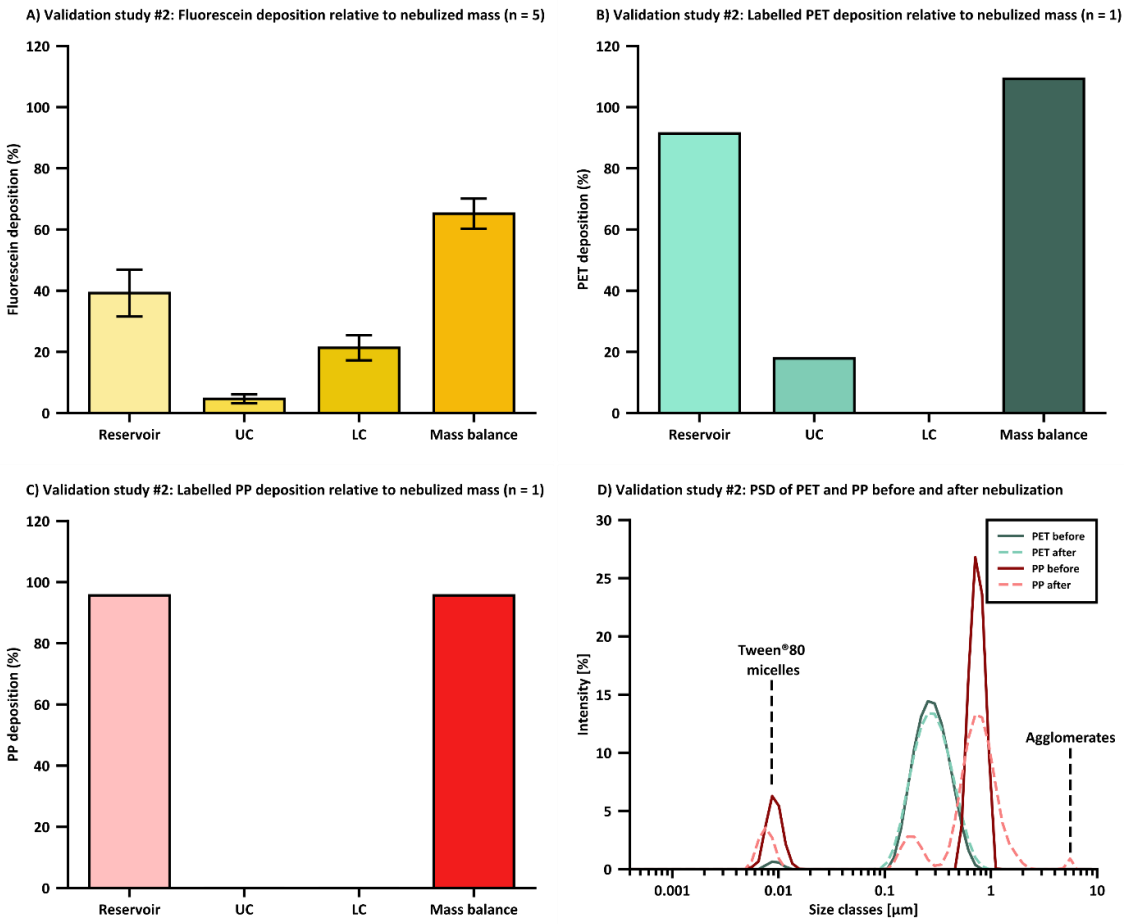

Figure 4.10: Deposition pattern of nebulized fluorescein in 0.33% Tween®80 (A). Deposition pattern of nebulized F8BT-labeled PET (B) and PP (C) nanoparticles and their respective particle size distribution (PSD) before and after nebulization (D).

A similar deposition pattern was anticipated for PET and PP NPs as they are expected to be carried by the droplets produced during nebulization. However, **Figure 4.10B-C** shows that 91% of the PET and 96% of the PP NPs were retained in the reservoir of the nebulizer. Furthermore, only PET was found to be nebulized and deposited in the UC (18%). The high fraction of NPs in the reservoir combined with the high mass balances of PET (109%) and PP (96%) showed that NPs could not be nebulized effectively. This is a phenomenon that has been reported for hydrophobic nanomaterials (such as concentrated PS and polylactic-co-glycolic acid suspensions; 600-1000 µg/mL), especially in combination with jet nebulizer systems[255]. In the current study, it was however hypothesized that lower

concentrations (10 µg/mL) would not lead to widespread NP agglomeration in the jet nebulizer used. To assess this, the PSD profiles of the dispersed NPs (10 µg/mL) before and after nebulization (sampled from the reservoir) were measured *via* DLS **(Figure 4.10D)**. The PSD of PET was not affected by nebulization, which partly explains the detection of PET NPs in the UC. However, the low concentration of the NPs may result in lower quality size measurements using DLS[256]. The PSD curves of PP after nebulization indicated agglomeration through an additional peak at around 6 µm. Furthermore, a peak at 0.2 µm emerged after nebulization indicating incomplete dispersion of PP NPs before nebulization. Peaks at around 10 nm in all samples were attributed to Tween®80, as it is used above its critical micelle concentration **(Figure 3.7)**. It is hypothesized that there are additional factors besides particle size and hydrophobicity that determine the nebulization efficiency of NPs into the GLI using a jet nebulizer, such as shear forces or foaming inside the reservoir. To fully understand those factors and their impact, further investigations are needed.

Validation study #3: Assessment of unlabeled nanoplastic recovery rate from different sections of the GLI after aerosolization into the device and TED-GC-MS analysis

In the next study, the overall recovery rate (including nebulization, collection, washing, and sample preparation), the limit of detection (LOD) and the limit of quantification (LOQ) for unlabeled NPs was determined by nebulizing a mixture of three polymers (PET, PP, PS) into the GLI (n = 3). Thereafter, the washing and sample preparation protocol was applied **(Chapter 0)** and the samples were analyzed by TED-GC-MS which reflected the method used for the field sampling campaigns. It was hypothesized that a similar deposition pattern across all fractions would be measured with the TED-GC-MS method compared to the validation study #2. TED-GC-MS measurements are pending but a manuscript is in preparation for publishing the results.

Field sampling campaigns

Two field sampling campaigns were carried out from September to October 2022 in Podersdorf at the Neusiedler Lake in Austria and the island Brač in Croatia. The Austrian lakeside location was proposed to capture freshwater aerosols as control with a low expected MNP abundance compared to the Croatian coast. Following an in-depth investigation of regional weather patterns, it was decided that the northwest coastline of Brač would provide the optimal wind and weather conditions for collecting coastal aerosol samples with a high probability of SSA entrainment. To account for possible inland sources, air sampling was conducted at two locations on Brač. One directly at the shoreline to capture SSA, and one about 100 m inland for sampling seaside aerosols. Aerosols were collected on at least four occasions (i.e. on separate days during dry weather conditions) and meteorological data was captured. The weight of particles per m^3 sampled air, as well and their chemical composition was determined.

From the five procedural blanks and eight air samples, two procedural blanks and two air samples were used for filtration and microscopic examination at the Fraunhofer-Institute in Halle (Saale). The remaining three procedural blanks and six air samples were sent to Berlin for TED-GC-MS analysis, where they were screened for eight commonly found polymers (PE, PP, PS, SBR, PET, PBAT, PLA, PMMA). None of those polymers except PP was above the LOD. Unfortunately, the measured PP was present in all samples, including the blanks and are most likely contamination through the PP screw caps used in that experiment. An unpaired t-test also showed no statistically significant difference for the PP mass found in the UC ($p = 0.78$) and LC ($p = 0.57$) compared to their respective blanks **(Figure 4.11)**. A second signal was detected which was, however, unspecific for PET and therefore not considered. Several key implications of the Podersdorf study were taken forward into the analysis of the Croatian study samples. First of all, it was concluded that any PP present in Croatian samples should be reported but is likely attributable contamination from PP vial lids and not environmental sources. Analysis of the data and variability of PP in the Podersdorf samples also indicate that the variability is too high for background subtraction of the PP contamination from the experimental samples. Therefore, we decided to exclude PP from the final interpretation of our results, although to

a certain extent, the presence of PP could act as a second, less homogenous internal control for the TED-GC-MS measurements.

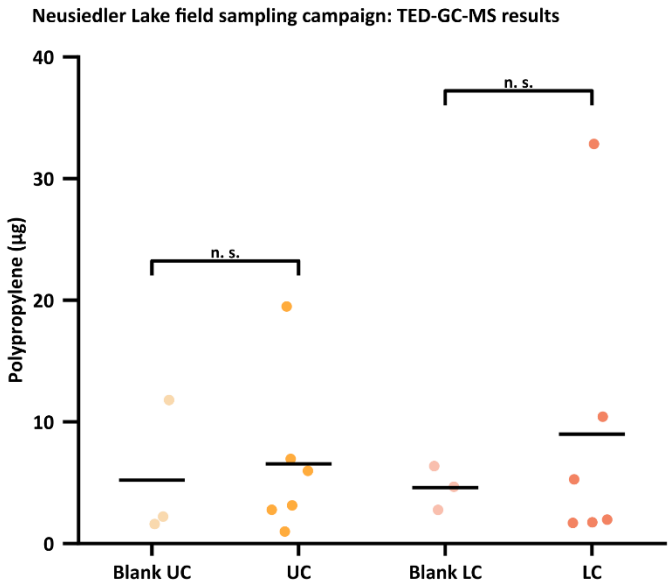

Figure 4.11: Mass of polypropylene detected in the upper compartment (UC) and lower compartment (LC) of the glass liquid impinger (GLI) from the field sampling campaign at the Neusiedler Lake in Austria. Statistical significance was tested using an independent t-test (CI: 95%) where n.s. = $p > 0.05$, * = $p < 0.05$, ** = $p < 0.01$, and *** = $p < 0.001$.

A second important question arising from the Austrian study is whether the volume of sampled air is sufficient to detect airborne MNPs above the LOD of the chosen method. A recent publication from Rindelaub & Miskelly (2025) measured concentrations of six polymers (PE, PC, PVC, PMMA, nylon, PET) in indoor air using Py-GC-MS. On average, 106 m^3 air per sample was actively pumped through an impactor device (PM size cut-off: 10 µm or 2.5 µm) and aerosol samples depositing on the filters analyzed. In all samples, the detected polymers were above procedural blank levels and concentrations ranged from 0.79 to 422 ng/m^3 air depending on the filter and polymer type[156]. These values are extremely close to the reported LOD and LOQ values of the Py-GC-MS used, indicating that 10-fold higher air volumes were required to collect sufficient mass for Py-GC-MS quantification. The Rindelaub and Miskelly (2025) study data indicates that it is likely that sampling of 10 m^3 air is not sufficient to detects airborne MNPs, unless the plastic content is particularly

high in the samples. Unfortunately, such observations were not available at the time the current sampling campaign was conducted in 2022. To increase the likelihood of MNP detection above the TED-GC-MS LOD, it was decided to pool two samples from the Croatian campaign collected on the same day and sampling site (seaside or sea spray sampling site). This decreased the number of samples from n = 6 per sampling site to n = 3 but increased the likelihood of detecting MNPs by doubling sampled air volume from 10 m^3 to 20 m^3. The sampling campaign was completed but results cannot be presented here since the sample measurement is pending.

Study limitations and future perspectives

Through the method validation study #1, it was established that the recovery rate of NPs from the GLI was fit-for-purpose, although more hydrophobic materials show slightly higher losses in the system. Unfortunately, the results of the method validation study #2 were inconclusive, due to the agglomeration and therefore poor aerosolization efficiency from the jet nebulizer system used. The suitability of the GLI as sampling device for MNPs in aerosols cannot be answered conclusively at this stage because samples from validation study #3 are not measured yet. Data from this study will help to identify differences between the nebulization of labeled and unlabeled, and hydrophobic (PP, PET) and hydrophilic (PS) NPs. It should be noted that the extreme hydrophobicity of the pristine test materials utilized may not be representative of the environmental situation. The surfaces of environmental NPs are expected to undergo aging, which typically reduces their hydrophobicity. Consequently, the low nebulization efficiency observed in this study is considered a limitation specific to the pristine test materials used and not a relevant factor for environmental samples, suggesting the procedure is fit for purpose. Furthermore, the LOD and LOQ for the whole sample collection and analysis method needs to be determined and compared to concentrations reported in the literature to, ultimately, assess its suitability. Finally, the field sampling campaigns represent an attempt to provide real-world exposure data but were limited by the comparably low sampled air volumes of 10 (or when pooled) to 20 m^3. Further field sampling campaigns with increased sample volumes, more

sampling points and repetitions per site should be performed to close existing knowledge gaps on MNP concentrations in lakeside and seaside aerosols.

4.4 Conclusions and contributions to the field of research

To assure comparability between studies, standardized and practical protocols need to be developed[257]. For this purpose, an entirely new method using a GLI for aerosol sampling and TED-GC-MS for analysis was explored and validation experiments performed. The list of available devices is long, ranging from passive to active pump systems with and without filters[25,258]. To my knowledge, validation specifically for sampling aerosols with a GLI to detect MNPs has not been performed before. This also presents the most significant contribution of this study to the field, as it will aid researchers in selecting the optimal method for their studies.

Chapter 5

CONTRIBUTIONS TO THE FIELD OF RESEARCH AND OUTLOOK

5 Perspective and future studies

5.1 Contribution of this study to the current status of micro- and nanoplastic test materials

The complexity of MNPs present in natural environments is also reflected in the wide array of requirements for test materials. In a real-world scenario, MNPs are polymer mixtures with broad size distributions and different degrees of degradation, possibly containing additives of concern and cargo from small molecules to microorganisms. Hence, developing a one-size-fits-all material compatible with all sorts of assays is unlikely. However, within this study it has been shown that quality-by-design is a highly flexible and useful framework for the development of MNP test materials with various intended application scenarios. The comparably low complexity of the presented materials can easily be increased. Depending on the specific research question and intended use case, the TPP with critical and desired quality attributes can be modified. Possible applications include the use of polymers containing defined types and amounts of additives to study their leaching behavior and health impacts or use particles that underwent ageing to determine adsorption and desorption processes of other contaminants. In the following paragraphs, short-, mid-, and long-term perspectives are described to further drive advancements in the field of micro- and nanoplastic research.

Short-term perspectives

This study showed that top-down procedures, particularly knife milling, were ineffective for producing MPs below 40 to 50 µm. However, bottom-up approaches rarely produce particles with primary sizes above 5-10 µm and are mostly spheroidal, leaving a substantial gap in available MP shapes and sizes. With respect to generating irregularly shaped NP fragments, future studies should focus on cryo-milling techniques with high energy inputs such as ball mills, since milling was most effective below the glass transition temperature of the milled material. Caldwell et al. (2020) showed that irregularly shaped NPs can be obtained by employing a combination of cryo-milling and regular ball milling, although their maximal test concentrations were limited to < 11 µg/mL due to comparably low yields[120]. Preliminary studies showed that larger particles or agglomerates can

effectively be removed by filtration with specialized silicone membranes, to optimize the PSD profile of milled materials. Further investigations, to assess its practicality when larger amounts of test materials are produced (e.g. filtration time, dependency on polymer type, or filter clogging) could make other time-consuming and yield reducing production steps obsolete (e.g. centrifugation). After production, in-depth characterization of the MNPs surface chemistry (e.g. *via* X-ray photoelectron spectroscopy, XPS) should be performed in future studies because changes in surface chemistry through production or ageing can influence the interaction of the produced particles with cells and their surrounding environment[259]. While methods to produce low complexity MNP test materials are now becoming available, materials that better reflect environmental samples are still scarce. It also became apparent that dispersing MNPs is substantial for reliable assay readouts. Yet, this issue is not commonly reported. Particles will behave differently depending on their material properties and size, the polarity, pH, or salt content of the medium, and the presence of dispersing agents in the medium. While dispersions in DMEM using FBS or BSA as dispersants were assessed in this study, a wider range of media and conditions needs to be tested. The same is true for testing sensitivity of other cell types than Calu-3 to hyperosmolarity, and biological assays for possible interactions with glycerol. In this way, the flexibility of the presented system of highly concentrated MNPs in glycerol stocks could be demonstrated and its limitations uncovered.

Mid-term to long-term perspectives

For the mid-term, alternatives like biopolymers or water-soluble polymers should also be investigated as they are intended to replace classical fossil-based and long-lasting polymers where applicable. A study by Nigro et al. (2025) showed that the highly used water-soluble polymer PEG negatively affected *Daphnia magna*[260], although PEG is generally considered as safe[261]. Safety assessment of such materials before they are widely used is recommended to uncover possible health risks early on. Approaches for such early-stage risk assessment of entirely new so called “advanced materials” are currently under development and might also be applicable to biopolymers with limited hazard data[262]. Another important point concerns standardization. Apart from a lack of widely agreed

standard protocols for sample collection, storage, preparation, or measurement, also particle standards are rare. To my knowledge, there are currently no MNP reference materials with an intended use in *in vitro* and *in vivo* biological assays. However, the demand for such materials has repeatedly been expressed by the research community[68,70–74]. To provide such a material, it may be necessary to certify multiple CQAs (i.e. properties of interest) as they should simultaneously be colloidally stable in complex aqueous media, sterile, and demonstrate a low endotoxin concentration. **Table 5.1** lists the CQAs which we propose and the acceptable specification limits for each attribute.

Table 5.1: Proposed list of critical quality attributes (CQAs) and their corresponding specifications recommended for reference micro- or nanoplastic materials intended for use in biological assays.

CQAs	Specification	Recommended methods/comments
Homogeneity of particle concentration (uniformity of nanoplastic content across several units)	Guidelines do not provide a recommendation for a maximal allowable variability. We suggest 85-115% of the target value[190].	For batches with > 100 units, a minimum of 10 units measured in duplicates. For batches with < 100 units, at least 3 units or 10% of the batch size measured with four technical replicates[190].
Homogeneity of the particle size distribution profile	> 85% of the particles are within the targeted size range using the validated QC dispersion protocol.	Particle size distribution data should be determined using a validated QC dispersion protocol combined with LD analysis.
Stability of the particle size distribution profile	D_{10} and D_{50} measured after 12 months storage at ambient room temperature should not differ > 15% from the original values. The fraction within the targeted size range should not drop below 85%.	Particle size distribution data should be determined using a validated QC dispersion protocol combined with LD analysis.
Sterility after manufacture and storage	0 CFU/mL after production and 12 months storage of unopened containers at ambient room temperature.	Sterility should be tested using a validated method following dispersion using a validated biorelevant dispersion protocol with sterile cell culture media.
Endotoxin content measured after manufacture	< 0.1 EU/mL[191] after production and 12 months storage of unopened containers at ambient room temperature.	Endotoxin content should be tested using a validated method following dispersion using a validated biorelevant dispersion protocol with sterile, low-endotoxin grade cell culture media.
Residual solvents from the production process	< 1% residual solvents in the final glycerol product.	If no biological effect is expected, higher amounts of residuals could be acceptable.

As described before, the obtained PP MPs did not meet these criteria. Mostly because the low particle yield impeded most of the necessary testing. With the current approach for NPs however, three out of six requirements of the proposed criteria could be fulfilled for both polymers. Additionally to the points highlighted in **Chapter 3.4** (dispersion of nanoPP in biorelevant media, storage stability and in-use shelf-life), also the quantification of residual solvents and content homogeneity of a higher number of vials needs to be investigated. The next step towards more realistic test materials is to include ageing into the

development process. Materials can be aged naturally by exposing plastics to environmental influences or artificially through methods like UV-irradiation, ozone, chemical oxidation, or heat treatment. For natural ageing, exposure times are long, and the result is highly variable because of the weather dependency. Therefore, typically artificial methods are used as they can accelerate and standardize this process[263]. While several standards exist for the routine weathering of polymers, none of them fully replicate the complex natural weathering process. This discrepancy has led to the use of various, non-standardized protocols, which limits the comparability of research findings[264]. Consequently, future research should focus on harmonizing protocols and explore combining aging processes and how they can be integrated into material production to ensure a representative and reproducible product.

5.2 Contribution of this study to the current status of MNP sampling in aerosols

At the present stage, the method described cannot be recommended without reservations. For a complete picture, the pending data from validation study #3 needs to be analyzed, and the LOD and LOQ of this method calculated. This is achievable short-term and comparing the LOD and LOQ with reported MNP concentrations from other air sampling studies will determine the volume of air needed to likely detect MNPs in the samples. Currently, the comparably low sample volume presents the biggest limitation of this study as a recent study by Rindelaub & Miskelly (2025) suggest that ten times higher sample volumes are needed to collect detectable amounts of MNPs[156]. In a second study, Rindelaub *et al.* (2025) sampled air at a remote coastal location in southern New Zealand and quantified MPs by number (> 10 µm) and mass (> 2.5 µm). Passive and active sampling devices were used, where the average air volume sampled actively was 308 m^3, thus, 30 times higher than in our study. They reported an average aerosol MP concentration of 65 ± 6 ng/m^3 (0.14% of all aerosol mass), where individual polymers reached aerosol mass concentrations of roughly 41 ng/m^3 (PE), 15 ng/m^3 (PET), 10 ng/m^3 (PVC), and < 1 ng/m^3 for Nylon, PMMA, PS, and PP[265].

Rindelaub *et al.* also experienced heterogeneously distributed polymer mass concentrations during their five-week campaign. These differences could not be attributed solely to meteorological conditions, but also local human activities like rubbish burning or agriculture[265]. Furthermore, they provided an overview over similar studies[266–268] and showed that the measured MP concentrations are comparable to urban areas. However, it has to be noted that the variability spans over six orders of magnitude due to differences in sampling methods and protocols[265]. Consequently, more sampling studies are needed in the long term, spanning both indoor and outdoor environments across different seasons and timepoints. To facilitate study comparability, standardization of all sampling aspects is desired. Wright *et al.* (2021) expressed the need for developing standardized protocols of existing methods and defined 11 criteria regarding sample collection and handling, controls, and sample analyzation. They also provided a scoring system to assess the robustness of a study sampling MPs in air[257]. By including experts from different disciplines, this approach should be used for the development of guidelines. While this can be achieved in a mid-term perspective, the development of standards like the ones issued by ISO takes more time and, thus, would provide a long-term goal. Unlike international standards, an advantage of guidelines or SOPs is that they can be provided *via* an open access policy. However, the lower findability must be compensated through intensive dissemination activities e.g. at relevant conferences, institutions, or international projects. ☙

References

1 K. Altmann, L. Wimmer, V. Alcolea-Rodriguez, T. Waniek, V. Wachtendorf, K. Matzdorf, D. Ciornii, P. Fengler, F. Milczewski, I. Otazo-Aseguinolaza, M. Ferrer, M. A. Bañares, R. Portela and L. A. Dailey. Quality-by-design and current good practices for the production of test and reference materials for micro- and nano-plastic research. *J Hazard Mater*, 2025, **497**, 139595. https://doi.org/10.1016/J.JHAZMAT.2025.139595.

2 L. Wimmer, M. V. Nguyen Hoang, J. Schwarzinger, V. B. Jovanović, B. Anđelković, T. Cirkovic Velickovic, T. Meisel, T. Waniek, C. Weimann, K. Altmann and L. A. Dailey. A quality-by-design inspired approach to develop PET and PP nanoplastic test materials for use in in vitro and in vivo biological assays. *Environ Sci Nano*, 2025, **12**, 2667–2686. https://doi.org/10.1039/D4EN01186D.

3 B. C. T. de Deus, T. C. Costa, L. N. Altomari, E. M. Brovini, P. S. D. de Brito and S. J. Cardoso. Coastal plastic pollution: A global perspective. *Mar Pollut Bull*, 2024, **203**, 116478. https://doi.org/10.1016/j.marpolbul.2024.116478.

4 European Commission. *Commission Staff Working Document - A European Strategy for Plastics in a Circular Economy*. *Commission Staff Working Document - A European Strategy for Plastics in a Circular Economy*, Brussels, 2018. https://eur-lex.europa.eu/legal-content/EN/TXT/?uri=SWD:2018:16:FIN, (accessed 30 April 2024).

5 5/14 United Nations Environment Assembly. *End Plastic Pollution: Towards an International Legally Binding Instrument - Resolution adopted by the United Nations Environment Assembly on 2 March 2022 [UNEP/EA.5/Res.14]*, 2022. https://wedocs.unep.org/20.500.11822/40597, (accessed 30 August 2024).

6 The White House. FACT SHEET: Biden-Harris Administration Releases New Strategy to Tackle Plastic Pollution, Takes Action to Reduce Single-Use Plastics in Federal Operations. https://www.whitehouse.gov/briefing-room/statements-releases/2024/07/19/fact-sheet-biden-harris-administration-releases-new-strategy-to-tackle-plastic-pollution-takes-action-to-reduce-single-use-plastics-in-federal-operations/?utm_source=link, (accessed 30 August 2024).

7 J. Soares, I. Miguel, C. Venâncio, I. Lopes and M. Oliveira. Public views on plastic pollution: Knowledge, perceived impacts, and pro-environmental behaviours. *J Hazard Mater*, 2021, **412**, 125227. https://doi.org/10.1016/j.jhazmat.2021.125227.

8 Plastics Europe. *Plastics - the fast Facts 2023*. https://plasticseurope.org/knowledge-hub/plastics-the-fast-facts-2023/, (accessed 30 August 2024).

9 N. Singh and T. R. Walker. Plastic recycling: A panacea or environmental pollution problem. *npj Materials Sustainability*, 2024, **2**, 17. https://doi.org/10.1038/s44296-024-00024-w.

10 W. W. Y. Lau, Y. Shiran, R. M. Bailey, E. Cook, M. R. Stuchtey, J. Koskella, C. A. Velis, L. Godfrey, J. Boucher, M. B. Murphy, R. C. Thompson, E. Jankowska, A. C. Castillo, T. D. Pilditch, B. Dixon, L. Koerselman, E. Kosior, E. Favoino, J. Gutberlet, S. Baulch, M. E. Atreya, D. Fischer, K. K. He, M. M. Petit, U. Rashid Sumaila, E. Neil, M. V Bernhofen, K. Lawrence and J. E. Palardy. Evaluating scenarios toward zero plastic pollution. *Science (1979)*, 2020, **369**, 1455–1461. https://doi.org/10.1126/science.aba9475.

11 V. Yadav, M. A. Sherly, P. Ranjan, R. O. Tinoco, A. Boldrin, A. Damgaard and A. Laurent. Framework for quantifying environmental losses of plastics from landfills. *Resour Conserv Recycl*, 2020, **161**, 104914. https://doi.org/10.1016/j.resconrec.2020.104914.

12 X. Fei, Y. Guo, Y. Wang, M. Fang, K. Yin and H. He. The long-term fates of land-disposed plastic waste. *Nat Rev Earth Environ*, 2022, **3**, 733–735. https://doi.org/10.1038/s43017-022-00354-0.

13 K. Zhang, A. H. Hamidian, A. Tubić, Y. Zhang, J. K. H. Fang, C. Wu and P. K. S. Lam. Understanding plastic degradation and microplastic formation in the environment: A review. *Elsevier Ltd*, 2021, preprint. https://doi.org/10.1016/j.envpol.2021.116554.

14 Y. K. Song, S. H. Hong, M. Jang, G. M. Han, S. W. Jung and W. J. Shim. Combined Effects of UV Exposure Duration and Mechanical Abrasion on Microplastic Fragmentation by Polymer Type. *Environ Sci Technol*, 2017, **51**, 4368–4376. https://doi.org/10.1021/acs.est.6b06155.

15 J. Gigault, B. Pedrono, B. Maxit and A. Ter Halle. Marine plastic litter: the unanalyzed nano-fraction. *Environ. Sci.: Nano*, 2016, **3**, 346–350. https://doi.org/10.1039/C6EN00008H.

16 O. S. Alimi, J. Farner Budarz, L. M. Hernandez and N. Tufenkji. Microplastics and Nanoplastics in Aquatic Environments: Aggregation, Deposition, and Enhanced Contaminant Transport. *Environ Sci Technol*, 2018, **52**, 1704–1724. https://doi.org/10.1021/acs.est.7b05559.

17 B. Kuizenga, P. F. Tasseron, K. Wendt-Potthoff and T. H. M. van Emmerik. From source to sea: Floating macroplastic transport along the Rhine river. *Front Environ Sci*. https://doi.org/10.3389/fenvs.2023.1180872.

18 V. S. Koutnik, J. Leonard, S. Alkidim, F. J. DePrima, S. Ravi, E. M. V Hoek and S. K. Mohanty. Distribution of microplastics in soil and freshwater environments: Global analysis and framework for transport modeling. *Environmental Pollution*, 2021, **274**, 116552. https://doi.org/10.1016/j.envpol.2021.116552.

19 D. Allen, S. Allen, S. Abbasi, A. Baker, M. Bergmann, J. Brahney, T. Butler, R. A. Duce, S. Eckhardt, N. Evangeliou, T. Jickells, M. Kanakidou, P. Kershaw, P. Laj, J. Levermore, D. Li, P. Liss, K. Liu, N. Mahowald, P. Masque, D. Materić, A. G. Mayes, P. McGinnity, I. Osvath, K. A. Prather, J. M. Prospero, L. E. Revell, S. G. Sander, W. J. Shim, J. Slade, A. Stein, O. Tarasova and S. Wright. Microplastics and nanoplastics in the marine-atmosphere environment. *Nat Rev Earth Environ*, 2022, **3**, 393–405. https://doi.org/10.1038/s43017-022-00292-x.

20 N. Evangeliou, H. Grythe, Z. Klimont, C. Heyes, S. Eckhardt, S. Lopez-Aparicio and A. Stohl. Atmospheric transport is a major pathway of microplastics to remote regions. *Nat Commun*, 2020, **11**, 3381. https://doi.org/10.1038/s41467-020-17201-9.

21 S. L. Wright, J. Ulke, A. Font, K. L. A. Chan and F. J. Kelly. Atmospheric microplastic deposition in an urban environment and an evaluation of transport. *Environ Int*, 2020, **136**, 105411. https://doi.org/10.1016/J.ENVINT.2019.105411.

22 M. Bergmann, S. Mützel, S. Primpke, M. B. Tekman, J. Trachsel and G. Gerdts. White and wonderful? Microplastics prevail in snow from the Alps to the Arctic. *Sci Adv*, 2019, **5**, eaax1157. https://doi.org/10.1126/sciadv.aax1157.

23 M. B. Tekman, T. Krumpen and M. Bergmann. Marine litter on deep Arctic seafloor continues to increase and spreads to the North at the HAUSGARTEN observatory. *Deep Sea Research Part I: Oceanographic Research Papers*, 2017, **120**, 88–99. https://doi.org/10.1016/j.dsr.2016.12.011.

24 L. Maurizi, L. Simon-Sánchez, A. Vianello, A. H. Nielsen and J. Vollertsen. Every breath you take: High concentration of breathable microplastics in indoor environments. *Chemosphere*, 2024, **361**, 142553. https://doi.org/10.1016/j.chemosphere.2024.142553.

25 World Health Organization (WHO). *Dietary and inhalation exposure to nano- and microplastic particles and potential implications for human health*. 2022. https://www.who.int/publications/i/item/9789240054608, (accessed 29 August 2025).

26 J.-L. Xu, S. Wright, C. Rauert and K. V. Thomas. Are microplastics bad for your health? More rigorous science is needed. *Nature*, 2025, **639**, 300–302. https://doi.org/10.1038/d41586-025-00702-2.

27 D. Crespy, M. Bozonnet and M. Meier. 100 Years of Bakelite, the Material of a 1000 Uses. *Angewandte Chemie International Edition*, 2008, **47**, 3322–3328. https://doi.org/10.1002/anie.200704281.

28 A. L. Andrady and M. A. Neal. Applications and societal benefits of plastics. *Philosophical Transactions of the Royal Society B: Biological Sciences*, 2009, **364**, 1977–1984. https://doi.org/10.1098/rstb.2008.0304.

29 I. E. Napper and R. C. Thompson. Plastic Debris in the Marine Environment: History and Future Challenges. *Global Challenges*, 2020, **4**, 1900081. https://doi.org/10.1002/gch2.201900081.

30 A. Frick and C. Stern. *DSC-Prüfung in der Anwendung*. *DSC-Prüfung in der Anwendung*, Carl Hanser Verlag GmbH & Co. KG, München, 2nd Edition., 2013. https://doi.org/10.3139/9783446436923.

31 H. Wiesinger, Z. Wang and S. Hellweg. Deep Dive into Plastic Monomers, Additives, and Processing Aids. *Environ Sci Technol*, 2021, **55**, 9339–9351. https://doi.org/10.1021/acs.est.1c00976.

32 R. Farrell, Y. J. Cortese, D. M. Devine, N. Gately, M. Rueda, L. Rodriguez and R. Pezzoli. The function and properties of common food packaging materials and their suitability for reusable packaging: The transition from a linear to circular economy. *Current Research in Green and Sustainable Chemistry*, 2024, **9**, 100429. https://doi.org/10.1016/j.crgsc.2024.100429.

33 N. Singh and T. R. Walker. Plastic recycling: A panacea or environmental pollution problem. *npj Materials Sustainability*, 2024, **2**, 17. https://doi.org/10.1038/s44296-024-00024-w.

34 R. Geyer, J. R. Jambeck and K. L. Law. Production, use, and fate of all plastics ever made. *Sci Adv*, 2017, **3**, e1700782. https://doi.org/10.1126/sciadv.1700782.

35 V. Yadav, M. A. Sherly, P. Ranjan, R. O. Tinoco, A. Boldrin, A. Damgaard and A. Laurent. Framework for quantifying environmental losses of plastics from landfills. *Resour Conserv Recycl*, 2020, **161**, 104914. https://doi.org/10.1016/j.resconrec.2020.104914.

36 A. Chamas, H. Moon, J. Zheng, Y. Qiu, T. Tabassum, J. H. Jang, M. Abu-Omar, S. L. Scott and S. Suh. Degradation Rates of Plastics in the Environment. *ACS Sustain Chem Eng*, 2020, **8**, 3494–3511. https://doi.org/10.1021/acssuschemeng.9b06635.

37 L. Liu, M. Xu, Y. Ye and B. Zhang. On the degradation of (micro)plastics: Degradation methods, influencing factors, environmental impacts. *Science of The Total Environment*, 2022, **806**, 151312. https://doi.org/10.1016/j.scitotenv.2021.151312.

38 Royal Society of New Zealand Te Apārangi. Plastics In The Environment - Te Ao Hurihuri - The Changing World. *Royal Society of New Zealand Te Apārangi*, 2019, https://www.royalsociety.org.nz/major-issues-and-projects/plastics/.

39 J. Boucher and D. Friot. Primary microplastics in the oceans: a global evaluation of sources, Gland, 2017. https://doi.org/10.2305/IUCN.CH.2017.01.en.

40 Y. Cai, D. M. Mitrano, R. Hufenus and B. Nowack. Formation of Fiber Fragments during Abrasion of Polyester Textiles. *Environ Sci Technol*, 2021, **55**, 8001–8009. https://doi.org/10.1021/acs.est.1c00650.

41 Y. Xu, M. C. Rillig and W. R. Waldman. New separation protocol reveals spray painting as a neglected source of microplastics in soils. *Environ Chem Lett*, 2022, **20**, 3363–3369. https://doi.org/10.1007/s10311-022-01500-2.

42 L. J. Knight, F. N. F. Parker-Jurd, M. Al-Sid-Cheikh and R. C. Thompson. Tyre wear particles: an abundant yet widely unreported microplastic? *Environmental Science and Pollution Research*, 2020, **27**, 18345–18354. https://doi.org/10.1007/s11356-020-08187-4.

43 N. B. Hartmann, T. Hüffer, R. C. Thompson, M. Hassellöv, A. Verschoor, A. E. Daugaard, S. Rist, T. Karlsson, N. Brennholt, M. Cole, M. P. Herrling, M. C. Hess, N. P. Ivleva, A. L. Lusher and M. Wagner. Are We Speaking the Same Language? Recommendations for a Definition and Categorization Framework for Plastic Debris. *Environ Sci Technol*, 2019, **53**, 1039–1047. https://doi.org/10.1021/acs.est.8b05297.

44 M. R. Gregory. Plastic 'scrubbers' in hand cleansers: a further (and minor) source for marine pollution identified. *Mar Pollut Bull*, 1996, **32**, 867–871. https://doi.org/10.1016/S0025-326X(96)00047-1.

45 S. J. Cusworth, W. J. Davies, M. R. McAinsh, A. S. Gregory, J. Storkey and C. J. Stevens. Agricultural fertilisers contribute substantially to microplastic concentrations in UK soils. *Commun Earth Environ*, 2024, **5**, 7. https://doi.org/10.1038/s43247-023-01172-y.

46 U.S. Food & Drug Administration (FDA). The Microbead-Free Waters Act: FAQs. The Microbead-Free Waters Act: FAQs. https://www.fda.gov/cosmetics/cosmetics-laws-regulations/microbead-free-waters-act-faqs, (accessed 13 June 2025).

47 European Commission. Restriction of microplastics in the EU - Regulation (EU) 2023/2055. https://trade.ec.europa.eu/access-to-markets/en/news/restriction-microplastics-eu-17-october-2023, (accessed 13 June 2025).

48 D. M. Mitrano and W. Wohlleben. Microplastic regulation should be more precise to incentivize both innovation and environmental safety. *Nat Commun*, 2020, **11**, 5324. https://doi.org/10.1038/s41467-020-19069-1.

49 European Commission and Directorate-General for Environment. *Nanoplastics – State of knowledge and environmental and human health impacts*. Publications Office of the European Union, 2023. https://doi.org/10.2779/632649.

50 International Organization for Standardization. *ISO 21960 (2020): Plastics - Environmental aspects - State of knowledge and methodologies*. 2020. https://www.iso.org/standard/72300.html.

51 V. Onink, M. L. A. Kaandorp, E. van Sebille and C. Laufkötter. Influence of Particle Size and Fragmentation on Large-Scale Microplastic Transport in the Mediterranean Sea. *Environ Sci Technol*, 2022, **56**, 15528–15540. https://doi.org/10.1021/acs.est.2c03363.

52 M. Al-Sid-Cheikh, S. J. Rowland, K. Stevenson, C. Rouleau, T. B. Henry and R. C. Thompson. Uptake, Whole-Body Distribution, and Depuration of Nanoplastics by the Scallop Pecten maximus at Environmentally Realistic Concentrations. *Environ Sci Technol*, 2018, **52**, 14480–14486. https://doi.org/10.1021/acs.est.8b05266.

53 R. Ambrosini, R. S. Azzoni, F. Pittino, G. Diolaiuti, A. Franzetti and M. Parolini. First evidence of microplastic contamination in the supraglacial debris of an alpine glacier. *Environmental Pollution*, 2019, **253**, 297–301. https://doi.org/10.1016/j.envpol.2019.07.005.

54 Y. Zhang, T. Gao, S. Kang, S. Allen, X. Luo and D. Allen. Microplastics in glaciers of the Tibetan Plateau: Evidence for the long-range transport of microplastics. *Science of The Total Environment*, 2021, **758**, 143634. https://doi.org/10.1016/j.scitotenv.2020.143634.

55 X. Peng, M. Chen, S. Chen, S. Dasgupta, H. Xu, K. Ta, M. Du, J. Li, Z. Guo and S. Bai. Microplastics contaminate the deepest part of the world's ocean. *Geochem Perspect Lett*, 2018, 1–5. https://doi.org/10.7185/geochemlet.1829.

56 M. Bergmann, F. Collard, J. Fabres, G. W. Gabrielsen, J. F. Provencher, C. M. Rochman, E. van Sebille and M. B. Tekman. Plastic pollution in the Arctictic. *Nature Reviews Earth & Environment 2022 3:5*, 2022, **3**, 323–337. https://doi.org/10.1038/s43017-022-00279-8.

57 E. Bergami, E. Rota, T. Caruso, G. Birarda, L. Vaccari and I. Corsi. Plastics everywhere: first evidence of polystyrene fragments inside the common Antarctic collembolan Cryptopygus antarcticus. *Biol Lett*, 2020, **16**, 20200093, https://doi.org/10.1098/rsbl.2020.0093.

58 S. Abbasi, A. Turner, M. Hoseini and H. Amiri. Microplastics in the Lut and Kavir Deserts, Iran. *Cite This: Environ. Sci. Technol*, 2021, **55**, 6000. https://doi.org/10.1021/acs.est.1c00615.

59 W. C. LI, H. F. TSE and L. FOK. Plastic waste in the marine environment: A review of sources, occurrence and effects. *Science of The Total Environment*, 2016, **566–567**, 333–349. https://doi.org/10.1016/j.scitotenv.2016.05.084.

60 Y. Arif, A. R. Mir, P. Zieliński, S. Hayat and A. Bajguz. Microplastics and nanoplastics: Source, behavior, remediation, and multi-level environmental impact. *J Environ Manage*, 2024, **356**, 120618. https://doi.org/10.1016/j.jenvman.2024.120618.

61 E. van Sebille, M. H. England and G. Froyland. Origin, dynamics and evolution of ocean garbage patches from observed surface drifters. *Environmental Research Letters*, 2012, **7**, 044040. https://doi.org/10.1088/1748-9326/7/4/044040.

62 S. Allen, D. Allen, K. Moss, G. Le Roux, V. R. Phoenix and J. E. Sonke. Examination of the ocean as a source for atmospheric microplastics. *PLoS One*, 2020, **15**, e0232746. https://doi.org/10.1371/JOURNAL.PONE.0232746.

63 K. Lyu, J. Li, Y. Wu, J. Asselman and Z. Yang. Changes in population fitness and gene co-expression networks reveal the boosted impact of toxic cyanobacteria on Daphnia magna through microplastic exposure. *J Hazard Mater*, 2025, **487**, 137225. https://doi.org/10.1016/J.JHAZMAT.2025.137225.

64 S. L. Wright and F. J. Kelly. Plastic and Human Health: A Micro Issue? *Environ Sci Technol*, 2017, **51**, 6634–6647. https://doi.org/10.1021/acs.est.7b00423.

65 E. E. Emecheta, P. M. Pfohl, W. Wohlleben, A. Haase and A. Roloff. Desorption of Polycyclic Aromatic Hydrocarbons from Microplastics in Human Gastrointestinal Fluid Simulants–Implications for Exposure Assessment. *ACS Omega*, 2024, **9**, 24281–24290. https://doi.org/10.1021/acsomega.3c09380.

66 I. Ali, X. Tan, C. Peng, I. Naz, Y. Zhang, A. Hernández, R. Marcos, R. Pervez, Z. Duan and Y. Ruan. Eco- and bio-corona-based microplastics and nanoplastics complexes in the environment: Modulations in the toxicological behavior of plastic particles and factors affecting. *Process Safety and Environmental Protection*, 2024, **187**, 356–375. https://doi.org/10.1016/j.psep.2024.04.035.

67 P. Li and J. Liu. Micro(nano)plastics in the Human Body: Sources, Occurrences, Fates, and Health Risks. *Environ Sci Technol*, 2024, **58**, 3065–3078. https://doi.org/10.1021/acs.est.3c08902.

68 K. Tanaka, Y. Takahashi, H. Kuramochi, M. Osako, S. Tanaka and G. Suzuki. Preparation of Nanoscale Particles of Five Major Polymers as Potential Standards for the Study of Nanoplastics. *Small*, 2021, **17**, 2105781. https://doi.org/10.1002/smll.202105781.

69 W. S. Lee, H. Kim, Y. Sim, T. Kang and J. Jeong. Fluorescent Polypropylene Nanoplastics for Studying Uptake, Biodistribution, and Excretion in Zebrafish Embryos. *ACS Omega*, 2022, **7**, 2467–2473. https://doi.org/10.1021/acsomega.1c06779.

70 J. Seghers, E. A. Stefaniak, R. La Spina, C. Cella, D. Mehn, D. Gilliland, A. Held, U. Jacobsson and H. Emteborg. Preparation of a reference material for microplastics in water-evaluation of homogeneity. *Anal Bioanal Chem*, 2022, 385–397. https://doi.org/10.1007/s00216-021-03198-7.

71 G. Balakrishnan, M. Déniel, T. Nicolai, C. Chassenieux and F. Lagarde. Towards more realistic reference microplastics and nanoplastics: preparation of polyethylene micro/nanoparticles with a biosurfactant. *Environ. Sci.: Nano*, 2019, **6**, 315. https://doi.org/10.1039/c8en01005f.

72 J. Hildebrandt and A. F. Thünemann. Aqueous Dispersions of Polypropylene: Toward Reference Materials for Characterizing Nanoplastics. *Macromol Rapid Commun*, 2023, 2200874. https://doi.org/10.1002/marc.202200874.

73 S. Ducoli, S. Federici, R. Nicsanu, A. Zendrini, C. Marchesi, L. Paolini, A. Radeghieri, P. Bergese and L. E. Depero. A different protein corona cloaks “true-to-life” nanoplastics with respect to synthetic polystyrene nanobeads. *Environ. Sci.: Nano*, 2022, **9**, 1414–1426. https://doi.org/10.1039/d1en01016f.

74 J. R. Peller, S. P. Mezyk, S. Shidler, J. Castleman, S. Kaiser, R. F. Faulkner, C. D. Pilgrim, A. Wilson, S. Martens and G. P. Horne. Facile nanoplastics formation from macro and microplastics in aqueous media. *Environmental Pollution*, 2022, **313**, 120171. https://doi.org/10.1016/j.envpol.2022.120171.

75 AURORA. Actionable european roadmap for early-life health risk assessment of micro- and nanoplastics. https://auroraresearch.eu/, (accessed 13 June 2025).

76 IMPTOX. An innovative analytical platform to investigate the effect and toxicity of micro and nano plastics. https://www.imptox.eu/en/, (accessed 13 June 2025).

77 PLASTICSFATE. Plastics fate and effects in the human body. https://www.plasticsfate.eu/, (accessed 13 June 2025).

78 PLASTICHEAL. Innovative tools to study the impact and mode of action of micro and nanoplastics on human health. https://www.plasticheal.eu/en, (accessed 13 June 2025).

79 POLYRISK. Understanding human exposure and health hazard of micro- and nanoplastic contaminants in our environment. https://polyrisk.science/, (accessed 13 June 2025).

80 CUSP. The European research cluster to understand the health impacts of micro- and nanoplastics. https://cusp-research.eu/, (accessed 13 June 2025).

81 PlascticsEurope. *Plastics - the Facts 2021 An analysis of European plastics production, demand and waste data*. 2021. https://plasticseurope.org/wp-content/uploads/2021/12/Plastics-the-Facts-2021-web-final.pdf, (accessed 29 August 2025)

82 P. Schwabl, S. Koppel, P. Konigshofer, T. Bucsics, M. Trauner, T. Reiberger and B. Liebmann. Detection of various microplastics in human stool: A prospective case series. *Ann Intern Med*, 2019, **171**, 453–457. https://doi.org/10.7326/M19-0618.

83 L. C. Jenner, J. M. Rotchell, R. T. Bennett, M. Cowen, V. Tentzeris and L. R. Sadofsky. Detection of microplastics in human lung tissue using μFTIR spectroscopy. *Science of The Total Environment*, 2020, **707**, 136073. https://doi.org/10.1016/j.scitotenv.2022.154907.

84 S. L. Wright, J. Ulke, A. Font, K. L. A. Chan and F. J. Kelly. Atmospheric microplastic deposition in an urban environment and an evaluation of transport. *Environ Int*, 2020, **136**, 105411. https://doi.org/10.1016/J.ENVINT.2019.105411.

85 V. Nava, S. Chandra, J. Aherne, M. B. Alfonso, A. M. Antão-Geraldes, K. Attermeyer, R. Bao, M. Bartrons, S. A. Berger, M. Biernaczyk, R. Bissen, J. D. Brookes, D. Brown, M. Cañedo-Argüelles, M. Canle, C. Capelli, R. Carballeira, J. L. Cereijo, S. Chawchai, S. T. Christensen, K. S. Christoffersen, E. de Eyto, J. Delgado, T. N. Dornan, J. P. Doubek, J. Dusaucy, O. Erina, Z. Ersoy, H. Feuchtmayr, M. L. Frezzotti, S. Galafassi, D. Gateuille, V. Gonçalves, H.-P. Grossart, D. P. Hamilton, T. D. Harris, K. Kangur, G. B. Kankılıç, R. Kessler, C. Kiel, E. M. Krynak, À. Leiva-Presa, F. Lepori, M. G. Matias, S. S. Matsuzaki, Y. McElarney, B. Messyasz, M. Mitchell, M. C. Mlambo, S. N. Motitsoe, S. Nandini, V. Orlandi, C. Owens, D. Özkundakci, S. Pinnow, A. Pociecha, P. M. Raposeiro, E.-I. Rõõm, F. Rotta, N. Salmaso, S. S. S. Sarma, D. Sartirana, F. Scordo, C. Sibomana, D. Siewert, K. Stepanowska, Ü. N. Tavşanoğlu, M. Tereshina, J. Thompson, M. Tolotti, A. Valois, P. Verburg, B. Welsh, B. Wesolek, G. A. Weyhenmeyer, N. Wu, E. Zawisza, L. Zink and B. Leoni. Plastic debris in lakes and reservoirs. *Nature*, 2023, **619**, 317–322. https://doi.org/10.1038/s41586-023-06168-4.

86 N. W. May, M. J. Gunsch, N. E. Olson, A. L. Bondy, R. M. Kirpes, S. B. Bertman, S. China, A. Laskin, P. K. Hopke, A. P. Ault and K. A. Pratt. Unexpected Contributions of Sea Spray and Lake Spray Aerosol to Inland Particulate Matter. *Environ Sci Technol Lett*, 2018, **5**, 405–412. https://doi.org/10.1021/acs.estlett.8b00254.

87 E. L. Romsos, C. R. Steffen and P. M. Vallone. *Development of a research grade test material for supporting community-wide validation efforts*. Washington D.C., 2022. https://strbase-archive.nist.gov/pub_pres/ISFG2022_Romsos_RGTM.pdf, (accessed 30 August 2024).

88 International Organization for Standardization. *ISO Guide 30 (2015): Reference materials - Selected terms and definitions*. *2015*. https://www.iso.org/standard/46209.html

89 National Institute of Standards and Technology. SRM Definitions. https://www.nist.gov/srm/srm-definitions, (accessed 30 August 2024).

90 G. Crosset-Perrotin, A. Moraz, R. Portela, V. A. Alcolea-Rodriguez, D. Burrueco-Subirà, C. Smith, M. Bañares, H. Foroutan and D. H. Fairbrother. Production, Labeling, and Applications of Micro- and Nanoplastic Reference and Test Materials. *Environ Sci Nano*, 2025, **12**, 2911-2964. https://doi.org/10.1039/D4EN00767K.

91 Bundesanstalt für Materialforschung und -prüfung (BAM). BAM Referenzmaterialien - Polymermaterialien. https://webshop.bam.de/webshop_de/referenzmaterialien/polymermaterialien.html, (accessed 3 September 2024).

92 National Institute of Standards and Technology (NIST). Reference Materials for Plastic Pollution Measurement Science. https://www.nist.gov/programs-projects/reference-materials-plastic-pollution-measurement-science, (accessed 3 September 2024).

93 CD Bioparticles. CD Bioparticles - Polymer Particles. https://www.cd-bioparticles.com/product/polymer-particles-list-172.html, (accessed 3 September 2024).

94 MicroplasticSolution. EasyMP™ - microplastic standards. https://www.microplasticsolution.com/microplastic-reference-materials, (accessed 13 June 2025).

95 O. Hagelskjær, F. Hagelskjær, H. Margenat, J. E. Sonke and G. Le Roux. EasyMP: Diverse and Environmentally Relevant Microplastic Reference Materials Encompassing Fragments and Fibers. *Nano Select*, e70004. https://doi.org/10.1002/nano.70004.

96 V. N. de Ruijter, P. E. Redondo-Hasselerharm, T. Gouin and A. A. Koelmans. Quality Criteria for Microplastic Effect Studies in the Context of Risk Assessment: A Critical Review. *Environ Sci Technol*, 2020, **54**, 11692–11705. https://doi.org/10.1021/acs.est.0c03057.

97 S. Lin, H. Zhang, C. Wang, X.-L. Su, Y. Song, P. Wu, Z. Yang, M.-H. Wong, Z. Cai and C. Zheng. Metabolomics Reveal Nanoplastic-Induced Mitochondrial Damage in Human Liver and Lung Cells. *Environ Sci Technol*, 2022, **56**, 12483–12493. https://doi.org/10.1021/acs.est.2c03980.

98 W. Peter, M. Antoine, M. Pius, M. Danielle, M.-A. Xenia, D. Liliane, D. Pierre-Andre, Z. Andreas, K. Harald F. and von M. Ursula. Barrier Capacity of Human Placenta for Nanosized Materials. *Environ Health Perspect*, 2010, **118**, 432–436. https://doi.org/10.1289/ehp.0901200.

99 A. Tavakolpournegari, B. Annangi, A. Villacorta, G. Banaei, J. Martin, S. Pastor, R. Marcos and A. Hernández. Hazard assessment of different-sized polystyrene nanoplastics in hematopoietic human cell lines. *Chemosphere*, 2023, **325**, 138360. https://doi.org/10.1016/j.chemosphere.2023.138360.

100 M. Tamayo-Belda, J. J. Vargas-Guerrero, K. Martín-Betancor, G. Pulido-Reyes, M. González-Pleiter, F. Leganés, R. Rosal and F. Fernández-Piñas. Understanding nanoplastic toxicity and their interaction with engineered cationic nanopolymers in microalgae by physiological and proteomic approaches. *Environ Sci Nano*, 2021, **8**, 2277–2296. https://doi.org/10.1039/D1EN00284H.

101 O. Pikuda, E. G. Xu, D. Berk and N. Tufenkji. Toxicity Assessments of Micro- and Nanoplastics Can Be Confounded by Preservatives in Commercial Formulations. *Environ Sci Technol Lett*, 2019, **6**, 21–25. https://doi.org/10.1021/acs.estlett.8b00614.

102 M. Heinlaan, K. Kasemets, V. Aruoja, I. Blinova, O. Bondarenko, A. Lukjanova, A. Khosrovyan, I. Kurvet, M. Pullerits, M. Sihtmäe, G. Vasiliev, H. Vija and A. Kahru. Hazard evaluation of polystyrene nanoplastic with nine bioassays did not show particle-specific acute toxicity. *Science of The Total Environment*, 2020, **707**, 136073. https://doi.org/10.1016/j.scitotenv.2019.136073.

103 Elijah. J. Petersen, A. C. Barrios, T. B. Henry, M. E. Johnson, A. A. Koelmans, A. R. Montoro Bustos, J. Matheson, M. Roesslein, J. Zhao and B. Xing. Potential Artifacts and Control Experiments in Toxicity Tests of Nanoplastic and Microplastic Particles. *Environ Sci Technol*, 2022, **56**, 15192–15206. https://doi.org/10.1021/acs.est.2c04929.

104 T. F. Lins, A. M. O'Brien, T. Kose, C. M. Rochman and D. Sinton. Toxicity of nanoplastics to zooplankton is influenced by temperature, salinity, and natural particulate matter. *Environ Sci Nano*, 2022, **9**, 2678–2690. https://doi.org/10.1039/D2EN00123C.

105 N. N. Phuong, A. Zalouk-Vergnoux, L. Poirier, A. Kamari, A. Châtel, C. Mouneyrac and F. Lagarde. Is there any consistency between the microplastics found in the field and those used in laboratory experiments? *Environmental Pollution*, 2016, **211**, 111–123. https://doi.org/10.1016/J.ENVPOL.2015.12.035.

106 L. A. Parker, E. M. Höppener, E. F. van Amelrooij, S. Henke, I. M. Kooter, K. Grigoriadi, M. G. A. Nooijens, A. M. Brunner and A. Boersma. Protocol for the production of micro- and nanoplastic test materials. *Microplastics and Nanoplastics*, 2023, **3**, 10. https://doi.org/10.1186/s43591-023-00058-2.

107 Y. Ji, L. Chen, Y. Wang, J. Zhang, Y. Yu, M. Wang, X. Wang, W. Liu, B. Yan, L. Xiao, X. Song, C. Lv and L. Chen. Realistic Nanoplastics Induced Pulmonary Damage via the Crosstalk of Ferritinophagy and Mitochondrial Dysfunction. *ACS Nano*, 2024, **18**, 16790–16807. https://doi.org/10.1021/acsnano.4c02335.

108 I. Inkielewicz-Stepniak, L. Tajber, G. Behan, H. Zhang, M. W. Radomski, C. Medina and M. J. Santos-Martinez. The role of mucin in the toxicological impact of polystyrene nanoparticles. *Materials*, 2018, **11**, 724. https://doi.org/10.3390/ma11050724.

109 M. Sultan, X.-Y. Wei, J.-J. Duan, B.-F. Zhang, M.-F. Wu, Z.-X. Cai and D.-S. Pei. Comparative toxicity of polystyrene, polypropylene, and polyethylene nanoplastics on Artemia franciscana nauplii: a multidimensional assessment. *Environ Sci Nano*, 2024, **11**, 1070–1084. https://doi.org/10.1039/D3EN00774J.

110 M. Auguste, T. Balbi, A. Miglioli, S. Alberti, S. Prandi, R. Narizzano, A. Salis, G. Damonte and L. Canesi. Comparison of Different Commercial Nanopolystyrenes: Behavior in Exposure Media, Effects on Immune Function and Early Larval Development in the Model Bivalve Mytilus galloprovincialis. *Nanomaterials*, 2011, **11**, 3291. https://doi.org/10.3390/nano11123291.

111 V. Mishra, S. Thakur, A. Patil and A. Shukla. Quality by design (QbD) approaches in current pharmaceutical set-up. *Expert Opin Drug Deliv*, 2018, **15**, 737–758. https://doi.org/10.1080/17425247.2018.1504768.

112 L. X. Yu, G. Amidon, M. A. Khan, S. W. Hoag, J. Polli, G. K. Raju and J. Woodcock. Understanding Pharmaceutical Quality by Design. *AAPS J*, 2014, **16**, 771–783. https://doi.org/10.1208/s12248-014-9598-3.

113 J. Ali, K. Pramod, Ma. Tahir, N. Charoo and S. Ansari. Pharmaceutical product development: A quality by design approach. *Int J Pharm Investig*, 2016, **6**, 129. https://doi.org/10.4103/2230-973x.187350.

114 International Organization for Standardization. *ISO 33401 (2024): Reference materials - Contents of certificates, labels and accompanying documentation*. 2024. https://www.iso.org/standard/84222.html.

115 International Organization for Standardization. *ISO 33405 (2024): Reference materials - Approaches for characterization and assessment of homogeneity and stability*. 2024. https://www.iso.org/standard/84226.html

116 D. Magrì, P. Sánchez-Moreno, G. Caputo, F. Gatto, M. Veronesi, G. Bardi, T. Catelani, D. Guarnieri, A. Athanassiou, P. P. Pompa and D. Fragouli. Laser Ablation as a Versatile Tool To Mimic Polyethylene Terephthalate Nanoplastic Pollutants: Characterization and Toxicology Assessment. *ACS Nano*, 2018, **12**, 7690–7700. https://doi.org/10.1021/acsnano.8b01331.

117 E. Von Der Esch, M. Lanzinger, A. J. Kohles, C. Schwaferts, J. Weisser, T. Hofmann, K. Glas, M. Elsner and N. P. Ivleva. Simple Generation of Suspensible Secondary Microplastic Reference Particles via Ultrasound Treatment. *Front. Chem*, 2020, **8**, 169. https://doi.org/10.3389/fchem.2020.00169.

118 Z. Gerdes, M. Hermann, M. Ogonowski and E. Gorokhova. A novel method for assessing microplastic effect in suspension through mixing test and reference materials. *Sci Rep*, 2019, **9**, 10695. https://doi.org/10.1038/s41598-019-47160-1.

119 J. Hwang, D. Choi, S. Han, J. Choi and J. Hong. An assessment of the toxicity of polypropylene microplastics in human derived cells. *Science of The Total Environment*, 2019, **684**, 657–669. https://doi.org/10.1016/j.scitotenv.2019.05.071.

120 J. Caldwell, R. Lehner, S. Balog, C. Rhême, X. Gao, D. Septiadi, C. Weder, A. Petri-Fink and B. Rothen-Rutishauser. Fluorescent plastic nanoparticles to track their interaction and fate in physiological environments. *Environ. Sci.: Nano*, 2021, **8**, 502–513. https://doi.org/10.1039/D0EN00944J.

121 A. G. Rodríguez-Hernández, J. Alejandro Muñoz-Tabares, J. Cristobal Aguilar-Guzmán and R. Vazquez-Duhalt. A novel and simple method for polyethylene terephthalate (PET) nanoparticle production. *Environ. Sci.: Nano*, 2019, **6**, 2031–2036. https://doi.org/10.1039/c9en00365g.

122 L. M. Johnson, J. B. Mecham, S. A. Krovi, M. M. Moreno Caffaro, S. Aravamudhan, A. L. Kovach, T. R. Fennell and N. P. Mortensen. Fabrication of polyethylene terephthalate (PET) nanoparticles with fluorescent tracers for studies in mammalian cells. *Nanoscale Adv*, 2021, **3**, 339–346. https://doi.org/10.1039/D0NA00888E.

123 K. Y. Santizo, H. S. Mangold, Z. Mirzaei, H. Park, R. R. Kolan, G. Sarau, S. Kolle, T. Hansen, S. Christiansen and W. Wohlleben. Microplastic Materials for Inhalation Studies: Preparation by Solvent Precipitation and Comprehensive Characterization. *Small*, 2025, **21**, 2405555. https://doi.org/10.1002/smll.202405555.

124 J. Jeyavani, A. Sibiya, S. Bhavaniramya, S. Mahboob, K. A. Al-Ghanim, Z. un Nisa, M. N. Riaz, M. Nicoletti, M. Govindarajan and B. Vaseeharan. Toxicity evaluation of polypropylene microplastic on marine microcrustacean Artemia salina: An analysis of implications and vulnerability. *Chemosphere*, 2022, **296**, 133990. https://doi.org/10.1016/J.CHEMOSPHERE.2022.133990.

125 L. Fang, Y. Wang and Y. Xu. Preparation of Polypropylene Powder by Dissolution-Precipitation Method for Selective Laser Sintering. *Advances in Polymer Technology*, 2019, **2019**, 5803895. https://doi.org/10.1155/2019/5803895.

126 D. S. Achilias, A. A. Giannoulis, A. G. Z. Papageorgiou, Á. A. Giannoulis and G. Z. Papageorgiou. Recycling of polymers from plastic packaging materials using the dissolution-reprecipitation technique. *Polym. Bull*, 2009, **63**, 449–465. https://doi.org/10.1007/s00289-009-0104-5.

127 Retsch. *Sieve Analysis - Taking a close look at quality: An expert guide to particle size analysis*. Haan, 2015. https://www.retsch.de/files/8785/expert-guide-sieving.pdf, (accessed 13 May 2025).

128 A. Al Harraq and B. Bharti. Microplastics through the Lens of Colloid Science. *ACS Environmental Au*, 2022, **2**, 3–10. https://doi.org/10.1021/acsenvironau.1c00016.

129 C. Ompala, J.-P. Renault, O. Taché, É. Cournède, S. Devineau and C. Chivas-Joly. Stability and dispersibility of microplastics in experimental exposure medium and their dimensional characterization by SMLS, SAXS, Raman microscopy, and SEM. *J Hazard Mater*, 2024, **469**, 134083. https://doi.org/10.1016/j.jhazmat.2024.134083.

130 M. Schvartz, F. Saudrais, S. Devineau, S. Chédin, F. Jamme, J. Leroy, K. Rakotozandriny, O. Taché, G. Brotons, S. Pin, Y. Boulard and J.-P. Renault. Role of the Protein Corona in the Colloidal Behavior of Microplastics. *Langmuir*, 2023, **39**, 4291–4303. https://doi.org/10.1021/acs.langmuir.2c03237.

131 B. W. Wheeler, M. White, W. Stahl-Timmins and M. H. Depledge. Does living by the coast improve health and wellbeing? *Health Place*, 2012, **18**, 1198–1201. https://doi.org/10.1016/j.healthplace.2012.06.015.

132 S. Moitra, M. Foraster, A. Arbillaga-Etxarri, A. Marín, A. Barberan-Garcia, D. A. Rodríguez-Chiaradia, E. Balcells, M. Koreny, P. Torán-Monserrat, P. Vall-Casas, R. Rodríguez-Roisin and J. Garcia-Aymerich. Roles of the physical environment in health-related quality of life in patients with chronic obstructive pulmonary disease. *Environ Res*, 2022, **203**, 111828. https://doi.org/10.1016/J.ENVRES.2021.111828.

133 A. N. Schuh D. Klimatherapie im Hochgebirge und im Meeresklima. *DMW - Deutsche Medizinische Wochenschrift*, 2011, **136**, 135–139. https://doi.org/10.1055/s-0031-1272496.

134 A. Kubincová, P. Takáč, L. Kendrová, P. Joppa and W. Mikuľáková. The Effect of Pulmonary Rehabilitation in Mountain Environment on Exercise Capacity and Quality of Life in Patients with Chronic Obstructive Pulmonary Disease (COPD) and Chronic Bronchitis. *Medical Science Monitor*, 2018, **24**, 6375–6386. https://doi.org/10.12659/MSM.909777.

135 S. Tong, Y. Yin and Y. Bao. Climatotherapy for asthma: Research progress and prospect. *Environ Res*, 2022, **214**, 113988. https://doi.org/10.1016/j.envres.2022.113988.

136 P. K. Quinn and T. S. Bates. Ocean-Derived Aerosol and Its Climate Impacts. *Treatise on Geochemistry: Second Edition*, 2014, **5**, 317–330. https://doi.org/10.1016/B978-0-08-095975-7.00416-2.

137 R. M. Harrison, C. Giorio, D. C. S. Beddows and M. Dall'Osto. Size distribution of airborne particles controls outcome of epidemiological studies. *Science of The Total Environment*, 2010, **409**, 289–293. https://doi.org/10.1016/j.scitotenv.2010.09.043.

138 E. B. Franklin, S. Amiri, D. Crocker, C. Morris, K. Mayer, J. S. Sauer, R. J. Weber, C. Lee, F. Malfatti, C. D. Cappa, T. H. Bertram, K. A. Prather and A. H. Goldstein. Anthropogenic and Biogenic Contributions to the Organic Composition of Coastal Submicron Sea Spray Aerosol. *Environ Sci Technol*, 2022, **56**, 16633–16642. https://doi.org/10.1021/acs.est.2c04848.

139 L. T. Cravigan, M. D. Mallet, P. Vaattovaara, M. J. Harvey, C. S. Law, R. L. Modini, L. M. Russell, E. Stelcer, D. D. Cohen, G. Olsen, K. Safi, T. J. Burrell and Z. Ristovski. Sea spray aerosol organic enrichment, water uptake and surface tension effects. *Atmos Chem Phys*, 2020, **20**, 7955–7977. https://doi.org/10.5194/acp-20-7955-2020.

140 J. Asselman, E. Van Acker, M. De Rijcke, L. Tilleman, F. Van Nieuwerburgh, J. Mees, K. A. C. De Schamphelaere and C. R. Janssen. Marine biogenics in sea spray aerosols interact with the mTOR signaling pathway. *Sci Rep*, 2019, **9**, 675. https://doi.org/10.1038/s41598-018-36866-3.

141 Y. Wang, M. Li and A. S. Zha. mTOR promotes an inflammatory response through the HIF1 signaling pathway in ulcerative colitis. *Int Immunopharmacol*, 2024, **134**, 112217. https://doi.org/10.1016/J.INTIMP.2024.112217.

142 World Health Organization (WHO). *WHO global air quality guidelines: particulate matter (PM2.5 and PM10), ozone, nitrogen dioxide, sulfur dioxide and carbon monoxide*. 2021. https://www.who.int/publications/i/item/9789240034228/.

143 J. Scales, H. Hajmohammadi, M. Priestman, L. C. McIlvenna, I. E. de Boer, H. Hassan, A. H. Tremper, G. Chen, H. E. Wood, D. C. Green, K. Katsouyanni, I. S. Mudway and C. Griffiths. Assessing the Impact of Non-Exhaust Emissions on the Asthmatic Airway (IONA) Protocol for a Randomised Three-Exposure Crossover Study. *Int J Environ Res Public Health*, 2024, **21**, 895. https://doi.org/10.3390/ijerph21070895.

144 R. Dris, J. Gasperi, V. Rocher, M. Saad, N. Renault and B. Tassin. Microplastic contamination in an urban area: a case study in Greater Paris. *Environmental Chemistry*, 2015, **12**, 592–599. https://doi.org/10.1071/EN14167.

145 S. Allen, D. Allen, V. R. Phoenix, G. Le Roux, P. Durántez Jiménez, A. Simonneau, S. Binet and D. Galop. Atmospheric transport and deposition of microplastics in a remote mountain catchment. *Nat Geosci*, 2019, **12**, 339–344. https://doi.org/10.1038/s41561-019-0335-5.

146 S. Lambert, M. Vercauteren, A. I. Catarino, Y. Li, J. Van Landuyt, N. Boon, G. Everaert, M. De Rijcke, C. R. Janssen and J. Asselman. Aerosolization of micro- and nanoplastics via sea spray: Investigating the role of polymer type, size, and concentration, and potential implications for human exposure. *Environmental Pollution*, 2024, **351**, 124105. https://doi.org/10.1016/j.envpol.2024.124105.

147 L. D. B. Mandemaker and F. Meirer. Spectro-Microscopic Techniques for Studying Nanoplastics in the Environment and in Organisms. *Angewandte Chemie International Edition*, 2023, **62**, e202210494. https://doi.org/10.1002/anie.202210494.

148 Å. Gustafsson, A. M. Krais, A. Gorzsás, T. Lundh and P. Gerde. Isolation and characterization of a respirable particle fraction from residential house-dust. *Environ Res*, 2018, **161**, 284–290. https://doi.org/10.1016/J.ENVRES.2017.10.049.

149 J. C. Prata. Airborne microplastics: Consequences to human health? *Environmental Pollution*, 2018, **234**, 115–126. https://doi.org/10.1016/j.envpol.2017.11.043.

150 J. Caldwell, L. Rodriguez-Lorenzo, B. Espiña, A. Beck, F. Stock, K. Voges, K. Pabortsava, C. Feltham, A. Horton, R. Lampitt, B. Rothen-Rutishauser, P. Taladriz-Blanco and A. Petri-Fink. Detection of submicron- and nanoplastics spiked in environmental fresh- and saltwater with Raman spectroscopy. *Mar Pollut Bull*, 2024, **203**, 116468. https://doi.org/10.1016/J.MARPOLBUL.2024.116468.

151 J. Caldwell, P. Taladriz-Blanco, L. Rodriguez-Lorenzo, B. Rothen-Rutishauser and A. Petri-Fink. Submicron- and nanoplastic detection at low micro- to nanogram concentrations using gold nanostar-based surface-enhanced Raman scattering (SERS) substrates. *Environ. Sci.: Nano*, 2024, **11**, 1000–1011. https://doi.org/10.1039/D3EN00401E.

152 F. Petersen and J. A. Hubbart. The occurrence and transport of microplastics: The state of the science. *Science of The Total Environment*, 2021, **758**, 143936. https://doi.org/10.1016/j.scitotenv.2020.143936.

153 W. J. Shim, S. H. Hong and S. E. Eo. Identification methods in microplastic analysis: a review. *Analytical Methods*, 2017, **9**, 1384–1391. https://doi.org/10.1039/C6AY02558G.

154 S. Primpke, S. H. Christiansen, W. Cowger, H. de Frond, A. Deshpande, M. Fischer, E. B. Holland, M. Meyns, B. A. O'Donnell, B. E. Ossmann, M. Pittroff, G. Sarau, B. M. Scholz-Böttcher and K. J. Wiggin. Critical Assessment of Analytical Methods for the Harmonized and Cost-Efficient Analysis of Microplastics. *Appl Spectrosc*, 2020, **74**, 1012–1047. https://doi.org/10.1177/0003702820921465.

155 F. A. Santos, R. S. Andre, A. D. Alvarenga, A. L. M. M. Alves and D. S. Correa. Micro- and nanoplastics in the environment: a comprehensive review on detection techniques. *Environ. Sci.: Nano*, 2025 **12**, 3442-3467. https://doi.org/10.1039/D4EN00319E.

156 J. D. Rindelaub and G. M. Miskelly. Inhalable microplastics and plastic additives in the indoor air of chemical laboratories. *J Expo Sci Environ Epidemiol*, 2025. https://doi.org/10.1038/s41370-025-00768-0.

157 D. Santillo. *Microplastic fibres and fragments in nearshore surface waters of 7 lakes in Austria in May and June 2023*. 2023. https://www.greenpeace.to/greenpeace/wp-content/uploads/GRL-AR-2023-04.pdf, (accessed 13 June 2025).

158 C. Schmid, L. Cozzarini and E. Zambello. A critical review on marine litter in the Adriatic Sea: Focus on plastic pollution. *Environmental Pollution*, 2021, **273**, 116430. https://doi.org/10.1016/j.envpol.2021.116430.

159 L. F. Amato-Lourenço, R. Carvalho-Oliveira, G. R. Júnior, L. dos Santos Galvão, R. A. Ando and T. Mauad. Presence of airborne microplastics in human lung tissue. *J Hazard Mater*, 2021, **416**, 126124. https://doi.org/10.1016/J.JHAZMAT.2021.126124.

160 L. Zhu, Y. Kang, M. Ma, Z. Wu, L. Zhang, R. Hu, Q. Xu, J. Zhu, X. Gu and L. An. Tissue accumulation of microplastics and potential health risks in human. *Science of The Total Environment*, 2024, **915**, 170004. https://doi.org/10.1016/J.SCITOTENV.2024.170004.

161 M. Klein and E. K. Fischer. Microplastic abundance in atmospheric deposition within the Metropolitan area of Hamburg, Germany. *Science of The Total Environment*, 2019, **685**, 96–103. https://doi.org/10.1016/J.SCITOTENV.2019.05.405.

162 J. Hänninen, M. Weckström, J. Pawłowska, N. Szymańska, E. Uurasjärvi, M. Zajaczkowski, S. Hartikainen and I. Vuorinen. Plastic debris composition and concentration in the Arctic Ocean, the North Sea and the Baltic Sea. *Mar Pollut Bull*, 2021, **165**, 112150. https://doi.org/10.1016/J.MARPOLBUL.2021.112150.

163 N. P. Mortensen, T. R. Fennell and L. M. Johnson. Unintended human ingestion of nanoplastics and small microplastics through drinking water, beverages, and food sources. *NanoImpact*, 2021, **21**, 100302. https://doi.org/10.1016/J.IMPACT.2021.100302.

164 Y. Li, P. Italiani, E. Casals, N. Tran, V. F. Puntes and D. Boraschi. Optimising the use of commercial LAL assays for the analysis of endotoxin contamination in metal colloids and metal oxide nanoparticles. *Nanotoxicology*, 2015, **9**, 462–473. https://doi.org/10.3109/17435390.2014.948090.

165 G. J. Oostingh, E. Casals, P. Italiani, R. Colognato, R. Stritzinger, J. Ponti, T. Pfaller, Y. Kohl, D. Ooms, F. Favilli, H. Leppens, D. Lucchesi, F. Rossi, I. Nelissen, H. Thielecke, V. F. Puntes, A. Duschl and D. Boraschi. Problems and challenges in the development and validation of human cell-based assays to determine nanoparticle-induced immunomodulatory effects. *Part Fibre Toxicol*, 2011, **8**, 8. https://doi.org/10.1186/1743-8977-8-8.

166 Y. Li, M. Fujita and D. Boraschi. Endotoxin Contamination in Nanomaterials Leads to the Misinterpretation of Immunosafety Results. *Front Immunol*, 2017, **8**, 472. https://doi.org/10.3389/fimmu.2017.00472.

167 H. A. Maddah. Polypropylene as a Promising Plastic: A Review. *American Journal of Polymer Science*, 2016, **6**, 1–11. https://doi.org/10.5923/j.ajps.20160601.01.

168 J. Almond, P. Sugumaar, M. N. Wenzel, G. Hill and C. Wallis. Determination of the carbonyl index of polyethylene and polypropylene using specified area under band methodology with ATR-FTIR spectroscopy. *E-Polymers*, 2020, **20**, 369–381. https://doi.org/10.1515/epoly-2020-0041.

169 Scientific Polymer Products Inc. *Refractive index of polymers by index*. https://scipoly.com/technical-library/refractive-index-of-polymers-by-index/, (accessed 10 March 2025).

170 D. Langevin, O. Lozano, A. Salvati, V. Kestens, M. Monopoli, E. Raspaud, S. Mariot, A. Salonen, S. Thomas, M. Driessen, A. Haase, I. Nelissen, N. Smisdom, P. P. Pompa, G. Maiorano, V. Puntes, D. Puchowicz, M. Stępnik, G. Suárez, M. Riediker, F. Benetti, I. Mičetić, M. Venturini, W. G. Kreyling, M. van der Zande, H. Bouwmeester, S. Milani, J. O. Rädler, S. Mülhopt, I. Lynch and K. Dawson. Inter-laboratory comparison of nanoparticle size measurements using dynamic light scattering and differential centrifugal sedimentation. *NanoImpact*, 2018, **10**, 97–107. https://doi.org/10.1016/j.impact.2017.12.004.

171 Food and Drug Administration. *Pharmaceutical Microbiology Manual*. 2020. https://www.fda.gov/media/88801/download, (accessed 30 August 2024).

172 Ph. Eur. 11. 4.5.4.2.1 Plattengussverfahren. in *European Pharmacopoeia 11*, 2023.

173 X. Song, W. Zhuang, H. Cui, M. Liu, T. Gao, A. Li and Z. Gao. Interactions of microplastics with organic, inorganic and bio-pollutants and the ecotoxicological effects on terrestrial and aquatic organisms. *Science of The Total Environment*, 2022, **838**, 156068. https://doi.org/10.1016/J.SCITOTENV.2022.156068.

174 C. R. Barber. The sublimation temperature of carbon dioxide. *British Journal of Applied Physics*, 1966, **17**, 391. https://doi.org/10.1088/0508-3443/17/3/312.

175 World Health Organization (WHO) and International Labour Organization (ILO). International Chemical Safety Cards (WHO and ILO). https://chemicalsafety.ilo.org/dyn/icsc/showcard.display?p_version=2&p_card_id=0044, (accessed 19 June 2025).

176 F. Müller. Wet Classification in the Fines Range < 10 µm. *Chem Eng Technol*, 2010, **33**, 1419–1426. https://doi.org/10.1002/ceat.200900540.

177 Terence Allen. Particle Size Measurement. in *Volume 1: Powder sampling and particle size measurement*, Springer Dordrecht, 5th edn., 1996, pp. 156–166.

178 SmartMembranes GmbH. SmartMembranes - Macroporous silicon. https://www.smartmembranes.de/en/products/macroporous-silicon/, (accessed 21 February 2025).

179 International Organization for Standardization. *ISO 17034 (2016): General requirements for the competence of reference material producers*. 2016. https://www.iso.org/standard/29357.html.

180 R. M. and M. S. E. Swierczewska Magdalena and Crist. Evaluating Nanomedicines: Obstacles and Advancements. in *Characterization of Nanoparticles Intended for Drug Delivery*, ed. S. E. McNeil, Springer New York, New York, NY, 2018, pp. 3–16. https://doi.org/10.1007/978-1-4939-7352-1_1.

181 P. D. Constable, K. W. Hinchcliff, S. H. Done and W. Grünberg, Eds. Disturbances of Free Water, Electrolytes, Acid-Base Balance, and Oncotic Pressure. in *Veterinary Medicine*, Elsevier, 11th edn., 2017, pp. 113–152. https://doi.org/10.1016/B978-0-7020-5246-0.00005-X.

182 R. Scherließ. The MTT assay as tool to evaluate and compare excipient toxicity in vitro on respiratory epithelial cells. *Int J Pharm*, 2011, **411**, 98–105. https://doi.org/10.1016/j.ijpharm.2011.03.053.

183 A. Nene, S. Sadeghzade, S. Viaroli, W. Yang, U. P. Uchenna, A. Kandwal, X. Liu, P. Somani and M. Galluzzi. Recent advances and future technologies in nano-microplastics detection. *Environ Sci Eur*, 2025, **37**, 7. https://doi.org/10.1186/s12302-024-01044-y.

184 Y. Yang, E. Xie, Z. Du, Z. Peng, Z. Han, L. Li, R. Zhao, Y. Qin, M. Xue, F. Li, K. Hua and X. Yang. Detection of Various Microplastics in Patients Undergoing Cardiac Surgery. *Environ Sci Technol*, 2023, **57**, 10911–10918. https://doi.org/10.1021/acs.est.2c07179.

185 A. Ragusa, A. Svelato, C. Santacroce, P. Catalano, V. Notarstefano, O. Carnevali, F. Papa, M. C. A. Rongioletti, F. Baiocco, S. Draghi, E. D'Amore, D. Rinaldo, M. Matta and E. Giorgini. Plasticenta: First evidence of microplastics in human placenta. *Environ Int*, 2021, **146**, 106274. https://doi.org/10.1016/J.ENVINT.2020.106274.

186 K. Mattsson, E. V Johnson, A. Malmendal, S. Linse, L.-A. Hansson and T. Cedervall. Brain damage and behavioural disorders in fish induced by plastic nanoparticles delivered through the food chain. *Sci Rep*, 2017, **7**, 11452. https://doi.org/10.1038/s41598-017-10813-0.

187 W. Wang, J. Zhang, Z. Qiu, Z. Cui, N. Li, X. Li, Y. Wang, H. Zhang and C. Zhao. Effects of polyethylene microplastics on cell membranes: A combined study of experiments and molecular dynamics simulations. *J Hazard Mater*, 2022, **429**, 128323. https://doi.org/10.1016/J.JHAZMAT.2022.128323.

188 L. Li, S. Li, Y. Xu, L. Ren, L. Yang, X. Liu, Y. Dai, J. Zhao and T. Yue. Distinguishing the nanoplastic–cell membrane interface by polymer type and aging properties: translocation, transformation and perturbation. *Environ. Sci.: Nano*, 2023, **10**, 440–453. https://doi.org/10.1039/D2EN00800A.

189 P. M. Gopinath, K. S. Twayana, P. Ravanan, J. Thomas, A. Mukherjee, D. F. Jenkins and N. Chandrasekaran. Prospects on the nano-plastic particles internalization and induction of cellular response in human keratinocytes. *Part Fibre Toxicol*, 2021, **18**, 35. https://doi.org/10.1186/s12989-021-00428-9.

190 International Organization for Standardization. *ISO Guide 35 (2017): Reference materials - guidance for characterisation and assessment of homogeneity and stability*. 2017. https://www.iso.org/standard/60281.html.

191 Y. Li, Z. Shi, I. Radauer-Preiml, A. Andosch, E. Casals, U. Luetz-Meindl, M. Cobaleda, Z. Lin, M. Jaberi-Douraki, P. Italiani, J. Horejs-Hoeck, M. Himly, N. A. Monteiro-Riviere, A. Duschl, V. F. Puntes and D. Boraschi. Bacterial endotoxin (lipopolysaccharide) binds to the surface of gold nanoparticles, interferes with biocorona formation and induces human monocyte inflammatory activation. *Nanotoxicology*, 2017, **11**, 1157–1175. https://doi.org/10.1080/17435390.2017.1401142.

192 R. Christoph, B. Schmidt, U. Steinberner, W. Dilla and R. Karinen. Glycerol. in *Ullmann's Encyclopedia of Industrial Chemistry*, 2006. https://doi.org/10.1002/14356007.a12_477.pub2.

193 S. S. Gaikwad, J. O. Morales, N. B. Lande, J. Catalán-Figueroa, U. D. Laddha and S. J. Kshirsagar. Exploring paediatric oral suspension development: Challenges, requirements, and formulation advancements. *Int J Pharm*, 2024, **657**, 124169. https://doi.org/10.1016/j.ijpharm.2024.124169.

194 L. R. Morrison. Glycerol. in *Kirk-Othmer Encyclopedia of Chemical Technology*, 2000. https://doi.org/10.1002/0471238961.0712250313151818.a01.

195 Pharmaceutical Press and American Pharmacists Association. *Handbook of Pharmaceutical Excipients*. *Handbook of Pharmaceutical Excipients*, Pharmaceutical Press & American Pharmacists Association, London, 6th edn., 2009.

196 M. S. B. Frank, M. C. Nahata and M. D. Hilty. Glycerol: A Review of Its Pharmacology, Pharmacokinetics, Adverse Reactions, and Clinical Use. *Pharmacotherapy: The Journal of Human Pharmacology and Drug Therapy*, 1981, **1**, 147–160. https://doi.org/10.1002/j.1875-9114.1981.tb03562.x.

197 DAC/NRF-KommissionABDA and Bundesvereinigung Deutscher Apothekerverbände e. V. Deutscher Arzneimittel-Codex® / Neues Rezeptur-Formularium® (DAC/NRF). in *DAC/NRF*, Deutscher Apotheker Verlag, 2024/1., 2024. https://dacnrf.pharmazeutische-zeitung.de/.

198 D. S. Wishart, C. Knox, A. C. Guo, D. Cheng, S. Shrivastava, D. Tzur, B. Gautam and M. Hassanali. DrugBank: a knowledgebase for drugs, drug actions and drug targets. *Nucleic Acids Res*, 2008, **36**, D901–D906. https://doi.org/10.1093/nar/gkm958.

199 K. Tanaka, H. Kuramochi, K. Maeda, Y. Takahashi, M. Osako and G. Suzuki. Size-Controlled Preparation of Polyethylene Nanoplastic Particles by Nanoprecipitation and Insights into the Underlying Mechanisms. *ACS Omega*, 2023, **8**, 14470–14477. https://doi.org/10.1021/acsomega.2c08233.

200 R. B. Schefer, A. Armanious and D. M. Mitrano. Eco-Corona Formation on Plastics: Adsorption of Dissolved Organic Matter to Pristine and Photochemically Weathered Polymer Surfaces. *Environ Sci Technol*, 2023, **57**, 14707–14716. https://doi.org/10.1021/acs.est.3c04180.

201 B. W. Neun and M. A. Dobrovolskaia. NCL Method STE-1.1: Detection and Quantification of Gram Negative Bacterial Endotoxin Contamination in Nanoparticle Formulations by End Point Chromogenic LAL Assay. https://doi.org/10.17917/5WSQ-7X78, (accessed 20 May 2025).

202 Corning Inc. *Endotoxins and Cell Culture - Technical Guide*. https://www.corning.com/catalog/cls/documents/application-notes/TC-305.pdf, (accessed 30 August 2024).

203 J. M. Costello and S. T. Bowden. The temperature variation of orthobaric density difference in liquid-vapour systems. III. Alcohols. *Recueil des Travaux Chimiques des Pays-Bas*, 1958, **77**, 36–46. https://doi.org/10.1002/recl.19580770106.

204 S. Stern, P. Adiseshaiah and T. Potter. NCL Method GTA-1: LLC-PK1 Kidney Cytotoxicity Assay. https://doi.org/10.17917/Q6EC-XC97, (accessed 13 February 2025).

205 D. Wang, Q. Sun, M. J. Hokkanen, C. Zhang, F.-Y. Lin, Q. Liu, S.-P. Zhu, T. Zhou, Q. Chang, B. He, Q. Zhou, L. Chen, Z. Wang, R. H. A. Ras and X. Deng. Design of robust superhydrophobic surfaces. *Nature*, 2020, **582**, 55–59. https://doi.org/10.1038/s41586-020-2331-8.

206 M. Yamamoto, N. Nishikawa, H. Mayama, Y. Nonomura, S. Yokojima, S. Nakamura and K. Uchida. Theoretical Explanation of the Lotus Effect: Superhydrophobic Property Changes by Removal of Nanostructures from the Surface of a Lotus Leaf. *Langmuir*, 2015, **31**, 7355–7363. https://doi.org/10.1021/acs.langmuir.5b00670.

207 K. Aljoumaa and M. Abboudi. Physical ageing of polyethylene terephthalate under natural sunlight: correlation study between crystallinity and mechanical properties. *Applied Physics A*, 2015, **122**, 6. https://doi.org/10.1007/s00339-015-9518-0.

208 A. Rjeb, L. Tajounte, M. C. El Idrissi, S. Letarte, A. Adnot, D. Roy, Y. Claire, A. Périchaud and J. Kaloustian. IR spectroscopy study of polypropylene natural aging. *J Appl Polym Sci*, 2000, **77**, 1742–1748. https://doi.org/10.1002/1097-4628(20000822)77:8<1742::AID-APP11>3.0.CO;2-T.

209 Y. Bide, M. A. Fashapoyeh and S. Shokrollahzadeh. Structural investigation and application of Tween 80-choline chloride self-assemblies as osmotic agent for water desalination. *Sci Rep*, 2021, **11**, 17068. https://doi.org/10.1038/s41598-021-96199-6.

210 Z. Weiszhár, J. Czúcz, C. Révész, L. Rosivall, J. Szebeni and Z. Rozsnyay. Complement activation by polyethoxylated pharmaceutical surfactants: Cremophor-EL, Tween-80 and Tween-20. *European Journal of Pharmaceutical Sciences*, 2012, **45**, 492–498. https://doi.org/10.1016/j.ejps.2011.09.016.

211 Alan Rawle. Basic principles of particle size analysis. *Surface Coatings International. Part A, Coatings Journal*, 2003, **86**, 58–65.

212 M. Kaszuba and M. T. Connah. Protein and Nanoparticle Characterisation Using Light Scattering Techniques. *Particle & Particle Systems Characterization*, 2006, **23**, 193–196. https://doi.org/10.1002/ppsc.200601030.

213 T. Du, X. Yu, S. Shao, T. Li, S. Xu and L. Wu. Aging of Nanoplastics Significantly Affects Protein Corona Composition Thus Enhancing Macrophage Uptake. *Environ Sci Technol*, 2023, **57**, 3206–3217. https://doi.org/10.1021/acs.est.2c05772.

214 Y. Ji, C. Wang, Y. Wang, L. Fu, M. Man and L. Chen. Realistic polyethylene terephthalate nanoplastics and the size- and surface coating-dependent toxicological impacts on zebrafish embryos. *Environ Sci Nano*, 2020, **7**, 2313–2324. https://doi.org/10.1039/D0EN00464B.

215 A. Vismara and A. Gautieri. Molecular insights into nanoplastics-peptides binding and their interactions with the lipid membrane. *Biophys Chem*, 2024, **308**, 107213. https://doi.org/10.1016/j.bpc.2024.107213.

216 C. Wunderlich, S. Schumacher and M. Kietzmann. Pyrogen detection methods: Comparison of bovine whole blood assay (bWBA) and monocyte activation test (MAT). *BMC Pharmacol Toxicol*, 2014, **15**, 50. https://doi.org/10.1186/2050-6511-15-50.

217 M. Grauso, A. Lan, M. Andriamihaja, F. Bouillaud and F. Blachier. Hyperosmolar environment and intestinal epithelial cells: impact on mitochondrial oxygen consumption, proliferation, and barrier function in vitro. *Sci Rep*, 2019, **9**, 11360. https://doi.org/10.1038/s41598-019-47851-9.

218 A. Guyot and J. W. Hanrahan. ATP release from human airway epithelial cells studied using a capillary cell culture system. *J Physiol*, 2002, **545**, 199–206. https://doi.org/10.1113/jphysiol.2002.030148.

219 M. D. Gundersen, K. B. Larsen, K. M. Johnsen, R. Goll, J. Florholmen and G. Haraldsen. Hypo-osmotic stress induces the epithelial alarmin IL-33 in the colonic barrier of ulcerative colitis. *Sci Rep*, 2022, **12**, 11550. https://doi.org/10.1038/s41598-022-15573-0.

220 A. Miermont, S. W. L. Lee, G. Adriani and R. D. Kamm. Quantitative screening of the effects of hyper-osmotic stress on cancer cells cultured in 2- or 3-dimensional settings. *Sci Rep*, 2019, **9**, 13782. https://doi.org/10.1038/s41598-019-50198-w.

221 J. D. Finan and F. Guilak. The effects of osmotic stress on the structure and function of the cell nucleus. *J Cell Biochem*, 2010, **109**, 460–467. https://doi.org/10.1002/jcb.22437.

222 H. M. Taïeb, D. S. Garske, J. Contzen, M. Gossen, L. Bertinetti, T. Robinson and A. Cipitria. Osmotic pressure modulates single cell cycle dynamics inducing reversible growth arrest and reactivation of human metastatic cells. *Sci Rep*, 2021, **11**, 13455. https://doi.org/10.1038/s41598-021-92054-w.

223 V. Dhaka, S. Singh, A. G. Anil, T. S. Sunil Kumar Naik, S. Garg, J. Samuel, M. Kumar, P. C. Ramamurthy and J. Singh. Occurrence, toxicity and remediation of polyethylene terephthalate plastics. A review. *Environ Chem Lett*, 2022, **20**, 1777–1800. https://doi.org/10.1007/s10311-021-01384-8.

224 R. Ahmad Khanbeigi, A. Kumar, F. Sadouki, C. Lorenz, B. Forbes, L. A. Dailey and H. Collins. The delivered dose: Applying particokinetics to in vitro investigations of nanoparticle internalization by macrophages. *Journal of Controlled Release*, 2012, **162**, 259–266. https://doi.org/10.1016/j.jconrel.2012.07.019.

225 P. M. Hinderliter, K. R. Minard, G. Orr, W. B. Chrisler, B. D. Thrall, J. G. Pounds and J. G. Teeguarden. ISDD: A computational model of particle sedimentation, diffusion and target cell dosimetry for in vitro toxicity studies. *Part Fibre Toxicol*, 2010, **7**, 36. https://doi.org/10.1186/1743-8977-7-36.

226 G. DeLoid, J. M. Cohen, T. Darrah, R. Derk, L. Rojanasakul, G. Pyrgiotakis, W. Wohlleben and P. Demokritou. Estimating the effective density of engineered nanomaterials for in vitro dosimetry. *Nat Commun*, 2014, **5**, 3514. https://doi.org/10.1038/ncomms4514.

227 International Organization for Standardization. *Biological evaluation of medical devices - Part 5: Tests for in vitro cytotoxicity (ISO Standard No. 10993:2009). 2009*. https://www.iso.org/standard/44908.html

228 V. Tolardo, D. Magrì, F. Fumagalli, D. Cassano, A. Athanassiou, D. Fragouli and S. Gioria. In Vitro High-Throughput Toxicological Assessment of Nanoplastics. *Nanomaterials*, 2022, **12**, 1947. https://doi.org/10.3390/nano12121947.

229 S. Yang, Y. Cheng, Z. Chen, T. Liu, L. Yin, Y. Pu and G. Liang. In vitro evaluation of nanoplastics using human lung epithelial cells, microarray analysis and co-culture model. *Ecotoxicol Environ Saf*, 2021, **226**, 112837. https://doi.org/10.1016/j.ecoenv.2021.112837.

230 L. Schröter and N. Ventura. Nanoplastic Toxicity: Insights and Challenges from Experimental Model Systems. *Small*, 2022, **18**, 2201680. https://doi.org/10.1002/smll.202201680.

231 C. Veclin, C. Desmet, A. Pradel, A. Valsesia, J. Ponti, H. El Hadri, T. Maupas, V. Pellerin, J. Gigault, B. Grassl and S. Reynaud. Effect of the Surface Hydrophobicity–Morphology–Functionality of Nanoplastics on Their Homoaggregation in Seawater. *ACS ES&T Water*, 2022, **2**, 88–95. https://doi.org/10.1021/acsestwater.1c00263.

232 L. Schröter and N. Ventura. Nanoplastic Toxicity: Insights and Challenges from Experimental Model Systems. *Small*, 2022, **18**, 2201680. https://doi.org/10.1002/smll.202201680.

233 L. M. A. Martin, N. Gan, E. Wang, M. Merrill and W. Xu. Materials, surfaces, and interfacial phenomena in nanoplastics toxicology research. *Environmental Pollution*, 2022, **292**, 118442. https://doi.org/10.1016/J.ENVPOL.2021.118442.

234 O. M. Morakinyo, M. I. Mokgobu, M. S. Mukhola and R. P. Hunter. Health Outcomes of Exposure to Biological and Chemical Components of Inhalable and Respirable Particulate Matter. *Int J Environ Res Public Health*, 2016, **13**, 592. https://doi.org/10.3390/ijerph13060592.

235 R. Lehner, C. Weder, A. Petri-Fink and B. Rothen-Rutishauser. Emergence of Nanoplastic in the Environment and Possible Impact on Human Health. *Environ Sci Technol*, 2019, **53**, 1748–1765. https://doi.org/10.1021/acs.est.8b05512.

236 Deutscher Apotheker Verlag. 2.9.18 Zubereitungen zur Inhalation: Aerodynamische Beurteilung feiner Teilchen. in *Europäisches Arzneibuch*, 2019, vol. 10.0, pp. 478–480.

237 A. R. Ferro and L. M. Hildemann. Inhalation Exposure, Uptake, and Dose. in *Exposure Analysis*, eds. W. R. Ott, A. C. Steinemann and L. A. Wallace, CRC Press, Boca Raton, 1st Edition., 2006, pp. 81–98.

238 E. D. Schreder, N. Uding and M. J. La Guardia. Inhalation a significant exposure route for chlorinated organophosphate flame retardants. *Chemosphere*, 2016, **150**, 499–504. https://doi.org/10.1016/j.chemosphere.2015.11.084.

239 World Health Organization (WHO). *Hazard prevention and control in the work environment: airborne dust.*, Geneva, 1999. https://www.who.int/publications/i/item/WHO-SDE-OEH-99-14, (accessed 29 August 2025).

240 G. Scheuch, M. J. Kohlhaeufl, P. Brand and R. Siekmeier. Clinical perspectives on pulmonary systemic and macromolecular delivery. *Adv Drug Deliv Rev*, 2006, **58**, 996–1008. https://doi.org/10.1016/j.addr.2006.07.009.

241 N. A. H. Janssen, P. Fischer, M. Marra, C. Ameling and F. R. Cassee. Short-term effects of PM2.5, PM10 and PM2.5–10 on daily mortality in the Netherlands. *Science of The Total Environment*, 2013, **463–464**, 20–26. https://doi.org/10.1016/j.scitotenv.2013.05.062.

242 J. Chen and G. Hoek. - Long-term exposure to PM and all-cause and cause-specific mortality: A systematic review and meta-analysis. *Environ Int*, 2020, **143**, 105974. https://doi.org/10.1016/j.envint.2020.105974.

243 P. Orellano, J. Reynoso, N. Quaranta, A. Bardach and A. Ciapponi. Short-term exposure to particulate matter (PM10 and PM2.5), nitrogen dioxide (NO2), and ozone (O3) and all-cause and cause-specific mortality: Systematic review and meta-analysis. *Environ Int*, 2020, **142**, 105876. https://doi.org/10.1016/j.envint.2020.105876.

244 G. W. Hallworth and D. G. Westmoreland. The twin impinger: a simple device for assessing the delivery of drugs from metered dose pressurized aerosol inhalers. *Journal of Pharmacy and Pharmacology*, 1987, **39**, 966–972. https://doi.org/10.1111/j.2042-7158.1987.tb03142.x.

245 C. C. Tseng and C. S. Li. Collection efficiencies of aerosol samplers for virus-containing aerosols. *J Aerosol Sci*, 2005, **36**, 593–607. https://doi.org/10.1016/J.JAEROSCI.2004.12.004.

246 M. Spanne, P. Grzybowski and M. Bohgard. Collection Efficiency for Submicron Particles of a Commonly Used Impinger. *Am Ind Hyg Assoc J*, 1999, **60**, 540–544. https://doi.org/10.1080/00028899908984476.

247 J. Hogan C.J., E. M. Kettleson, M. -H. Lee, B. Ramaswami, L. T. Angenent and P. Biswas. Sampling methodologies and dosage assessment techniques for submicrometre and ultrafine virus aerosol particles. *J Appl Microbiol*, 2005, **99**, 1422–1434. https://doi.org/10.1111/j.1365-2672.2005.02720.x.

248 B. Miljevic, R. L. Modini, S. E. Bottle and Z. D. Ristovski. On the efficiency of impingers with fritted nozzle tip for collection of ultrafine particles. *Atmos Environ*, 2009, **43**, 1372–1376. https://doi.org/10.1016/J.ATMOSENV.2008.12.001.

249 K. P. Yu, Y. P. Chen, J. Y. Gong, Y. C. Chen and C. C. Cheng. Improving the collection efficiency of the liquid impinger for ultrafine particles and viral aerosols by applying granular bed filtration. *J Aerosol Sci*, 2016, **101**, 133–143. https://doi.org/10.1016/J.JAEROSCI.2016.08.002.

250 W. Jin, W. Zhang, H. Tang, P. Wang, Y. Zhang, S. Liu, J. Qiu, H. Chen, L. Wang, R. Wang, Y. Sun, P. Liu, H. Tang and Y. Zhu. Microplastics exposure causes the senescence of human lung epithelial cells and mouse lungs by inducing ROS signaling. *Environ Int*, 2024, **185**, 108489. https://doi.org/10.1016/J.ENVINT.2024.108489.

251 L. Chen, Y. Liu, H. Li, S. Lin, X. Wang, J. Fang, X. Diao, L. Wang, Z. Yang and Z. Cai. Size-Dependent Pulmonary Toxicity and Whole-Body Distribution of Inhaled Micro/Nanoplastic Particles in Male Mice from Chronic Exposure. *Environ Sci Technol*, 2025, **59**, 6993–7003. https://doi.org/10.1021/acs.est.4c14232.

252 C. Goedecke, P. Eisentraut, K. Altmann, A. M. Elert, C. G. Bannick, M. Ricking, N. Obermaier, A.-K. Barthel, T. Schmitt, M. Jekel and U. Braun. Development of a Routine Screening Method for the Microplastic Mass Content in a Wastewater Treatment Plant Effluent. *Frontiers in Environmental Chemistry*; 2022; **3**; 844633. https://doi.org/10.3389/fenvc.2022.844633.

253 M. Kittner, P. Eisentraut, D. Dittmann and U. Braun. Decomposability versus detectability: First validation of TED-GC/MS for microplastic detection in different environmental matrices. *Applied Research*, 2024, **3**, e202200089. https://doi.org/10.1002/appl.202200089.

254 R. Sijs, S. Kooij and D. Bonn. How surfactants influence the drop size in sprays from flat fan and hollow cone nozzles. *Physics of Fluids*, 2021, **33**, 113608. https://doi.org/10.1063/5.0066775.

255 L. A. Dailey, T. Schmehl, T. Gessler, M. Wittmar, F. Grimminger, W. Seeger and T. Kissel. Nebulization of biodegradable nanoparticles: impact of nebulizer technology and nanoparticle characteristics on aerosol features. *Journal of Controlled Release*, 2003, **86**, 131–144. https://doi.org/10.1016/S0168-3659(02)00370-X.

256 K. Takahashi, J. A. Kramar, N. Farkas, K. Takahata, I. Misumi, K. Sugawara, S. Gonda and K. Ehara. Interlaboratory comparison of nanoparticle size measurements between NMIJ and NIST using two different types of dynamic light scattering instruments. *Metrologia*, 2019, **56**, 055002. https://doi.org/10.1088/1681-7575/ab3073.

257 S. L. Wright, T. Gouin, A. A. Koelmans and L. Scheuermann. Development of screening criteria for microplastic particles in air and atmospheric deposition: critical review and applicability towards assessing human exposure. *Microplastics and Nanoplastics*, 2021, **1**, 6. https://doi.org/10.1186/s43591-021-00006-y.

258 Y. Logvina, I. M. Matas, H. Ribeiro, L. da Silva, P. Rodrigues, J. Leitão and J. E. da Silva. Micro- and Nanoplastics in the Atmosphere: Methodology for Microplastics Size-Fractionation Sampling. *Microplastics*, 2024, **3**, 82–97. https://doi.org/10.3390/microplastics3010006.

259 T. Di Giulio, G. E. De Benedetto, N. Ditaranto, C. Malitesta and E. Mazzotta. Insights into Plastic Degradation Processes in Marine Environment by X-ray Photoelectron Spectroscopy Study. *Int J Mol Sci*, 2024, **25**, 5060. https://doi.org/10.3390/ijms25105060.

260 L. Nigro, A. Binelli, I. Herman, S. Gazzotti, M. A. Ortenzi and J. Asselman. Transgenerational effects of water-soluble polymers on Daphnia magna at environmentally relevant concentrations: The role of multigenerational plasticity. *Environ Res*, 2025, **275**, 121436. https://doi.org/10.1016/J.ENVRES.2025.121436.

261 A. Kolate, D. Baradia, S. Patil, I. Vhora, G. Kore and A. Misra. PEG — A versatile conjugating ligand for drugs and drug delivery systems. *Journal of Controlled Release*, 2014, **192**, 67–81. https://doi.org/10.1016/J.JCONREL.2014.06.046.

262 J. Prinz, G. Nagel, S. Dekkers, E. P. van Someren, V. Adam, V. Di Battista, B. Suarez-Merino, W. Wohlleben, M. Persson, A. Baun, O. Schmid and A. Haase. HARMLESS Early Warning System for Advanced Materials. *Adv Sustain Syst*, 2025, **9**, 2500217. https://doi.org/10.1002/adsu.202500217.

263 G. Binda, G. Kalčíková, I. J. Allan, R. Hurley, E. Rødland, D. Spanu and L. Nizzetto. Microplastic aging processes: Environmental relevance and analytical implications. *TrAC Trends in Analytical Chemistry*, 2024, **172**, 117566. https://doi.org/10.1016/J.TRAC.2024.117566.

264 O. S. Alimi, D. Claveau-Mallet, R. S. Kurusu, M. Lapointe, S. Bayen and N. Tufenkji. Weathering pathways and protocols for environmentally relevant microplastics and nanoplastics: What are we missing? *J Hazard Mater*, 2022, **423**, 126955. https://doi.org/10.1016/J.JHAZMAT.2021.126955.

265 J. D. Rindelaub, J. A. Salmond, W. Fan, G. M. Miskelly, K. N. Dirks, S. Henning, T. Conrath, F. Stratmann and G. Coulson. Aerosol mass concentrations and dry/wet deposition of atmospheric microplastics at a remote coastal location in New Zealand. *Environmental Pollution*, 2025, **372**, 126034. https://doi.org/10.1016/J.ENVPOL.2025.126034.

266 C. H. Wu, T. T. M. Dang, J. K. Mutuku, L. M. Lin, B. W. Huang and G. P. Chang-Chien. Evaluation of PM2.5 bound microplastics and plastic additives in several cities in Taiwan: Spatial distribution and human health risk. *Science of The Total Environment*, 2025, **959**, 178213. https://doi.org/10.1016/J.SCITOTENV.2024.178213.

267 B. Kirchsteiger, D. Materić, F. Happenhofer, R. Holzinger and A. Kasper-Giebl. Fine micro- and nanoplastics particles (PM2.5) in urban air and their relation to polycyclic aromatic hydrocarbons. *Atmos Environ*, 2023, **301**, 119670. https://doi.org/10.1016/J.ATMOSENV.2023.119670.

268 X. Sheng, Y. Lai, S. Yu, Q. Li, Q. Zhou and J. Liu. Quantitation of Atmospheric Suspended Polystyrene Nanoplastics by Active Sampling Prior to Pyrolysis–Gas Chromatography–Mass Spectrometry. *Environ Sci Technol*, 2023, **57**, 10754–10762. https://doi.org/10.1021/acs.est.3c02299.